Tânia Sofia Cardoso Ribeiro Rebelo

Mestre em Engenharia Química – Otimização Energética na Indústria Química

Improving the early diagnostic of prostate cancer by multiple biomarker detection with new biosensing devices

Dissertação para obtenção do Grau de Doutor em

Química Sustentável

Setembro, 2015

Improving the early diagnostic of prostate cancer by multiple biomarker detection with new biosensing devices

Bolsa de Doutoramento da Fundação para a Ciência e a Tecnologia com a referência SFRH/BD/79221/2011, financiada pelo POPH – QREN – Tipologia 4.1 – Formação Avançada, comparticipada pelo Fundo Social Europeu e por fundos nacionais do MCTES

Dedico esta dissertação ao meu marido, Rui Rebelo, pela paciência que demonstrou ao longo destes 4 anos, mas principalmente por todo o carinho, apoio e dedicação.

Ao meu filho Rui, que deu um sentido especial à minha vida e me tem proporcionado grandes alegrias.

Aos meus pais e restante família por todo o apoio e compreensão.

Acknowledgments

I thank Prof. Goreti Sales for the scientific supervision, dedication, affection, confidence she had on me, for all the availability, encouragement and patience demonstrated at various times over the last four years.

To Prof. João Paulo Noronha for accepting the supervision of this work, for the support and scientific contribution.

To Prof. João Rodrigues for the dedication, help, and scientific contribution.

To Prof. Carlos Pereira from *Centro de Investigação em Química, Faculdade de Ciências da Universidade do Porto* for his help, dedication, affection and hospitality with which he received me in his group.

To all my colleagues of the CIQ group for all the help, the constructive discussions, friendship and mainly the companionship. I thank to Renata Costa, Paula Fernandes, Inês Miranda, Tatiana Andreani, Nuno Pereira, José Ribeiro and all others colleagues.

To all my colleagues of the BioMarK group that, direct or indirectly, contributed to this work. I thank to Felismina Moreira, Joana Guerreiro and all others colleagues.

To all my friends for their comprehension and support. In particularly to Renata Costa and Sofia Almeida.

To my family: my husband, son and parents for the patience, the love, dedication but especially for being present in every moment of my life.

Resumo

O cancro da próstata é o cancro mais comum nos homens Europeus (dados da Organização Mundial de Saúde). Os dados estatísticos mais recentes, relativos ao território português, confirmam este cenário, referindo que cerca de 50% dos homens portugueses poderão vir a padecer de cancro da próstata e que 15% destes morrerão desta condição.

A deteção precoce do cancro da próstata é por isso muito importante no sucesso do tratamento da doença. Atualmente, o rastreio é realizado através do biomarcador antigénio específico da próstata (PSA) que é excretado na urina. Todavia, aparecimento de resultados falsos positivos/negativos, é recorrente, levando a que os doentes sejam enviados desnecessariamente para procedimentos de biópsia. Este protocolo pode ser melhorado através do desenvolvimento de dispositivos de deteção do cancro da próstata em "point-of-care", não só para o PSA mas também para outros marcadores.

Neste sentido, o presente trabalho tem como objetivo desenvolver sensores de baixo custo, baseados em novos biomateriais sintéticos, que permitam rastrear vários biomarcadores em culturas de linhas celulares do cancro da próstata, em amostras de sangue e em amostras de urina. Os biomarcadores considerados neste estudo são os seguintes: antigénio específico da próstata (PSA), anexina A3 (ANXA3), microseminoproteina-beta (MSMB) e sarcosina (SAR).

Para o reconhecimento dos biomarcadores em estudo foram utilizadas duas abordagens distintas: a síntese de polímeros de impressão moleculares, um tipo de anticorpos plásticos, e o reconhecimento enzimático. O crescimento de um polímero rígido e quimicamente estável na presença do biomarcador possibilita a criação dos anticorpos plásticos. Os MIPs apresentam elevada sensibilidade/seletividade, uma maior estabilidade e preço mais baixo, quando

comparados com anticorpos naturais. O crescimento destas unidades sensoras nanoestruturadas foi efetuada sobre um suporte sólido de carbono. A interação entre o biomarcador e o material sensor traduz-se na produção de sinais elétricos quantitativos ou semi-quantitativos. Estes dispositivos permitem a deteção barata e portátil nos teste "point-of-care".

Palavras-chave: Biosensores; Biomarcadores do cancro da próstata; Eletroquímica; Polímeros de impressão molecular.

Abstract

Prostate cancer (PCa) is the most common form of cancer in men, in Europe (World Health Organization data). The most recent statistics, in Portuguese territory, confirm this scenario, which states that about 50% of Portuguese men may suffer from prostate cancer and 15% of these will die from this condition.

Its early detection is therefore fundamental. This is currently being done by Prostate Specific Antigen (PSA) screening in urine but false positive and negative results are quite often obtained and many patients are sent to unnecessary biopsy procedures. This early detection protocol may be improved, by the development of point-of-care cancer detection devices, not only to PSA but also to other biomarkers recently identified.

Thus, the present work aims to screen several biomarkers in cultured human prostate cell lines, serum and urine samples, developing low cost sensors based on new synthetic biomaterials. Biomarkers considered in this study are the following: prostate specific antigen (PSA), annexin A3 (ANXA3), microseminoprotein-beta (MSMB) and sarcosine (SAR).

The biomarker recognition may occurs by means of molecularly imprinted polymers (MIP), which are a kind of plastic antibodies, and enzymatic approaches. The growth of a rigid polymer, chemically stable, using the biomarker as a template allows the synthesis of the plastic antibody. MIPs show high sensitivity/selectivity and present much longer stability and much lower price than natural antibodies. This nanostructured material was prepared on a carbon solid. The interaction between the biomarker and the sensing-material produces electrical signals generating quantitative or semi-quantitative data. These devices allow inexpensive and portable detection in point-of-care testing.

Keywords: Biosensors; Prostate cancer biomarkers; Surface imprinting; Electrochemistry.

"O mundo está nas mãos daqueles que tem a coragem de sonhar e correr o risco de viver seus sonhos."

Paulo Coelho

Index

List of figures

List of tables

List of abbreviations

A	Ampere
AA	Acrylamide
AFM	Atomic-force microscopy
AMH	2-Aminoethyl methacrylate hydrochloride
ANXA3	Annexin A3
AR	Androgen receptor
ATR	Attenuated Total Reflectance
BOP	Benzoyl peroxide
BPH	Benign prostate hyperplasia
BSA	Bovine Serum Albumin
CAF	Caffeic Acid
cDNA	Complementary Deoxyribonucleic acid
C_{dl}	Capacitance of the double layer
C/NIM	Charged Non-Imprinted Materials
C/PIM	Charged Protein Imprinted Materials
CT	Cycle threshold
CV	Cyclic Voltammetry
DMEM	Dulbecco's Modified Eagle Medium
DNA	Deoxyribonucleic acid
DTT	DL-Dithiothreitol
E	Applied potential
EDAC	*N*-ethyl-*N*-(3-dimethylaminopropyl) carbodiimide hydrochloride

EDTA	Ethylenediaminetetraacetic acid
EIS	Electrochemical Impedance Spectroscopy
ELISA	Enzyme linked immunosorbent assay
Emf	Electromotive force
F	Faraday
FB	Human gingival fibroblasts
FBS	Fetal bovine serum
FTIR	Fourier Transformed Infrared
GO	Graphene oxide
GUSB	Beta-glucuronidase
HEPES	4-(2-hydroxyethyl)-1-piperazineethanesulfonic acid
hKLK3	Human kallikrein 3
Hz	Frequency
I	Electrical current
IAA	Iodoacetamide
ISE	Ion-Selective Electrode
IUPAC	International Union of Pure and Applied Chemistry
K_{eq}	Equilibrium constant
KLK2	Kallikrein-2
KLK4	Kallikrein-4
K^{POT}	Potentiometric selectivity coefficients
LLLR	Lower limit of linear range
LOD	Limit of detection
MALDI-TOF	Matrix Assisted Laser Desorption Ionization Time-of-Flight
MIP	Molecularly Imprinted Polymer

mRNA	Messenger Ribonucleic acid
MS	Mass Spectrometry
MSMB	Microseminoprotein-beta
NHS	*N*-hydroxysuccinimide
NIM	Non Imprinted Materials
NIP	Non Imprinted Polymer
NMAA	*N,N*-methylenebis(acrylamide)
N/NIM	Neutral monomers Non Imprinted Materials
N/PIM	Neutral monomers Protein Imprinted Materials
oNPOE	*ortho*-Nitrophenyloctyl ether
PBS	Phosphate buffer solutions
PCa	Prostate Cancer
PC3	Prostate cancer cell line
PCTA1	Prostate Carcinoma Tumor Antigen-1
PIM	Protein Imprinted Materials
PMF	Peptide Mass Fingerprint
PrLZ	Prostate Leucine Zipper
PSA	Prostate Specific Antigen
PSCA	Prostate Stem Cell Antigen
PSMA	Prostate-Specific Membrane Antigen
PSMB6	Proteasome subunit beta type-6
PSP94	Prostatic Secretory Protein 94
PVC	Poly(vinylchloride)
QCM	Quartz Crystal Microbalance
qPCR	Quantitative polymerase chain reaction

R	Universal gas constant
R_{ct}	Charge transfer resistance
RMS	Root Mean Square
RNA	Ribonucleic acid
RPMI	Roswell Park Memorial Institute - medium
R_s	Resistance of the solution
RT-PCR	Reverse transcription polymerase chain reaction
SAR	Sarcosine
SOX	Sarcosine Oxidase
SPE	Screen-Printed Electrode
SPR	Surface Plasmon Resonance
SWV	Square Wave Voltammetry
T	Temperature
t	Time
TEM	Transmission Electron Microscopy
TFA	Trifluoroacetic acid
TGM4	Protein-glutamine gamma-glutamyltransferase 4
THF	Tetrahydrofuran
ULLR	Upper limit of linear range
UV	Ultraviolet
VB	Vinyl benzoate
VTA	(Vinylbenzyl)trimethylammonium chloride
W	Warburg diffusion element
WE	Working electrode
Z′	Imaginary component of impedance

Z''	Warburg impedance
α-CHCA	Alpha-cyano-4-hydroxycinnamic acid
α-MEM	Alpha-Minimal Essential Medium
ΔG	Free energy change
ω	Angular frequency

1

Framework

1.1 Motivation

Prostate cancer (PCa) is the commonest form of cancer in men in Europe, with a 61.4 % incidence among all cancer diseases and 12.1 % mortality [1]. Accurate and early detection of PCa is thus very important, attributing early diagnosis a major role in the successful treatment of the disease.

Early detection of prostate cancer biomarkers is currently made by PSA screening in men over 45 years old, combined with other alterations in serum and urine parameters. However, in PSA testing, many false positive/negative results are obtained, thereby leading several patients to unnecessary biopsy procedures. In addition, a non-invasive method for an accurate diagnosis of PCa would decrease the discomfort of patients in routine analytical procedures, while permitting a significant reduction in the number of repeated biopsies in patients. Also, an early detection protocol could benefit from the screening of additional specific biomarkers that may complement PSA testing, or replace it over time.

Many other biomolecules besides PSA have been correlated to PCa [2, 3], but only a few of these molecules may turn out a successful biomarker for analytical purposes. These should have analytical suitability (measured by cost-effective assay, simple to perform, rapid turnaround time and sufficient precision and accurateness), clinical suitability (ability to influence therapy and to improve patient outcome) and specificity for prostate cancer (so that the identification and

characterization of a unique blood-based marker for the disease would provide a more accurate diagnosis, reducing both unnecessary biopsies and patient uncertainty). Thus, along with the currently used PSA, Annexin A3 (ANXA3), Microseminoprotein-beta (MSMB) and Sarcosine (SAR) are here considered as suitable as PCa biomarkers.

The conventional methods for screening PCa biomarkers include immunological-based assays that have to be established in laboratorial context. Electrochemical (bio)sensors are emerging as a promising alternative tool to the conventional methodologies mostly due to their portability/automation feasibility. They offer high robustness, easy miniaturization, excellent detection limits with small analyte volumes, and ability to be used in turbid biofluids with optically absorbing and fluorescing compounds. A suitable architecture may allow good sensitivity and selectivity with the desired biochemical event. The biomarker recognition may be established by means of molecularly imprinted polymers that are a kind of plastic antibodies, which show high sensitivity/selectivity and present much longer stability and a much lower cost than natural antibodies [4].

Thus, this work describes the development of new biosensors for selected biomarker screening, with the purpose of combining these, in the future, in a multi-sensory platform for the screening of PCa. The electrical signal produced by each biomarker is produced by the interaction between a suitable biorecognition element and the corresponding target analyte. The electrical transduction is possible due to the modification of the transducer surface. Techniques such as Potentiometry and Voltammetry are used for this purpose. Conventional solid-contact carbon electrodes are designed for PSA sensing using potentiometric techniques. Voltammetry studies are adjusted for ANXA3, MSMB and SAR screening purposes, with screen-printed electrodes (SPEs). SPEs enable

simple and inexpensive procedures, providing selective readings with low concentrations of analyte and low sample volumes. Furthermore, they may offer portable versions to carry out assays in point-of-care testing.

1.2 Structure of the thesis

This thesis is organized in eight chapters.

Chapter 1, the present chapter, gives the motivation of the present work, describes the structure and the framework of the thesis and lists the publications and communications associated with this PhD research program.

Chapter 2 presents a literature overview about the main topics discussed in this work: the prostate cancer biomarkers detection, the recognition elements and the transducing processes. Special relevant issues are focused on PSA, ANXA3, MSMB and SAR biomarkers.

Chapter 3 to 7 presents the construction, characterization and application of biosensors for the quantification of different biomarkers.

Chapter 3 describes the synthesis of protein plastic antibodies tailored with selected charged monomers around the binding site to enhance protein binding. The presence of charged labels was beneficial for the production of more sensitive electrical responses. These were synthesized by surface imprinting over graphene layers, producing an inexpensive material that was successfully applied to produce PSA sensors of potentiometric transduction. The resulting materials were included as ionophores in plasticized PVC membranes, and tested over electrodes of solid or liquid conductive contacts, made of conductive carbon packed into a plastic syringe body or of inner reference solution over micropipette tips. However, although the results obtained were promising, the apparatus employed herein was more suitable for bench routine applications

than point-of-care use. The device could be reused and hardly disposed of after each application.

Therefore, the construction of a disposable biosensor is essential for tests in point-of-care, and was reported in **chapter 4,** which describes the construction of a simple and low cost ANXA3 electrochemical biosensor by electropolymerization procedures on the carbon surface of a SPE. The monomer selected for this purpose was Caffeic acid (CAF), coexisting in solution with the target protein. The biosensor was successfully applied to spiked urine samples.

With the aim of improving the construction of the above biosensor, **chapter 5** describes a molecular imprinting process over the surface of a carbon-SPE where charged labels in the imprinting stage enabled the production of a simple and low cost electrochemical sensor. This principle was applied to the determination of MSMB in biological fluids. The corresponding biosensor was obtained in the surface of a carbon-SPE by electropolymerizing CAF in the presence of MSMB and having dopamine as charged label.

In **chapter 6**, a biosensor device was developed for the quantification of sarcosine *via* electrochemical detection of hydrogen peroxide, H_2O_2 (at 0.6 V), generated from the catalyzed oxidation of sarcosine. The detection was carried out after the modification of carbon-SPEs by immobilization of sarcosine oxidase (SOX), using *N*-ethyl-*N'*-(3-dimethylaminopropyl)carbodiimide (EDC) and *N*-hydroxysuccinimide (NHS), on the surface of the carbon-SPE. The selectivity of the electrochemical biosensor was improved by covering the electrode surface with Nafion®. Nafion is used due to its film hydrophobicity and enzyme-favored environment as well as to enhance selectivity of the sensor by electrostatic repulsion of unwanted species.

The performance and effectiveness of the developed PSA biosensor, described in chapter 3, for screening PSA in biological fluids of complex composition, collected from different PCa cell line cultures, was studied in **chapter 7**. The electrochemical biosensor was able to specifically detect PSA in complex media and values obtained were similar to those achieved by a commercial ELISA kit, the most commonly used method for PSA quantification in PCa diagnosis. Thus, the described biosensor may represent a useful alternative as a diagnostic tool for PSA determination in biological samples.

Chapter 8 summarizes the main results obtained and presents guidelines for future research work.

1.3 List of publications

1.3.1 Papers published in international scientific journals

1: Tânia S.C.R. Rebelo, Carlos M. Pereira, M. Goreti F. Sales, João P. Noronha and Fernando Silva, Protein Imprinted Materials designed with charged binding sites on screen-printed electrode for Microseminoprotein-Beta determination in biological samples, *Sensors and Actuators B: Chemical*, 2016, 223, 846-852.

2: Tânia S.C.R. Rebelo, Carlos M. Pereira, M. Goreti F. Sales, João P. Noronha and Fernando Silva, Protein Imprinted Materials electrochemical sensor for determination of Annexin A3 in biological samples, *Electrochimica Acta*, 2016.

3: Tânia S.C.R. Rebelo, João P. Noronha, Marco Galésio, Hugo Santos, Mário Diniz, M. Goreti F. Sales, M.H. Fernandes and J. Costa-Rodrigues, Testing the variability of PSA expression by different human prostate cancer cell lines by means of a new potentiometric device employing molecularly antibody assembled on graphene surface, *Materials Science and Engineering: C*, 2016, 59, 1069–1078.

4: Tânia S.C.R. Rebelo, Carlos M. Pereira, M. Goreti F. Sales, João P. Noronha, J. Costa-Rodrigues, Fernando Silva, and M.H. Fernandes, Sarcosine oxidase composite screen-printed electrode for sarcosine determination in biological samples, *Analytica Chimica Acta*, 2014, 850, 26-32.

5: Tânia S.C.R. Rebelo, C. Santos, Costa-Rodrigues, M.H. Fernandes, João P.C. Noronha, and M. Goreti F. Sales, Novel Prostate Specific Antigen plastic antibody designed with charged binding sites for an improved protein binding and its application in a biosensor of potentiometric transduction, *Electrochimica Acta*, 2014, 132, 142-150.

1.3.2 Communications presented in national and international scientific conferences

1: Tânia S.C.R. Rebelo, Carlos M. Pereira, M. Goreti F. Sales, João P. Noronha, J. Costa-Rodrigues, Fernando Silva, and M.H. Fernandes, Sarcosine oxidase composite screen-printed electrode for sarcosine determination in biological samples. Poster, XIX Meeting of the Portuguese Electrochemical Society to be presented at Universidade de Aveiro, on 30th June - 2nd July, 2014.

2: Tânia S.C.R. Rebelo, M. Goreti F. Sales, João P.C. Noronha, J. Costa-Rodrigues and M.H. Fernandes, Oriented tailoring of plastic antibodies for prostate specific antigen and application of the imprinted material as ionophore in potentiometric detection. Poster, presented at Nanobio Europe, Varese, Italy, 18 - 20 June, 2012.

1.4 References

[1] World Health Organization (WHO), www.who.int/mediacentre/factsheets/fs297/en, accessed in September 2010.

[2] V.M. Velonas, H.H. Woo, C.G. Remedios, and S.J. Assinder, Current Status of Biomarkers for Prostate Cancer. *International Journal of Molecular Sciences* 14 (2013) 11034-11060.

[3] N. Cernei, Z. Heger, J. Gumulec, O. Zitka, M. Masarik, P. Babula, T. Eckschlager, M. Stiborova, R. Kizek, and V. Adam, Sarcosine as a Potential Prostate Cancer Biomarker—A Review. *International Journal of Molecular Sciences* 14 (2013) 13893-13908.

[4] K.Haupt and K. Mosbach, Molecularly Imprinted Polymers and Their Use in Biomimetic Sensors. *Chemical Reviews* 100 (2000) 2495-2504.

2

Literature Review

2.1. Prostate Cancer

PCa is the third most common cancer diagnosed in Europe today, and it has emerged as the most frequent cancer amongst men [1]. PCa develops in the prostate, a gland in the male reproductive system located directly beneath the bladder, which adds secretions to the sperm during the ejaculation of semen.

Genes, dietary factors, and lifestyle-related factors have been widely recognized as contributors to the development of PCa. During the past decade, molecular studies have provided unexpected clues about how PCa disease arises and develops. The presence of genes associated with inherited susceptibility to PCa and somatic alterations in prostatic cells provoked by infection or inflammation processes of the prostate contributes to the development of PCa. In addition, newly mechanisms by which environmental carcinogens might promote the progression of PCa were recognized [2].

Therefore, PCa early detection is fundamental for the successful treatment of the disease, and thus for the increase in the survival rate. The only medical recommendation for PCa early screening suggests monitoring the levels of PSA in serum, in men over 45 years old, combined with other alterations in serum and urine parameters. However, the PSA test, which may give false positive or negative information, is not reliable and does not allow an accurate differentiation of benign prostate hyperplasia (BPH), non-aggressive PCa and

aggressive PCa leading several patients to unnecessary biopsy procedures [3]. A non-invasive approach is important in this context, for an accurate diagnosis of PCa. It would permit a significant reduction in the number of repeated biopsies. The screening of additional specific biomarkers that may supplement PSA testing, or replace it over time, should be important not only for the determination of an appropriate treatment strategy for individual patients, but also for disease detection at an earlier stage, metastatic cancer prediction and re-occurring disease following prostatectomy.

Thus this thesis is meant to establish novel strategies for screening PCa biomarkers. Some considerations about these biomarkers and detection approaches under study will be presented in the following chapters.

2.2. Prostate cancer biomarkers

A biomarker is a molecule that is objectively measured and evaluated as an indicator of normal biologic processes, pathogenic processes, or pharmacologic responses to a therapeutic intervention. A biomarker reveals further information to presently existing clinical and pathological analysis. It facilitates the screening and detection of pathologies like cancer, monitoring the progression of the disease, and predicting the prognosis and survival after clinical intervention. A biomarker can also be used to evaluate the process of drug development, and, optimally, to improve the efficacy and safety of a cancer treatment by enabling physicians to tailor treatment for individual patients [4]. As defined by the National Cancer Institute, a biomarker is "a biological molecule found in the blood, other body fluids, or tissues that is a sign of a normal or abnormal process or of a condition or disease"[5].

Thus, in cancer research, molecular biomarkers refer to substances that are indicative of the presence of cancer in the body. The form of PCa biomarkers can

vary from metabolites to chemical products, genes and genetic variations, differences in messenger RNA (miRNA) and/or protein expression and post-translational modifications of proteins present in biological fluids, such as blood, urine or saliva [6].

However, not all of molecules are appropriate to this aim. The ideal biomarker, when screened, should allow detection of the disease and its progression, identify high-risk individuals, predict recurrence, and monitor response to treatments. It should be inexpensive, reliable, easily accessible, and quickly quantifiable [4]. Biomarkers used for screening need to be able to detect early stage disease with high precision and sensitivity. Ideally, these biomarkers should be detected in specimens that can be collected by noninvasive means.

Among the several biomarkers in PCa, PSA is the one used more often. However, it has been linked to false positive or negative results, creating the need to identify other biomarkers that may complement routine PSA testing. Thus, along with the PSA currently used in clinical practice, ANXA3, MSMB, and SAR are tested herein as complementary biomarkers. The simultaneous monitoring of these biomarkers may allow clinicians to diagnose PCa quickly and/or to accurately design a patient care strategy.

2.2.1 Prostate specific antigen

PSA is one of the best-known biomarkers in medicine. This is the only medical recommendation for PCa early screening: PSA levels in serum should be monitored in men over 45 years old. Monitoring PSA levels to follow up the evolution of prostate cancer disease is also recommended, especially for being a non-invasive procedure [7].

PSA is a glycoprotein that belongs to the kallikrein family of proteases, with a molecular mass of approximately 33 kDa, produced by the secretory epithelium

of human prostate [8]. It has several isoforms, with isoelectric points ranging from 6.8 to 7.2 [3].

Low levels of PSA may be found in the blood circulation since PSA is secreted in the seminal plasma of healthy man. Nowadays, the PSA quantification test measures the total amount of PSA in the blood. A total PSA level in the blood <4 ng/mL indicates that prostate cancer is improbable, while PSA levels >10 ng/mL mean cancer is likely; values ranging from 4–10 ng/mL are in a gray zone [9], corresponding to unclear clinical condition.

However, PSA testing is not perfect, due to its limitations, mainly the false positive or negative results. PSA levels are affected by a high number of factors, like several physiological/pathological conditions, as well as a consequence of different therapeutic approaches [10]. Moreover, several types of non-prostatic neoplasm can express PSA [11]. Also, among PCa cells, expression of PSA varies widely and, furthermore, it appears to be significantly affected by the surrounding environment [10, 12]. Despite this significant variability, PSA detection is still very important for early detection of PCa and for monitoring disease evolution, creating the need to have accurate and reliable methods for PSA detection, within a broad range of protein concentrations, in biological fluids.

2.2.2 Annexin A3

ANXA3 is a specific noninvasive biomarker for PCa early detection. It is detected in urine [13] or tissue [14]. ANXA3 belongs to a family of calcium and phospholipid binding proteins that plays an important role in cell differentiation, cell migration and also in immunomodulation. Furthermore it participates as an important component of matrix vesicles in cartilage formation and bone mineralization [15]. The differential expression of ANXA3 is particularly

interesting with regard to the unusual frequency of occurrence of osteoblastic bone metastases in the case of prostate carcinoma [16]. ANXA3 occurs intracellularly as well as extracellularly, for example in exosomes in urine. Exosomes are derivatives of so-called "multivesicular bodies" and may play an alternative, but decisive role, in the antigen presentation of immune cells [17, 18]. The exosomes detected in urine are possibly identical to the so-called prostasomes, that are small vesicles of prostatic origin contained in human semen [19]; in any case, both contain ANXA3.

ANXA3 is stable in exprimate urine samples for more than 48 h at 25 °C and is stable during the course of reiterate measurements within at least 24 h [13]. Therefore, its use as biomarker is feasible, being potentially valuable for the detection of the early stages of PCa in urine samples. Although there are no standard values of ANXA3 levels to determine a positive answer for PCa until now, when detection of ANXA3 is combined with PSA, or any other cancer marker, it can be a powerful tool, obviating the drawbacks of single PSA detection.

2.2.3 Microseminoprotein-beta

MSMB is one of the more abundant proteins in the secretions produced by the human prostate, present in the seminal plasma and can be detected in serum and urine of healthy men and PCa patients [20]. Other glands, including breast tissue and other hormone responsive epithelial tissues, also produce MSMB but in small quantities [21]. It is also called Prostatic Secretory Protein 94 (PSP94), a small nonglycosylated peptide, consisting of 94 amino acids, with a molecular mass of 10.7 kDa [22].

MSMB has systemic functions, which includes growth regulation and induction of apoptosis in prostate cancer cells *in vitro* and *in vivo* [20]. While for PSA the

risk of PCa is detected by higher levels, for MSMB the levels measured in biological fluids have been shown to be statistically significantly lower in men with prostate cancer and even lower in men with aggressive disease [23-25]. Not only as a biomarker of PCa development, progression and recurrence, but also as a potential target for therapeutic intervention, MSMB is an interesting choice as PCa biomarker [26]. As described previously for ANXA3, the combined detection of MSMB and PSA can be a powerful and more accurate tool in diagnosing prostate cancer in a clinical setting.

2.2.4 Sarcosine

The SAR is a molecule produced by human metabolism and is considered a new marker to identify the presence and aggressiveness of PCa [27]. Also known as *N*-methylglycine with the chemical formula CH_3NHCH_2COOH, SAR is a metabolite that occurs as an intermediate product in the synthesis and degradation of amino acid glycine, detected in urine [28].

SAR has been identified among ten metabolites that are more abundant in prostate cells as cancer progresses. It seems to help cancer cells to invade adjacent tissues [29]. Other studies were also performed with SAR in the context of PCa. This included knowing how SAR affected the *in vitro* behavior of cells, by adding the metabolite to prostate cells and manipulating the biochemical pathways to increase molecule producing. It was noted that benign cells became cancerous and invasive. By blocking the production of SAR, invasion was terminated [30].

In biological samples (urine and blood plasma) SAR concentration can range between 1 and 20 μM [31]. But as PCa progresses, SAR levels increase in both tumor cells and urine samples, suggesting that monitoring this metabolite can help in the construction of a non-invasive diagnostic method for this disease [28].

Such complementary test, together with PSA and ANXA3, may reduce the risk of false positive/negative results.

2.3 Quantification of biomarkers

Several conventional methods have been used to detect and quantify biomarkers for PCa. Currently, the standard clinical method used more often to monitor PCa biomarkers is immunoassay-based, like Enzyme-Linked Immunosorbent Assay (ELISA) [13, 23, 32]. Other methods, such as spectrophotometric [33, 34] and chromatographic methods [35, 36] are also used. Although, some of these methods are highly sensitive and specific for the detection of proteins, they also present some important drawbacks, such as being complex, time consuming and labor intensive procedures for routine diagnostics. Furthermore, immunoassays are very expensive methods because they require specific and expensive natural antibodies, with special handling and storage conditions. As an alternative, biosensors have emerged in recent years as an attractive tool to carry out quick and local clinical analysis [37]. Some of these also make use of an antibody as biological recognition element, but other materials may be employed, such as artificial antibodies [38]. A brief overview of these approaches is presented next.

2.3.1 Immunoassays

The immunoassay is an analytical technique based on molecular recognition between an antibody and its antigen. It allows the detection of different species, with a high degree of sensitivity and specificity, being considered as one of the most widely used biomedical diagnostic methods [39].

Today, fully automated instruments in medical laboratories around the world use the immunoassay principle, with an enzyme as the reporter label for routine measurements of innumerable analytes in patient samples. The most commonly used immunoassay method is ELISA.

ELISA is an analytical technique wherein an antigen must be immobilized in a solid surface and then complexed with an antibody that is linked to an enzyme. The enzyme acts on the colorless substrate to give a colored product which is readily detectable. Detection is accomplished by assessing the conjugated enzyme activity via incubation with a substrate. Color development of the substrate by catalytic action of the enzyme is used to quantify antigen–antibody interaction [40].

In ELISA assays, the immobilization of the antigen of interest can be accomplished by direct adsorption to the assay plate or indirectly via a capture antibody that has been attached to the plate. The antigen is then detected either directly (labeled primary antibody) or indirectly (labeled secondary antibody). The ELISA format most used in laboratories is the sandwich assay, where the analyte to be measured is bound between two primary antibodies – the capture antibody and the detection antibody [40]. Based on the specific recognition of an antigen by an antibody, this method is sensitive and robust. In the literature, there are some studies that quantify the biomarkers studied in the present work by this technique, namely, it is possible to find ELISA assays for PSA [32], ANXA3 [41], and MSMB [23, 42].

But some drawbacks arise in ELISA from the use of natural antibodies. These biologically derived materials require special handling/storage conditions, are expensive and have little stability, becoming easily denatured in the presence of organic solvents. In addition, the antigen binding to the antibody is very strong, turning this method irreversible and of single use.

2.3.2 Biosensors

Biosensors have emerged in recent years as an attractive tool to carry out quick and local clinical analysis, being today an alternative concept to ELISA-based

methods [37]. Such devices are used in a wide range of practical applications in medicine, pharmacology, food and process control, environmental monitoring, defense and security, but most of the market is driven by medical diagnostics. Most applications require the detection/identification of ligands or molecules with particular binding properties, aiming at high speed, good precision, and feasibility to carry out analysis in point of care or on-site [43].

Biosensors are analytical devices that incorporate a biological/biochemical sensing element and a physicochemical transducer, to deliver analyte measurements [44]. The interaction of analyte with the recognition element (mostly of biological origin) determines the overall selectivity of the analytical approach, while generating chemical/physical changes that may be monitored by a suitable transducer (Figure 2.1).

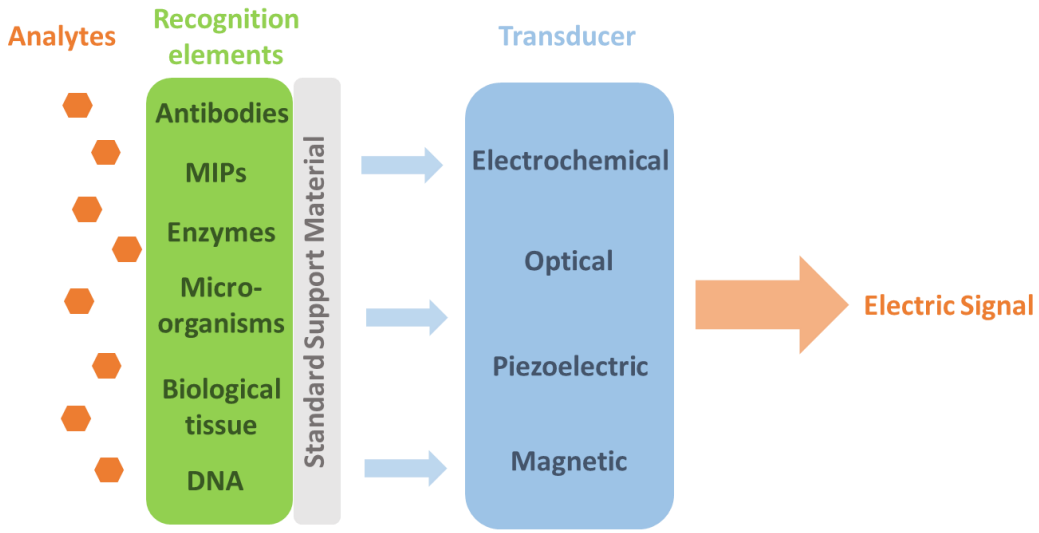

Figure **2.1**: General structure of a biosensing device.

In general, the selection of the recognition element should be made according to the analytical method under development and intended application. The surface of the sensor where the recognition element is immobilized is also a sensitive

parameter, meaning that a good development of the biosensor also depends on this choice. Depending on the measuring mode in use, a wide range of different materials can be chosen as surface. Among them are gold, silver, diamond, graphene and carbon nanotubes.

So, one of the characteristic features of biosensors is their high selectivity. It results from the possibility to tailor the specific interaction of compounds by immobilizing recognition elements on the sensor substrate that have a specific binding affinity to the desired molecule. The nature of recognition element is fundamental for the selectivity provided by biosensors. These can be biological molecules and/or artificial materials, which include enzymes, antibodies, micro-organisms, biological tissue, DNA, aptamers, and molecularly-imprinted polymers (MIPs) [43].

When the recognition element of biosensor is an antibody, the device becomes recognized as an immunosensor. Due to their similarity with biological systems and high/specific molecular affinity, the biological elements are widely used. Although, the use of an antibody as biological receptor confers a selective response, the drawbacks related to the irreversible nature and of single use of the determination remain to be solved. As an alternative, a new strategy based on the use of artificial antibodies instead of the natural ones could offer higher chemical/thermal stability [38] and promote a reversible analytical response, enabling an 'infinite' re-use of the biosensor devices.

The construction of the biosensors not only relies on the recognition element or surface but also with the transduction used for quantification of template. The method of transduction depends on the type of physicochemical change resulting from the sensing event. The physico-chemical transducer can be electrochemical, optical [45-47], piezoelectric [48] or magnetic [49].

2.3.3 (Bio)recognition elements

As mentioned previously, there are several (bio)molecules that may be employed as (bio)recognition elements. As the use of antibodies has been extensively reported in the literature [50-53], they will be left out from this overview of (bio)recognition elements. Instead, the used MIPs and enzymes as (bio)recognition elements will be regarded.

2.3.3.1 Molecularly Imprinted Material

MIPs are synthetic materials prepared by molecular imprinting technology to display a selective affinity for specific targets (Figure 2.2). These materials are a promising alternative to those naturally-derived, such as antibodies, enzymes or other biological receptors. MIPs have the ability to selectively recognize important molecules, such as drugs, proteins and biomolecules [54]. The technologies based on molecular molding provide efficient polymer systems with ability to recognize specific bioactive molecules, where the interaction depends on the properties and on the concentration of the template molecule present in the surrounding medium.

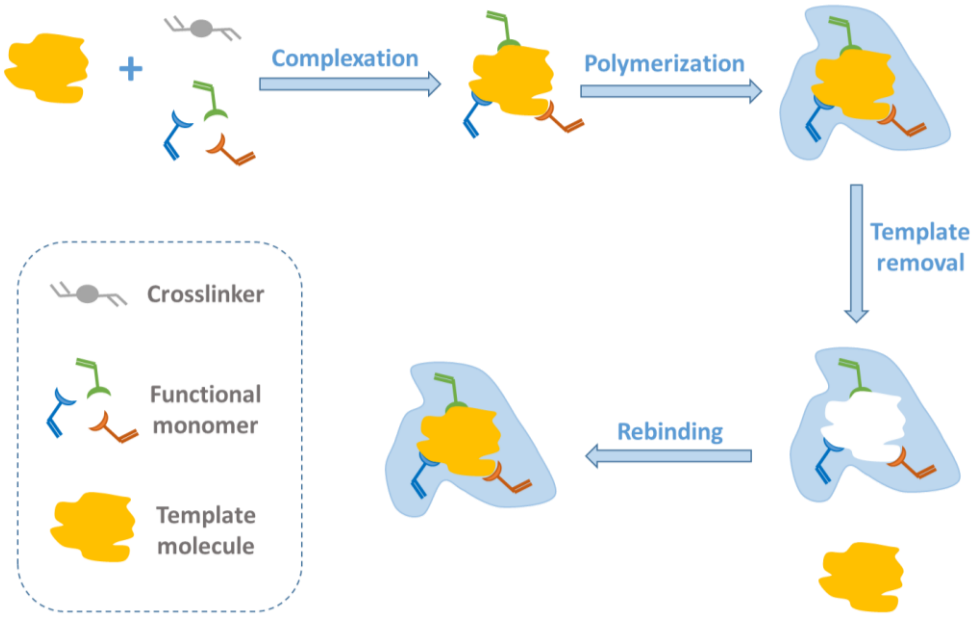

Figure **2.2**: Generic scheme of molecular imprinting process.

MIPs are rigid and three-dimensional materials synthesized around a certain molecule through covalent or non-covalent bonds. The recognition sites are obtained by pre-arrangement between target compound and selected monomers, followed by suitable polymerization procedures that lead to the formation of a rigid matrix. After removing the target molecule from the polymeric matrix, the recognition sites are exposed and display affinity for that specific target [55]. Thus, the resulting polymer recognizes and binds selectively to the template molecules. It should also be mentioned that a non-imprinted polymer (NIP) may be synthesized as control of the imprinting effect. It is obtained in the same way as the corresponding MIP, but in the absence of the template.

The target molecules in molecular imprinting processes are of diverse nature, yielding more or less difficult processes of molding. When the target molecule is a compound of low molecular weight, the imprinting process is relatively simple, with many papers demonstrating its success [56, 57]. In contrast, the imprinting of proteins (among which most PCa biomarkers are included) is still a field under development [58]. Proteins are a tricky material to carry out such tailoring processes, because they undergo conformational changes quite easily and have multiple charge locations varying with the specific conformation they exhibit. These critical points under the preparation of MIP may be avoided by using mild conditions, preferably close to those in the native environment of the protein. This includes room temperature polymerization procedures and use of compatible materials.

Among molecular imprinting techniques there are different approaches such as *in situ* polymerization, using either photochemical or thermal initiation, or surface grafting, with chemical or UV initiation, both in bulk or in surface approaches [59]. Each one has its own advantages and disadvantages. Bulk protein imprinting uses simple experimental procedures and is easy to achieve

but could suffer from poor protein extraction, slow binding kinetics, template entrapment and bleeding. Surface imprinting methods provides a controlled modification of the surface, template removal is much easier to achieve and non-specific binding is quite lower, however, the number of binding sites is highly reduced [55].

Summing all up, the suitable method should be carefully chosen taking into account which kind of template is under study. Nowadays, the most used and well succeeded method for imprinting proteins is surface imprinting, due to its higher binding capacity and faster mass transfer/binding kinetics than traditional bulk processes [55].

Previously to the studies presented herein, a biosensor was developed for SAR making use of bulk molecular-imprinted [60]. A solid-phase extraction was used and the MIP was prepared using methacrylic acid as functional monomer and a mixture of acetonitrile/water as porogenic agent. It was successfully used for the selective clean up and pre-concentration of SAR from real urine samples, although the presence of acetonitrile within this process may question the real shape of the imprinted protein.

But the most successful imprinting strategies for proteins employ surface imprinting [61, 62]. The overall process is shown in Figure 2.3. In this, the polymeric matrix is grown around the target protein that is immobilized on a nanostructure surface. The protein is extracted afterwards, in order to generate the specific rebinding sites close to the surface. These rebinding sites are more accessible than in bulk based approaches [61].

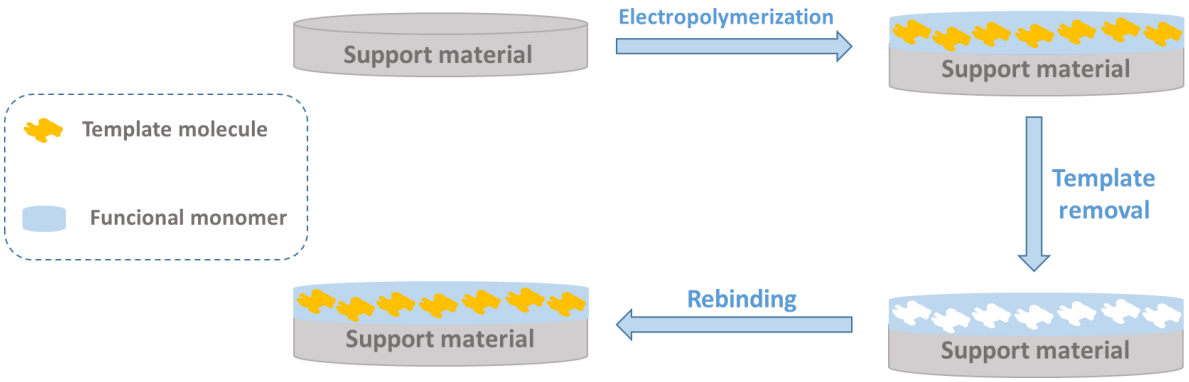

Figure **2.3**: Generic scheme of by electropolymerization.

Different techniques can be used to molecularly imprint the film into electrode surface, such as stamp-coating/micro-contact, polymer-brush imprinting, surface grafting and electropolymerization. Surface grafting and electropolymerization are of particular interest for proteins, as these turn out simple and successful processes for assembling a polymeric matrix around complex protein structures.

Surface grafting has emerged as a simple, useful, and versatile approach to improve surface properties of polymers and consists of the polymerization of monomers initiated from a solid surface bearing initiating functional sites, to give the polymers of which one chain ends covalently bonded to the solid surface [63]. This technique has advantages, when compared with in-bulk imprinting, including easy and controllable introduction of graft chains with a high density and exact localization. Furthermore, the process in which graft chains are covalent attached to the polymer surface avoid their delamination, and assure a long-term chemical stability of the chains, in contrast to physically coated polymer chains [64]. Surface grafting was also employed herein, to produce a successful sensing device for PSA.[65]. This work is described later, in chapter 3.

Electrochemical polymerization is a clean production method to generate raw monomer aggregates directly on the substrate, avoiding the use of volatile organic solvents or the need for physical/chemical initiator [66]. It is also a very useful technique since it allows the control of the rate of polymer nucleation and growth by the proper selection of the electropolymerization parameters. In addition the film thickness can be controlled by the amount of charge passed during film deposition, and the film morphology can be modified by suitable selection of an appropriate solvent and supporting electrolyte [67]. These factors are regarded to be very important in achieving the desired sensitivity of a sensor.

The preparation of MIP-based biosensors by electropolymerization processes has been shown a successful approach for the recognition and detection of complex template molecules [68-70]. It is a promising tool for the construction of simple design, high stability, rapid response and enhanced selectivity sensors devices [71]. Electrochemical polymerization is typically conducted by mixing the template and the monomer in solution and by applying the necessary electrical conditions to form a polymeric matrix directly on the transducer surface. Nevertheless, the monomer selection is crucial, leading to more or less conductive polymer layers [71], with different physical features. This technique was also employed along this work, aiming at the construction of biosensors for ANXA3 and MSMB. These works will be described in Chapter 4 and 5.

2.3.3.2 Enzyme

Enzymatic biosensors are a promising choice compared with traditional analytical methods, presenting several advantages such as high sensitivity and specificity for their substrates, portability, the possibilities of miniaturization and mass production and in some cases the sensors are re-used decreasing the cost of the detection process, they can be used for real-time diagnosis and monitoring of diseases (Figure 2.4). Thus, this is a valuable technique for qualitative and

quantitative analysis of a variety of target analytes in biomedicine, environmental, and food quality control, agricultural, and pharmaceutical industry and clinical sector [72].

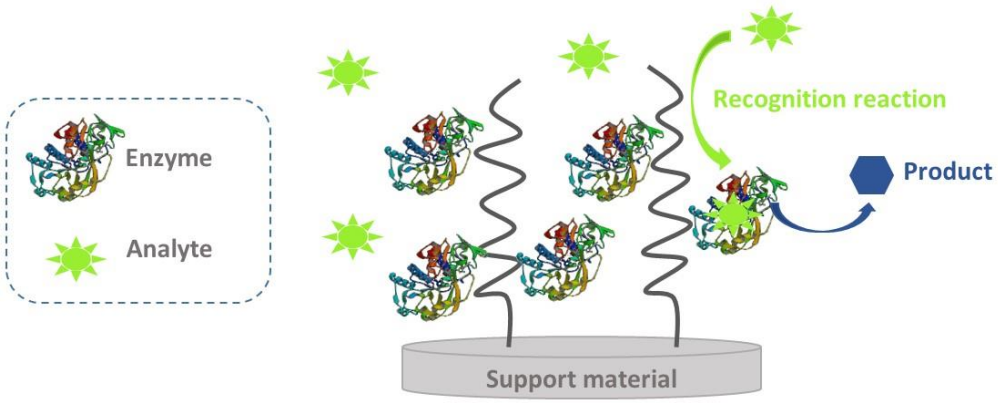

Figure **2.4**: Generic scheme of an enzymatic approach of biosensors.

Today, few enzyme biosensors are commercially available (e.g., sensors for monitoring blood glucose), while many are still under development. Although biosensors based on other (bio)recognition elements are rapidly progressing, enzyme biosensors are still one of the most frequently used in the biomedical field [73].

Usually the enzyme is immobilized on/within the surface of the transducer, and the effect created by the interaction of enzyme with the analyte is usually converted into an electrical signal. The immobilizing step has to be effective for the good performance of the biosensor. To reach accurate measurements, reproducible data and operational lifetimes, it is imperative that enzymes remain tightly bound to the surface. The immobilization step must lead to a stable binding of the enzyme, in order not be desorbed during the use of the biosensor, while holding the desired catalytic activity of the immobilized enzyme.

Since the sensitivity, selectivity and stability of a biosensor are strongly affected by the type of immobilization method used in the process – by influencing enzyme orientation, loading, mobility, stability, structure and biological activity –, intensive efforts have been done to develop successful immobilization strategies [74]. This includes adsorption, covalent, entrapment, cross-linking, and affinity or a combination of the previous approaches [75-77]. Each of these has advantages and disadvantages. The choice of the most appropriate technique depends on the enzyme nature, the transducer and the associated detection mode. The best method of enzyme immobilization can vary if the biosensor application requires maximum sensitivity or rather focuses on stability. Reproducibility, cost and difficulty of the immobilization process also need to be considered. Sensitivity decreases if immobilization causes enzyme denaturation or conformational changes or if the enzyme has been modified, especially on its active site. A better sensitivity is obtained with oriented immobilization of enzymes on the transducer surface which properly expose their active site to the solution phase [74].

Direct covalent coupling of enzymes onto the transducer surface is a popular chemical immobilization method used to develop enzymatic biosensors. In this, biocatalysts are bound to the surface through functional groups that they contain and are not essential for their catalytic activity. The binding of the enzymes to the solid support is generally carried out by initial activation of the surface using multifunctional reagents, followed by enzyme coupling to the activated support, and then the excess of unbound biomolecules is removed [74]. Covalent immobilization was also the approach used along this work to build a SAR biosensor [78]. The corresponding results are extensively discussed in chapter 6.

Conventional enzyme-based biosensing designs report mainly optical [45, 46, 79] and electrochemical [80-82] transduction systems. Recent advances in the

development of electrochemical and optical enzyme-based biosensors, in the last three to five years, provided information about its relevancy, specific applications and analytical performance in the biomedical field. New emerging technologies and innovative biosensing designs, such as nanosensors, paper based-sensors, lab-on-a-chip, biochips, and microfluidic devices are also reported in the literature employing enzyme-based sensing systems [72].

2.4 Transducers

Advances in transduction methods are closely linked with the development in areas such as electronics and computing. There is enough research into the basic principles of transduction to be able to build a large variety of commercial devices, and solve most of the problems associated with the transduction event. There are different types of transducers, depending on the physicochemical property (electron transfer, mass change, heat transfer). New horizons might be achieved by combining different transduction platforms (electrochemical/optical/mass sensitive) for enhanced data acquisition in biosensor applications [44].

In general, the choice of the transducer to be used depends on the analyte and the sample properties. For PCa biomarkers, different kinds of sensors have been reported in the literature, where the transducer is of electrochemical, optical or piezoelectric. These have been summarized in Table 2.1, highlighting the target biomarker, the (bio)recognition element, the transduction, the concentration levels and limit of detection (LOD).

Independently of the transduction platform, all methods reported in literature for the determination of the biomarkers under study are highly specific, since antibodies or enzymes were used as (bio)recognition element of the sensor devices.

As can be seen Table 2.1, various methodologies have been applied for the determination of biomarkers, including SPR, QCM, Elisa and electrochemical approaches, among others. In the case of PSA, the methods applied for the detection of the biomarker present similar concentration linear ranges, with the exception of SPR and piezoresistive micro-cantilever, in which the linear ranges and LODs obtained are higher. On the other hand, ELISA methods exhibit superior sensitivity performance for the detection of PSA, presenting lower concentration linear ranges and LODs.

Regarding the biomarkers ANXA3 and MSMB, no electrochemical methods were found in the literature reporting their determination. Within the methods shown in Table 2.1, QCM procedures allowed obtaining better LOD and linear concentration range for ANXA3. In the case of MSMB, the linear range obtained by the ELISA method is better than the others.

Within the existing methods in literature for the determination of SAR, the use of colorimetric method allowed to obtain a LOD of about one order of magnitude lower than the amperometric and fluorimetric detection methods. Although the colorimetric determination can be typically considered as a simple, inexpensive and sensitive methodology, the detection procedure is not suitable for quick analysis in the point-of-care, because it requires a reaction between specific chemicals with the biomarker under controlled temperature before reading. Overall, the electrochemical sensors are an attractive and important class of chemical sensors among the sensors used for the determination of PCa biomarkers.

Table **2.1**: Biosensors for PCa biomarkers with different transducers and their detection range reported in the literature.

Target Biomarker	(Bio)recognition element	Transduction platform	Response range (ng/mL)	LOD (ng/mL)	Reference
PSA	Antibody	Potentiometric	4.0–13	3.4	[9]
PSA	Antibody	Amperometric	4–10	0.4	[83]
PSA	Antibody	Amperometric (CV)	1–10	—	[84]
PSA	Antibody	SPR	—	100	[85]
PSA	Antibody	SPR	100–10000	—	[86]
PSA	Antibody	UV-Vis spectroscopy	5–8	4	[47]
PSA	Antibody	Fluorimetric	4–12.6	4	[87]
PSA	Antibody	Piezoresistive micro-cantilever	10–1000	—	[88]
PSA	Antibody	Piezoelectric	1.5–40	—	[89]
PSA	Antibody	QCM	2.3–150	4.7	[90]
PSA	Antibody	ELISA	0.12–25	0.1	[32]
PSA	Antibody	ELISA	0.9–60	0.4	[91]
ANXA3	Antibody	QCM	0.075–50	0.075	[92]

Table **2.1**: Biosensors for PCa biomarkers with different transducers and their detection range reported in the literature (cont.).

Target Biomarker	(Bio)recognition element	Transduction platform	Response range (ng/mL)	LOD (ng/mL)	Reference
ANXA3	Antibody	ELISA	2–18	—	[41]
ANXA3	Antibody	VIDAS® automated	1.5–100	—	[93]
MSMB	Antibody	ELISA	0.50–13.70	—	[23]
MSMB	Antibody	ELISA	0.50–22.8	—	[42]
MSMB	Antibody	AutoDelfia automatic	4.9–26	4.9	[22]
SAR	Enzyme	Colorimetric	0.89–4.45	0.45	[45]
SAR	Enzyme	Fluorimetric	2.05–151.8	1.78	[79]
SAR	Enzyme	Amperometric	89.1–356.4	—	[80]
SAR	Enzyme	Amperometric	10–250	2.5	[94]

These sensors have boosted the development of new diagnostic tools [95] displaying high sensitivity, specificity, and fast/accurate analysis. These sensors also offer experimental simplicity, low cost, portability allowing the possibility to carry out on-site analysis and adjust the technique to disposable devices. Such main features justify the selection of this kind of transduction by many authors.

The electrochemical transduction was selected in the context of this thesis and a brief description of the relevant electrochemical techniques employed herein is described then. .

2.4.1 Electrochemical

The general principle of electrochemical sensors is the electron flow between an electroactive species and an electrode surface (subjected to a pre-defined pattern fixed or variable potential). Such electron flow may be used both for qualitative and quantitative analysis, by means of direct or indirect reading of any chemical compound that is electroactive, i.e., it may be oxidized and/or reduced under the specified conditions. This technique may also be used to carry out fundamental studies such as, oxidation and reduction processes in various electrolytes, adsorption processes in different materials and electron transfer mechanisms at chemically modified electrode surfaces [96].

Electrochemical sensors can be classified taking into account the characteristics of the signal obtained by the transducer. Each type of electrochemical sensor is associated with various electrochemical techniques. According to the type of signal, which can be voltage, current or impedance changes, these sensors can be classified into three groups: potentiometric, amperometric and impedimetric, respectively [96-98].

2.4.1.1 Potentiometry

Potentiometry measures the potential difference between two electrodes (indicating and reference electrodes) immersed in a solution and its relationship to the activity of ionic species present in the same solution at near-zero current condition [99]. It is the electroanalytical technique with the widest response range, making use of the potential difference to quantity almost any chemical species of interest [98]. Such potential difference accounts the free energy change (ΔG) that would occur if the chemical phenomena were to proceed until the equilibrium condition had been satisfied. The correlation between free energy change and potential developed can be observed in equation 2.1,

$$\Delta G = -nFE \qquad \textbf{2.1}$$

where E is the maximum potential between two electrodes, F is the Faraday's constant (1F = 96,485 C mol^{-1}) and n is the number of electrons exchanged. For an electrochemical cell that contains an anode and a cathode, the potential of the electrochemical cell is the difference between the cathode electrode potential and the anode electrode potential. If the reaction is conducted under standard state conditions, this equation allows the calculation of the standard cell potential.

When the reaction conditions are not standard state, the Nernst equation – displayed in equation 2.2 – should be used to determine the cell potential,

$$E_{Cell} = E_0 - \frac{RT}{nF} LnK_{eq} \qquad \textbf{2.2}$$

in which, $E0$ is the cell potential at standard conditions, R is the universal gas constant (8.314 J/Kmol), T is the temperature in kelvin, n is the charge of the ion or number of electrons participating in the reaction and K_{eq} is the equilibrium constant.

If the potentiometric technique relies on ion-selective electrodes (ISEs), the potential difference is generated by the presence of ions at the selective membrane that is part of the indicating electrode. Thus, this specific potentiometric readings there are no explicit redox reactions, but an ion concentration gradient formed across the semi-permeable selective membrane [100, 101]. The observed potential difference is generated by the transfer of the ionized analyte across the interface between the sample and membrane phase. The interface of the inner side of the membrane may be a liquid or a solid-phase; the former yields lower detection limits but the latter is easier to handle among laboratory experiments. A schematic representation of the solid-state contact electrode is shown in Figure 2.5. This overall principal may be used for determination of almost any ionic species, including proteins.

ISEs provide a stable potential at the interface electrode/solution and have to be combined with a reference electrode to form an electrochemical cell. This need for a reference electrode comes from the inability to measure directly the potential of a single electrode. With the purpose of measuring the electromotive force (emf) of the cell, the working electrode immersed in the test solution is linked through a salt bridge, to the reference. The reference is made by an aqueous bridge electrolyte in contact with the sample solution via liquid junction. During all experiments, the potential of the reference electrode should be kept constant, stable and independent of the environmental conditions. The Ag/AgCl reference electrode is the most widely used due to its simplicity and inexpensive design. It is composed by a silver wire coated electrolytically with a thin layer of silver chloride. The wire is immersed in a known concentration solution of potassium chloride (KCl), saturated with AgCl [101].

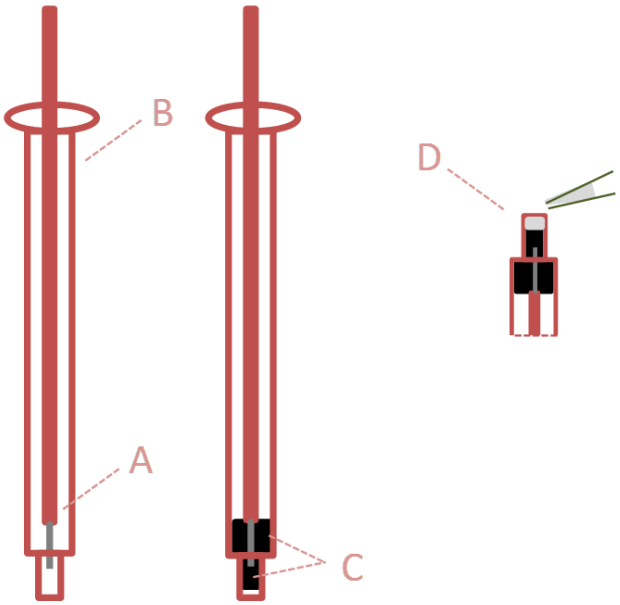

Figure **2.5**: Scheme of the ion-selective electrode construction of solid contact. **A**: copper electrical wire; **B**: syringe body; **C**: conductive carbon-based support material; **D**: casting of the selective membrane over the solid-contact.

Today, it is possible to find ISEs based on a small film or a selective membrane as recognition element and constructed with various configurations, ranging from an equivalent shape to a glass electrode, or a planar/tubular arrangement. The sensing surface is typically formed by incorporating a recognition element in a plasticized PVC matrix. One of the most important aspects in the development of an ISE is related to the electroactive material incorporated into the membrane, and ensures selective interaction with the analyte. This may be achieved by doping the membranes with MIPs.

Overall, the use of ISEs among screening procedures in biomedical context may offer several advantages. ISEs have fast responses, high precision and rapidity, low cost of analysis and enhanced selectivity [102]. The overall procedure is simple because the measures are targeted to a particular element. Typically, the

analysis is carried out over few milliliters of aqueous solvent, containing only the analyte and buffer/ionic strength adjuster. The analysis is also non-destructive, allowing subsequent reading(s) of other parameter(s) [103]. Thus, potentiometric-based electrochemical sensors were also developed along this work [65]. PSA was the target biomarker and the corresponding details may be found in chapter 3.

2.4.1.2 Amperometry

In amperometric measures the current intensity flows between two electrodes due to an electrolytic reaction. A reagent is the analyte under study and the measured current is proportional to its concentration [98]. The analyte, or the species involved with it via a (bio)chemical reaction, changes its oxidation state at one electrode. The electron flux is then monitored and is proportional to the amount of the species electrochemically transformed at the electrode [98]. The signal obtained from the transducer is presented in the form of current. The current intensity can be measured as a function of an applied potential (voltammetry), which can lead to lower detection limits. Several species in solution can be determined in the same experience if they react on the electrode surface at different potentials [104].

When an amperometric biosensor is used, the current varies upon the addition of a particular compound (e.g. a redox-enzyme substrate) to render a particular product that is electro-transformed at the electrode. The current change is proportional to the amount of electro-oxidized/reduced species, which in turn may be directly or inversely proportional to the analyte concentration, depending on the assay format [105].

The coupling of enzymes in amperometric electrodes permits the rapid, simple and direct determination of various metabolites and therapeutic drugs in

biological fluids. An enzyme electrode consists of a thin layer of an enzyme immobilized on the electrode surface. The enzyme is chosen to catalyze a reaction which generates a product or consumes a reactant which can be monitored amperometrically [106].

2.4.1.2.1 Voltammetry

Among the amperometric techniques, voltammetry includes the assays which involve disturbance of a system for applying a potential difference that varies over time, measuring the resulting current intensity. A resulting stream is comprised of two components: faradaic current (current due to oxidation-reduction reactions of the species under investigation) and the residual current. This residual current is due to a faradaic current generated by the presence of impurities in the electrodes. The electrode potential is controlled in relation to the potential of a reference electrode, which ideally preserves itself unchanged [107].

Voltammetry is widely used for chemical analytical purposes, not including fundamental studies of oxidation and reduction processes in several ways, adsorption processes on surfaces or electron transfer mechanisms chemically modified electrodes in surfaces [108].

Different voltammetric techniques can be defined according to the way the potential varies over time. Excitation due to the potential applied can origin different functions of potential-time, such as linear screening, triangular screening or pulse application [108]. The choice of a specific voltammetric technique is related to the type and quantitative and/or qualitative information to be obtained about the analyte or process, which involves the interaction between the analyte and the working electrode. Most of the approaches taken in the literature include cyclic voltammetry (CV) or square wave voltammetry (SWV), used along this study and resumed next.

2.4.1.2.1.1 Cyclic voltammetry

CV is the most widely used technique to get all the qualitative information about electrochemical reactions. This technique has the ability to rapidly provide thermodynamic information about redox processes, the kinetics of heterogeneous electron transfer reactions and also kinetic information of coupled chemical reactions or adsorptive processes. Particularly, CV allows the rapid detection of the oxidation-reduction potential of any electroactive species, and an evaluation of the effect of the medium composition in redox processes [98].

It consists in applying a linear potential (E) sweep at a steady scan-rate (the rate of potential change with time, $\nu=\Delta E/\Delta t$) to the working electrode (WE), leading to sequential linear potential increases and decreases between a minimum and a maximum potential limit. The CV plot obtained by this measurement is named voltammogram and depicts the resulting electrical current at the electrode surface (I) as a function of applied potential [98]. The application of this potential sweep is controlled by a reference electrode and has a triangular waveform when plotted against time, with minimum and maximum potential limits (E_{min} and E_{max}, respectively) established within the procedure (Figure 2.6).

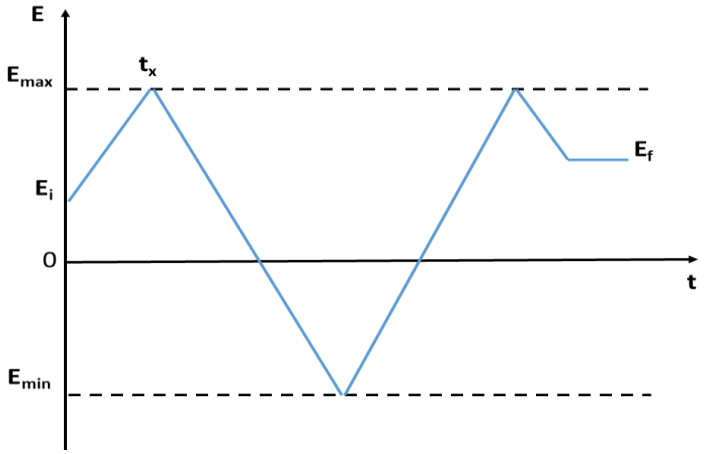

Figure **2.6**: Potential variation applied to the working electrode over time in CV: $\mathbf{E_i}$ – initial potential; $\mathbf{E_f}$ – final potential; $\mathbf{E_{min}}$ – minimum potential; $\mathbf{E_{max}}$ – maximum potential, $\mathbf{t_x}$ – time for the reverse scan.

The most important parameters in a voltammogram are the potentials of cathode and anode peak and the cathodic and anodic peak current intensities. As shown in Figure 2.7, the cathode potential scanning is followed by the anodic scanning, where the reduced species formed in the cathodic cycle can be oxidized according to the reverse reaction, yielding two peaks in the voltammogram. When the system is irreversible or quasi-reversible, the cathodic and anodic direction becomes not exactly reverse. Kinetic parameters can be inferred from the shape of the voltammograms [98].

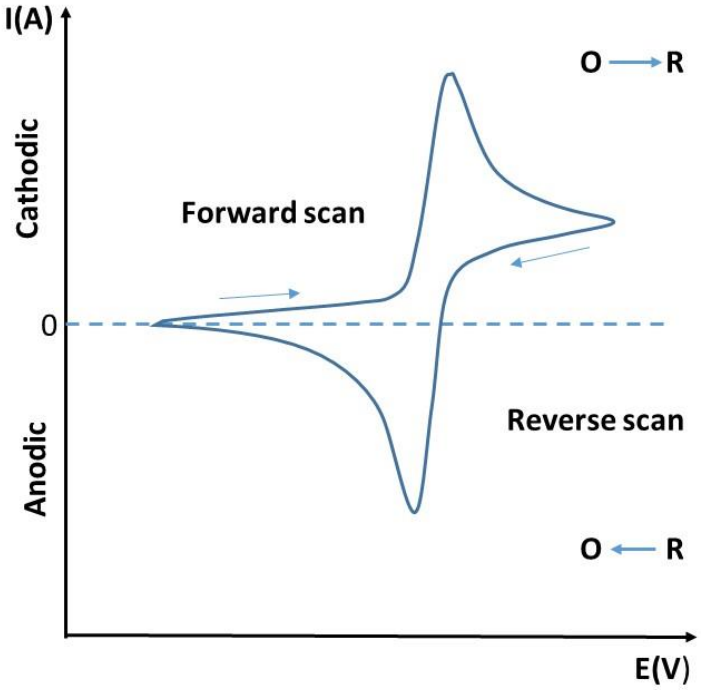

Figure **2.7**: Typical voltammogram for a reversible system.

2.4.1.2.1.2 Square wave voltammetry

The use of voltammetric techniques in the analysis of biological molecules is closely related to the development of more sensitive methods. SWV has been widely used for this end, being one of the most rapid and sensitive electrochemical techniques. The detection limits may be compared with the

chromatographic and spectroscopic techniques. Furthermore, the analysis of the characteristic parameters of this technique also enables kinetic and mechanistic evaluation of the electrode process.

In SWV, the excitation signal is obtained by overlapping the sequence pulses with a signal in the form of stairs. The current measurement is made two times in each cycle, in the end of the direct pulse and, the other, in the end of the reverse pulse [109]. The corresponding voltammogram shows the resulting current, i.e., the difference between the direct and reverse currents. The higher the reversibility of the reaction, the greater the contribution of the reverse current, significantly increasing the resulting current and, therefore, the response in terms of current intensity which can increase the sensitivity of the measurements [110], as seen in Figure 2.8.

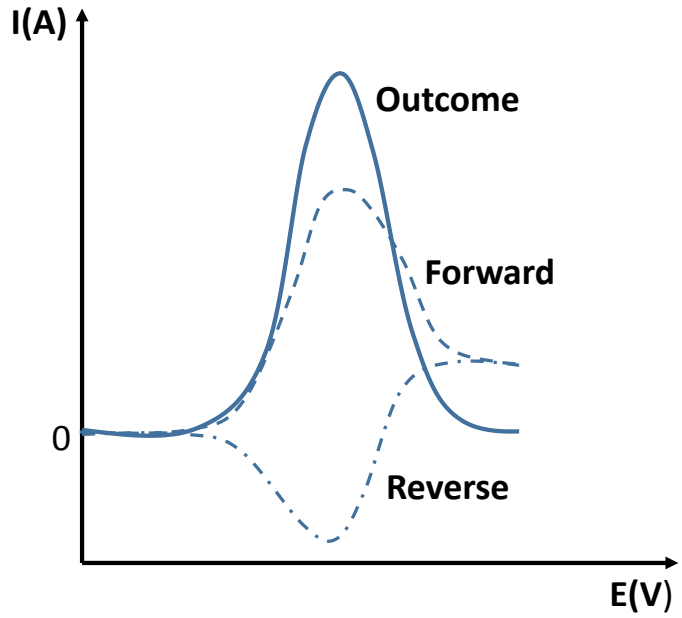

Figure **2.8**: Schematic square-wave voltammogram of a redox reversible process.

2.4.1.2.2 Chronoamperometry

Another pulse technique that involves amperometric techniques is the chronoamperometry. This technique consists in the study of current variation response as a function of time at a controlled potential - potential pulse. This pulse usually corresponds to the potential at which the current response is limited by mass transport, which is called faradaic current. A typical cronoamperogram has an initial peak current that matches the load of the double layer capacitive current in Figure 2.9. It is possible to see the evolution of capacitive current and faradaic by applying a potential pulse in chronoamperometry [98].

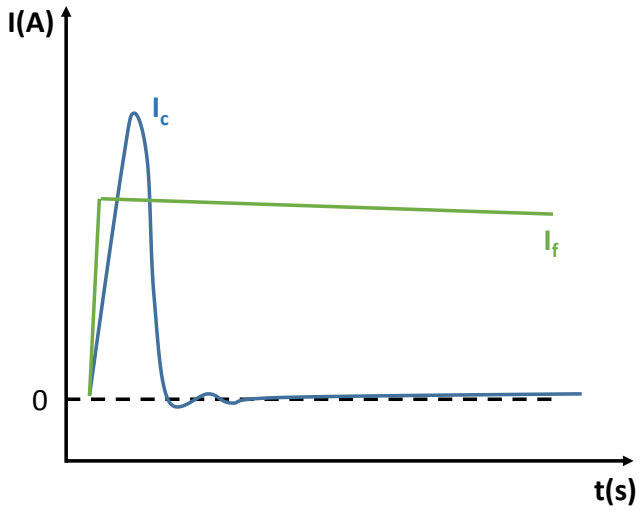

Figure **2.9**: Evolution of the current with time by applying a pulse potential to an electrode. In that I_f corresponds the faradaic current and I_c the capacitive current.

This technique was used in particular to electropolymerize CAF at electrode surface for the construction of ANXA3 and MSMB biosensor, described later in chapters 4 and 5.

2.4.1.3 Electrochemical impedance spectroscopy

The electrochemical impedance spectroscopy (EIS) allows one to obtain detailed information about the electrical characteristics of the interface between the electrode and the solution. It is used in various studies, ranging from the kinetic study of electrochemical processes up to the electron transport semiconductor devices [98].

This method involves the application of a small perturbation of the potential or current. The perturbation is a single sine wave with different frequencies. From the applied perturbation and the measured response, the magnitude of the impedance and phase shifts are determined [111] and the changes that occur at the electrodes are exhibited as the resistive or capacitive properties of materials, also called as impedance.

Impedance is calculated as the ratio of the system voltage (U) and the current (I), j is the imaginary component and ω is the angular frequency, generated by a frequency analyzer that is connected to a potentiostat (equation 2.3)[112].

$$Z(j\omega) = \frac{U(j\omega)}{I(j\omega)} = Z_{real}(\omega) + jZ_{imagine}(\omega) \qquad \textbf{2.3}$$

where $j = (-1)^{1/2}$, $\omega = 2\pi f$ (rad s^{-1}) and f is the frequency (Hz). Faradaic impedance is generally conducted in the presence of a redox probe.

From the measurements of impedance and phase angle it is possible to evaluate processes such as charge transfer, conductivity films, and capacity or diffusion coefficients. To enable the interpretation of data obtained, it is necessary to adjust the experimental results to an equivalent electrical circuit. The impedance will arise from the solution resistance (R_s), double layer capacitor (C_{dl}), charge transfer resistance (R_{ct}), and Warburg diffusion element (W) as depicted inset in

Figure 2.10. The combination of these elements is known as a Randles circuit [112].

In an impedance measurement, the typical Nyquist diagram obtained (Figure 2.10) has a semicircle segment, observed at high frequencies, which corresponds to electron-transfer limited process, and a straight-line segment that represents diffusion limited electron transfer process at low frequencies [113].

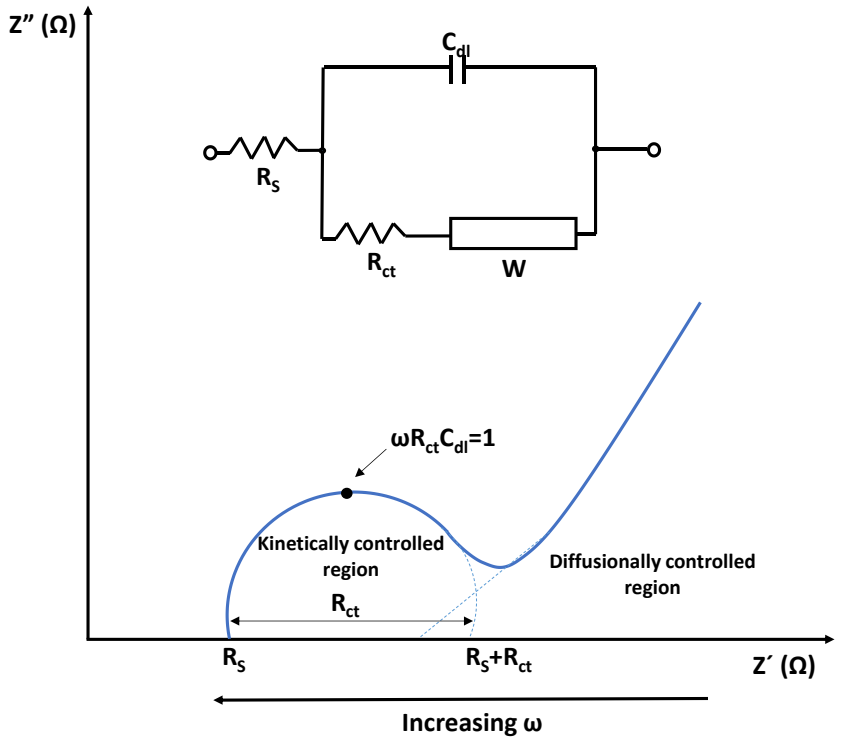

Figure **2.10**: Simple Randles equivalent circuit for an electrochemical cell. Reproduced from [112].

The elements obtained from Randles circuit, such as R_{ct} and capacitance, will depend on the dielectric and insulating features of the system. If the system under study is an interface electrode/solution, the immobilization steps taking place at the electrode surface will control the signal variations obtained in each stage of modification [113]. Thus, electrochemical impedance was employed herein mostly to follow the electrode surface modifications.

2.5 Final considerations

This chapter presented a brief review about PCa biomarkers and the existing methods and technologies applied to their quantification. A description of the recognition elements used in this work for biosensors design was presented. From all of them, synthetic materials, acting like natural antibodies, showed up as the logical choice. Still, new approaches are necessary in order to achieve the desired selectivity when compared to natural receptors. Several configurations of different electrochemical systems were also reviewed with emphasis to the desired biosensor characteristics. Of the different approaches described in this chapter, this thesis is focused on the design of combined systems of recognition elements and electrochemical transducers that can be suitable for point-of-care determination of PCa biomarkers.

2.6 References

[1] World Health Organization (WHO), www.who.int/mediacentre/factsheets/fs297/en, accessed in September 2010.

[2] W.G. Nelson, A.M. De Marzo, W.B. Isaacs, Prostate Cancer, *New England Journal of Medicine*, 349 (2003) 366-381.

[3] J. You, P. Cozzi, B. Walsh, M. Willcox, J. Kearsley, P. Russell, Y. Li, Innovative biomarkers for prostate cancer early diagnosis and progression, *Critical Reviews in Oncology Hematology*, 73 (2010) 10-22.

[4] V.M. Velonas, H.H. Woo, C.G. Remedios, S.J. Assinder, Current Status of Biomarkers for Prostate Cancer, *International Journal of Molecular Sciences*, 14 (2013) 11034-11060.

[5] N.C. Institute, NCI Dictionary of Cancer Terms, www.cancer.gov/dictionary?cdrid=45618, accessed in July 2010.

[6] P. Maruvada, W. Wang, P.D. Wagner, S. Srivastava, Biomarkers in molecular medicine: cancer detection and diagnosis, *BioTechniques*, 38 (2005) S9-S15.

[7] J.G. Huang, N. Campbell, S.L. Goldenberg, PSA and beyond: Biomarkers in prostate cancer, *BC Medical Journal*, 56 (2014) 334-341.

[8] S. Michel, G. Deléage, J.-P. Charrier, J. Passagot, N. Battail-Poirot, G. Sibai, M. Jolivet, C. Jolivet-Reynaud, Anti-Free Prostate-specific Antigen Monoclonal Antibody Epitopes Defined by Mimotopes and Molecular Modeling, *Clinical Chemistry*, 45 (1999) 638-650.

[9] Y. Liu, Electrochemical detection of pro state-specific antigen based on gold colloids/alumina derived sol-gel film, *Thin Solid Films*, 516 (2008) 1803-1808.

[10] I. Giusti, V. Dolo, Extracellular Vesicles in Prostate Cancer: New Future Clinical Strategies?, *BioMed Research International*, 2014 (2014) 14.

[11] J.C. Chen, C.L. Ho, H.W. Tsai, T.S. Tzai, H.S. Liu, N.H. Chow, W.H. Yang, H.L. Cheng, Immunohistochemical Detection of Prostate-specific Antigen Expression in Primary Urothelial Carcinoma of the Urinary Bladder, *Anticancer Research*, 28 (2008) 4149-4154.

[12] Z. Nosratollah, O. Habib, A. Behrangh, Association between steroid hormone receptors and PSA gene expression in breast cancer cell lines, *African Journal of Biotechnology*, 4 (2005) 1415-1420.

[13] M. Schostak, G.P. Schwall, S. Poznanovic, K. Groebe, M. Mueller, D. Messinger, K. Miller, H. Krause, A. Pelzer, W. Horninger, H. Klocker, J. Hennenlotter, S. Feyerabend, A. Stenzl, A. Schrattenholz, Annexin A3 in Urine: A Highly Specific Noninvasive Marker for Prostate Cancer Early Detection, *Journal of Urology*, 181 (2009) 343-353.

[14] W. Wozny, K. Schroer, G.P. Schwall, S. Poznanović, W. Stegmann, K. Dietz, H. Rogatsch, G. Schaefer, H. Huebl, H. Klocker, A. Schrattenholz, M.A. Cahill, Differential radioactive quantification of protein abundance ratios between benign and malignant prostate tissues: Cancer association of annexin A3, *Proteomics*, 7 (2007) 313-322.

[15] V. Gerke, C.E. Creutz, S.E. Moss, Annexins: linking Ca^{2+} signalling to membrane dynamics, *Nature Reviews Molecular Cell Biology*, 6 (2005) 449-461.

[16] E.T. Keller, J. Zhang, C.R. Cooper, P.C. Smith, L.K. McCauley, K.J. Pienta, R.S. Taichman, Prostate carcinoma skeletal metastases: cross-talk between tumor and bone, *Cancer and Metastasis Reviews*, 20 (2001) 333-349.

[17] T. Pisitkun, R.F. Shen, M.A. Knepper, Identification and proteomic profiling of exosomes in human urine, *Proceedings of the National Academy of Sciences of the United States of America*, 101 (2004) 13368-13373.

[18] N.E. Schartz, N. Chaput, F. Andre, L. Zitvogel, From the antigen-presenting cell to the antigen-presenting vesicle: the exosomes, *Current Opinion in Molecular Therapeutics*, 4 (2002) 372-381.

[19] G. Arienti, E. Carlini, C. Saccardi, C.A. Palmerini, Role of human prostasomes in the activation of spermatozoa, *Journal of Cellular and Molecular Medicine*, 8 (2004) 77-84.

[20] S.V. Garde, V.S. Basrur, L. Li, M.A. Finkelman, A. Krishan, L. Wellham, E. Ben-Josef, M. Haddad, J.D. Taylor, A.T. Porter, D.G. Tang, Prostate secretory protein (PSP94) suppresses the growth of androgen-independent prostate cancer cell line (PC3) and xenografts by inducing apoptosis, *The Prostate*, 38 (1999) 118-125.

[21] D. Wu, Y. Guo, A.F. Chambers, J.I. Izawa, J.L. Chin, J.W. Xuan, Serum bound forms of PSP94 (prostate secretory protein of 94 amino acids) in prostate cancer patients, *Journal of Cellular Biochemistry*, 76 (1999) 71-83.

[22] C. Valtonen-André, C. Sävblom, P. Fernlund, H. Lilja, A. Giwercman, Å. Lundwall, Beta-Microseminoprotein in Serum Correlates With the Levels in Seminal Plasma of Young, Healthy Males, *Journal of Andrology*, 29 (2008) 330-337.

[23] R.K. Nam, J.R. Reeves, A. Toi, H. Dulude, J. Trachtenberg, M. Emami, L. Daigneault, C. Panchal, L. Sugar, M.A.S. Jewett, S.A. Narod, A Novel Serum Marker, Total Prostate Secretory Protein of 94 Amino Acids, Improves Prostate Cancer Detection and Helps Identify High Grade Cancers at Diagnosis, *The Journal of Urology*, 175 (2006) 1291-1297.

[24] H.C. Whitaker, Z. Kote-Jarai, H. Ross-Adams, A.Y. Warren, J. Burge, A. George, E. Bancroft, S. Jhavar, D. Leongamornlert, M. Tymrakiewicz, E. Saunders, E. Page, A. Mitra, G. Mitchell, G.J. Lindeman, D.G. Evans, I. Blanco, C. Mercer, W.S. Rubinstein, V. Clowes, F. Douglas, S. Hodgson, L. Walker, A. Donaldson, L. Izatt, H. Dorkins, A. Male, K. Tucker, A. Stapleton, J. Lam, J. Kirk, H. Lilja, D. Easton, C. Cooper, R. Eeles, D.E. Neal, The rs10993994 Risk Allele for Prostate Cancer Results in Clinically Relevant Changes in Microseminoprotein-Beta Expression in Tissue and Urine, *Public Library of Science*, 5 (2010) e13363.

[25] C.A. Haiman, D.O. Stram, A.J. Vickers, L.R. Wilkens, K. Braun, C. Valtonen-André, M. Peltola, K. Pettersson, K.M. Waters, L.L. Marchand, L.N. Kolonel, B.E. Henderson, H. Lilja, Levels of Beta-Microseminoprotein in Blood and Risk of Prostate Cancer in Multiple Populations, *Journal of the National Cancer Institute*, 105 (2013) 237-243.

[26] H.C. Whitaker, A.Y. Warren, R. Eeles, Z. Kote-Jarai, D.E. Neal, The potential value of microseminoprotein-β as a prostate cancer biomarker and therapeutic target, *The Prostate*, 70 (2010) 333-340.

[27] H.J. Issaq, T.J. Waybright, T.D. Veenstra, Cancer biomarker discovery: Opportunities and pitfalls in analytical methods, *Electrophoresis*, 32 (2011) 967-975.

[28] N. Cernei, Z. Heger, J. Gumulec, O. Zitka, M. Masarik, P. Babula, T. Eckschlager, M. Stiborova, R. Kizek, V. Adam, Sarcosine as a Potential Prostate Cancer Biomarker—A Review, *International Journal of Molecular Sciences*, 14 (2013) 13893-13908.

[29] A. Sreekumar, L.M. Poisson, T.M. Rajendiran, A.P. Khan, Q. Cao, J. Yu, B. Laxman, R. Mehra, R.J. Lonigro, Y. Li, M.K. Nyati, A. Ahsan, S. Kalyana-Sundaram, B. Han, X. Cao, J. Byun, G.S. Omenn, D. Ghosh, S. Pennathur, D.C. Alexander, A. Berger, J.R. Shuster, J.T. Wei, S. Varambally, C. Beecher, A.M. Chinnaiyan, Metabolomic profiles delineate potential role for sarcosine in prostate cancer progression, *Nature*, 457 (2009) 910-914.

[30] S. Mukherjee, O. Cruz-Rodriguez, E. Bolton, J.A. Iniguez-Lluhi, The in vivo role of androgen receptor SUMOylation as revealed by androgen insensitivity syndrome and prostate cancer mutations targeting the proline/glycine residues of synergy control motifs, *Journal of Biological Chemistry*, 287 (2012) 31195-31206.

[31] N. Cernei, O. Zitka, M. Ryvolova, V. Adam, M. Masarik, J. Hubalek, R. Kizek, Spectrometric and Electrochemical Analysis of Sarcosine as a Potential Prostate Carcinoma Marker, *International Journal of Electrochemical Science*, 7 (2012) 4286-4301.

[32] B. Acevedo, Y. Perera, M. Ruiz, G. Rojas, J. Benítez, M. Ayala, J. Gavilondo, Development and validation of a quantitative ELISA for the measurement of PSA concentration, *Clinica Chimica Acta*, 317 (2002) 55-63.

[33] K. Ramachandran, C.G. Speer, S. Fiddy, I.M. Reis, R. Singal, Free circulating DNA as a biomarker of prostate cancer: comparison of quantitation methods, *Anticancer Research*, 33 (2013) 4521-4529.

[34] A.M. Hawkridge, D.C. Muddiman, Mass Spectrometry–Based Biomarker Discovery: Toward a Global Proteome Index of Individuality, *Annual Review of Analytical Chemistry*, 2 (2009) 265-277.

[35] F. Jentzmik, C. Stephan, M. Lein, K. Miller, B. Kamlage, B. Bethan, G. Kristiansen, K. Jung, Sarcosine in prostate cancer tissue is not a differential metabolite for prostate cancer aggressiveness and biochemical progression, *Journal of Urology*, 185 (2011) 706-711.

[36] X. Zang, C.M. Jones, T.Q. Long, M.E. Monge, M. Zhou, L.D. Walker, R. Mezencev, A. Gray, J.F. McDonald, F.M. Fernández, Feasibility of Detecting Prostate Cancer by Ultraperformance Liquid Chromatography–Mass Spectrometry Serum Metabolomics, *Journal of Proteome Research*, 13 (2014) 3444-3454.

[37] N.P. Sardesai, K. Kadimisetty, R. Faria, J.F. Rusling, A microfluidic electrochemiluminescent device for detecting cancer biomarker proteins, *Analytical and bioanalytical chemistry*, 405 (2013) 3831-3838.

[38] K.H.a.K. Mosbach, Molecularly Imprinted Polymers and Their Use in Biomimetic Sensors, *Chemical Reviews*, 100 (2000) 2495-2504.

[39] X. Pei, B. Zhang, J. Tang, B. Liu, W. Lai, D. Tang, Sandwich-type immunosensors and immunoassays exploiting nanostructure labels: A review, *Analytica Chimica Acta*, 758 (2013) 1-18.

[40] R. O'Kennedy, M. Byrne, C. O'Fagain, G. Berns, Experimental section: A Review of Enzyme-Immunoassay and a Description of a Competitive Enzyme-Linked Immunosorbent Assay for the Detection of Immunoglobulin Concentrations, *Biochemical Education*, 18 (1990) 136-140.

[41] J. Yin, X. Yan, X. Yao, Y. Zhang, Y. Shan, N. Mao, Y. Yang, L. Pan, Secretion of annexin A3 from ovarian cancer cells and its association with platinum resistance in ovarian cancer patients, *Journal of Cellular and Molecular Medicine*, 16 (2012) 337-348.

[42] J.R. Reeves, H. Dulude, C. Panchal, L. Daigneault, D.M. Ramnani, Prognostic Value of Prostate Secretory Protein of 94 Amino Acids and its

Binding Protein after Radical Prostatectomy, *Clinical Cancer Research*, 12 (2006) 6018-6022.

[43] A.P.F. Turner, Biosensors: sense and sensibility, *Chemical Society Reviews*, 42 (2013) 3184-3196.

[44] J. Kirsch, C. Siltanen, Q. Zhou, A. Revzin, A. Simonian, Biosensor technology: recent advances in threat agent detection and medicine, *Chemical Society Reviews*, 42 (2013) 8733-8768.

[45] J. Lan, W. Xu, Q. Wan, X. Zhang, J. Lin, J. Chen, J. Chen, Colorimetric determination of sarcosine in urine samples of prostatic carcinoma by mimic enzyme palladium nanoparticles, *Analytica Chimica Acta*, 825 (2014) 63-68.

[46] C.S. Pundir, N. Chauhan, G. Kumari, Vandana, Immobilization of *Arthrobacter* sarcosine oxidase onto alkylamine and arylamine glass and its application in serum sarcosine determination, *Indian Journal of Biotechnology*, 10 (2011) 219-223.

[47] H. Jans, K. Jans, P.J. Demeyer, K. Knez, T. Stakenborg, G. Maes, L. Lagae, A simple double-bead sandwich assay for protein detection in serum using UV-vis spectroscopy, *Talanta*, 83 (2011) 1580-1585.

[48] L. Su, L. Zou, C.C. Fong, W.L. Wong, F. Wei, K.Y. Wong, R.S.S. Wu, M. Yang, Detection of cancer biomarkers by piezoelectric biosensor using PZT ceramic resonator as the transducer, *Biosensors and Bioelectronics*, 46 (2013) 155-161.

[49] K.L. Zakian, A. Shukla-Dave, E. Ackerstaff, H. Hricak, J.A. Koutcher, 1H magnetic resonance spectroscopy of prostate cancer: biomarkers for tumor characterization, *Cancer Biomark*, 4 (2008) 263-276.

[50] N.J.O. Ronkainen, Stanley L., Nanomaterial-Based Electrochemical Immunosensors for Clinically Significant Biomarkers, *Materials*, 7 (2014) 4669-4709.

[51] B.V. Chikkaveeraiah, A. Bhirde, N.Y. Morgan, H.S. Eden, X. Chen, Electrochemical Immunosensors for Detection of Cancer Protein Biomarkers, *ACS nano*, 6 (2012) 6546-6561.

[52] J.F. Rusling, G. Sotzing, F. Papadimitrakopoulosa, Designing nanomaterial-enhanced electrochemical immunosensors for cancer biomarker proteins, *Bioelectrochemistry*, 76 (2009) 189-194.

[53] D.A. Healy, C.J. Hayes, P. Leonard, L. McKenna, R. O'Kennedy, Biosensor developments: application to prostate-specific antigen detection, *Trends in Biotechnology*, 25 (2007) 125-131.

[54] G. Vasapollo, R. Del Sole, L. Mergola, M.R. Lazzoi, A. Scardino, S. Scorrano, G. Mele, Molecularly Imprinted Polymers: Present and Future Prospective International, *Journal of Molecular Sciences*, 12 (2011) 15908-15945.

[55] F.T.C. Moreira, R.A.F. Dutra, J.P.C. Noronha, A.E.G. Cass, M.G.F. Sales, Smart Plastic Antibody Material (SPAM) tailored on disposable screen printed electrodes for protein recognition: application to Myoglobin detection, *Biosensors and Bioelectronics*, 45 (2013) 237-244.

[56] N. Maier, W. Lindner, Chiral recognition applications of molecularly imprinted polymers: a critical review, *Analytical and Bioanalytical Chemistry*, 389 (2007) 377-397.

[57] L. Chen, S. Xu, J. Li, Recent advances in molecular imprinting technology: current status, challenges and highlighted applications, *Chemical Society Reviews*, 40 (2011) 2922-2942.

[58] E. Verheyen, J.P. Schillemans, M.V. Wijk, M.A. Demeniex, W.E. Hennink, C.F.V. Nostrum, Challenges for the effective molecular imprinting of proteins, *Biomaterials*, 32 (2011) 3008-3020.

[59] M.J. Whitcombe, I. Chianella, L. Larcombe, S.A. Piletsky, J. Noble, R. Porter, A. Horgan, The rational development of molecularly imprinted polymer-based sensors for protein detection, *Chemical Society Reviews*, 40 (2011) 1547-1571.

[60] H. Hashemi-Moghaddam, M. Rahimian, B. Niromand, Molecularly Imprinted Polymers for Solid-Phase Extraction of Sarcosine as Prostate Cancer Biomarker from Human Urine, *Bulletin of the Korean Chemical Society*, 34 (2013) 2330-2334.

[61] N.W. Turner, C.W. Jeans, K.R. Brain, C.J. Allender, V. Hlady, D.W. Britt, From 3D to 2D: A Review of the Molecular Imprinting of Proteins, *Biotechnology Progress*, 22 (2006) 1474-1489.

[62] C. Tan, Y. Tong, Molecularly imprinted beads by surface imprinting, *Analytical and Bioanalytical Chemistry*, 389 (2007) 369-376.

[63] M. Kobayashi, Graft Polymerization from Surface, in: S.M. Kobayashi, Klaus (Ed.) Encyclopedia of Polymeric Nanomaterials, (2014) 1-9.

[64] K. Kato, E. Uchida, E.-T. Kang, Y. Uyama, Y. Ikada, Polymer surface with graft chains, *Progress in Polymer Science*, 28 (2003) 209-259.

[65] T.S.C.R. Rebelo, C. Santos, J. Costa-Rodrigues, M.H. Fernandes, J.P. Noronha, M.G.F. Sales, Novel Prostate Specific Antigen plastic antibody designed with charged binding sites for an improved protein binding and its application in a biosensor of potentiometric transduction, *Electrochimica Acta*, 132 (2014) 142-150.

[66] F.T.C. Moreira, S. Sharma, R.A.F. Dutra, J.P.C. Noronha, A.E.G. Cass, M.G.F. Sales, Protein-responsive polymers for point-of-care detection of cardiac biomarker, *Sensors and Actuators B*: Chemical, 196 (2014) 123-132.

[67] P.S. Sharma, A. Pietrzyk-Le, F. D'Souza, W. Kutner, Electrochemically synthesized polymers in molecular imprinting for chemical sensing, *Analytical and Bioanalytical Chemistry*, 10 (2012) 3177-3204.

[68] A. Ramanaviciene, A. Ramanavicius, Molecularly imprinted polypyrrole-based synthetic receptor for direct detection of bovine leukemia virus glycoproteins, *Biosensors and Bioelectronics*, 20 (2004) 1076-1082.

[69] X. Kan, Z. Xing, A. Zhu, Z. Zhao, G. Xu, C. Li, H. Zhou, Molecularly imprinted polymers based electrochemical sensor for bovine hemoglobin recognition, *Sensors and Actuators B: Chemical*, 168 (2012) 395-401.

[70] M.R. Subrayal, S. Giulia, P. Quan, Electrochemical probing of selective haemoglobin binding in hydrogel-based molecularly imprinted polymers, *Electrochimica Acta*, 56 (2011) 9203-9208.

[71] X. Qin, H. Xiao-Ya, H. Shi-Rong, Electrochemical sensors based on electropolymerized films, in: E. Schab-Balcerzak (Ed.) Electropolymerization, (2011) 226.

[72] C.R. Ispas, G. Crivat, S. Andreescu, Review: Recent Developments in Enzyme-Based Biosensors for Biomedical Analysis, *Analytical Letters*, 45 (2012) 168-186.

[73] G.S. Wilson, Y. Hu, Enzyme-based biosensors for in vivo measurements, *Chemical Reviews*, 100 (2000) 2693-2704.

[74] A. Sassolas, L.J. Blum, B.D. Leca-Bouvier, Immobilization strategies to develop enzymatic biosensors, *Biotechnology Advances*, 30 (2012) 489-511.

[75] S. Andreescu, J.L. Marty, Twenty years research in cholinesterase biosensors: From basic research to practical applications, *Biomolecular Engineering*, 23 (2006) 1-15.

[76] S.K. Arya, M. Datta, B.D. Malhotra, Recent advances in cholesterol biosensor, *Biosensors and Bioelectronics*, 23 (2008) 1083-1100.

[77] M.M.F. Choi, Progress in Enzyme-Based Biosensors Using Optical Transducers, *Microchimica Acta*, 148 (2004) 107-132.

[78] T.S.C.R. Rebelo, C.M. Pereira, M.G.F. Sales, J.P. Noronha, J. Costa-Rodrigues, F. Silva, M.H. Fernandes, Sarcosine oxidase composite screen-printed electrode for sarcosine determination in biological samples, *Analytica Chimica Acta*, 850 (2014) 26-32.

[79] C. Burton, S. Gamagedara, Y. Ma, A novel enzymatic technique for determination of sarcosine in urine samples, *Analytical Methods*, 4 (2012) 141-146.

[80] A. Ramanavicius, Amperometric biosensor for the determination of creatine, *Analytical and Bioanalytical Chemistry*, 387 (2007) 1899-1906.

[81] S. Yadav, R. Devi, P. Bhar, S. Singhla, C.S. Pundir, Immobilization of creatininase, creatinase and sarcosine oxidase on iron oxide nanoparticles/chitosan-g-polyaniline modified Pt electrode for detection of creatinine, *Enzyme and Microbial Technology*, 50 (2012) 247-254.

[82] C.H. Chen, M.S. Lin, A novel structural specific creatinine sensing scheme for the determination of the urine creatinine, *Biosensors and Bioelectronics*, 31 (2012) 90-94.

[83] X. Yu, B. Munge, V. Patel, G. Jensen, A. Bhirde, J.D. Gong, S.N. Kim, J. Gillespie, J.S. Gutkind, F. Papadimitrakopoulos, J.F. Rusling, Carbon Nanotube Amplification Strategies for Highly Sensitive Immunodetection of Cancer Biomarkers, *Journal of the American Chemical Society*, 128 (2006) 11199-11205.

[84] V. Escamilla-Gomez, D. Hernandez-Santos, M. Begona Gonzalez-Garcia, J. Manuel Pingarron-Carrazon, A. Costa-Garcia, Simultaneous detection of free and total prostate specific antigen on a screen-printed electrochemical dual sensor, *Biosensors and Bioelectronics*, 24 (2009) 2678-2683.

[85] J.W. Cho, D.Y. Kang, Y.H. Jang, H.H. Kim, J. Min, B.K. Oh, Ultra-sensitive surface plasmon resonance based immunosensor for prostate-specific antigen using gold nanoparticle-antibody complex, *Colloids and Surfaces A: Physicochemical and Engineering Aspects*, 313 (2008) 655-659.

[86] H.S. Jang, K.N. Park, C.D. Kang, J.P. Kim, S.J. Sim, K.S. Lee, Optical fiber SPR biosensor with sandwich assay for the detection of prostate specific antigen, *Optics Communications*, 282 (2009) 2827-2830.

[87] X. Wang, M. Zhao, D.D. Nolte, T.L. Ratliff, Prostate specific antigen detection in patient sera by fluorescence-free BioCD protein array, *Biosensors and Bioelectronics*, 26 (2011) 1871-1875.

[88] K.W. Wee, G.Y. Kang, J. Park, J.Y. Kang, D.S. Yoon, J.H. Park, T.S. Kim, Novel electrical detection of label-free disease marker proteins using piezoresistive self-sensing micro-cantilevers, *Biosensors and Bioelectronics*, 20 (2005) 1932-1938.

[89] B. Zhang, X. Zhang, H.H. Yan, S.J. Xu, D.H. Tang, W.L. Fu, A novel multi-array immunoassay device for tumor markers based on insert-plug model of piezoelectric immunosensor, *Biosensors and Bioelectronics*, 23 (2007) 19-25.

[90] Y. Uludag, I.E. Tothill, Development of a sensitive detection method of cancer biomarkers in human serum (75%) using a quartz crystal microbalance sensor and nanoparticles amplification system, *Talanta*, 82 (2010) 277-282.

[91] A.I. Barbosa, P. Gehlot, K. Sidapra, A.D. Edwards, N.M. Reis, Portable smartphone quantitation of prostate specific antigen (PSA) in a fluoropolymer microfluidic device, *Biosensors and Bioelectronics*, 70 (2015) 5-14.

[92] Y.J. Kim, M.M. Rahman, J.J. Lee, Ultrasensitive and label-free detection of annexin A3 based on quartz crystal microbalance, *Sensors and Actuators B: Chemical*, 177 (2013) 172-177.

[93] C. Hamelin-Peyron, V. Vlaeminck-Guillem, H. Haidous, G.P. Schwall, S. Poznanovic, E. Gorius-Gallet, S. Michel, A. Larue, M. Guillotte, A. Ruffion, G. Choquet-Kastylevsky, Y. Ataman-Onal, Prostate cancer biomarker annexin A3 detected in urines obtained following digital rectal examination presents antigenic variability, *Clinical Biochemistry*, 47 (2014) 901-908.

[94] P. Kotzian, N.W. Beyene, L.F. Llano, H. Moderegger, P. Tunón-Blanco, K. Kalcher, K. Vytras, Amperometric determination of sarcosine with sarcosine oxidase entrapped with nafion on manganese dioxide-modified screen-printed electrodes, *Scientific papers of the University of Pardubice. Serie A, Faculty of Chemical Technology*, 8 (2002) 93-101.

[95] M.U. Ahmed, M.M. Hossain, E. Tamiya, Electrochemical Biosensors for Medical and Food Applications, *Electroanalysis*, 20 (2008) 616-626.

[96] C. Mousty, Sensors and biosensors based on clay-modified electrodes—new trends, *Applied Clay Science*, 27 (2004) 159-177.

[97] Z. Samec, E. Samcová, H.H. Girault, Ion amperometry at the interface between two immiscible electrolyte solutions in view of realizing the amperometric ion-selective electrode, *Talanta*, 63 (2004) 21-32.

[98] A.M.O. Brett, C.M.A. Brett, Electrochemistry principles, methods and applications, (1996).

[99] S. Amemiya, Potentiometric Ion-Selective Electrodes, Chapter 7, Elsevier (2007).

[100] R.P. Buck, E. Lindner, Recommendations for nomenclature of ion-selective electrodes (IUPAC Recommendations 1994), *Pure and Applied Chemistry*, 66 (1994) 2527-2536.

[101] M. Ciobanu, J.P. Wilburn, M.L. Krim, D.E. Cliffel, Fundamentals, in: C.G. Zoski (Ed.) Handbook of Electrochemistry, Elsevier (2007) 1-28.

[102] V.V. Cosofret, R.P. Buck, Recent Advances in Pharmaceutical Analysis with Potentiometric Membrane Sensors, *Critical Reviews in Analytical Chemistry*, 24 (1993) 1-58.

[103] T.S.C.R. Rebelo, S.A.A. Almeida, J.R.L. Guerreiro, M.C.B.S.M. Montenegro, M.G.F. Sales, Trimethoprim-selective electrodes with molecularly imprinted polymers acting as ionophores and potentiometric transduction on graphite solid-contact, *Microchemical Journal*, 98 (2011) 21-28.

[104] A.J. Bard, G. Inzelt, F. Scholz, Electrochemical Dictionary, 2 ed., Springer (2012).

[105] M.S. Belluzo, M.E. Ribone, C.M. Lagier, Assembling Amperometric Biosensors for Clinical Diagnostics, *Sensors*, 8 (2008) 1366-1399.

[106] J. Wang, Amperometric biosensors for clinical and therapeutic drug monitoring: a review, *Journal of Pharmaceutical and Biomedical Analysis*, 19 (1999) 47-53.

[107] D.C. Harris, Quantitative Chemical Analysis, 7 ed., W.H. Freeman and Campany, (2007).

[108] A.D. Skoog, D.M. West, F.J. Holler, S.R. Crouch, Fundamentos de Química Analítica, 8 ed., Thomson, (2007).

[109] A.J. Bard, L.R. Faulkner, Electrochemical Methods - Fundamentals and Applications, 2 ed., John Wiley & Sons, (2001).

[110] D. Souza, L. Codognoto, A.R. Malagutti, R.A. Toledo, V.A. Pedrosa, R.T.S. Oliveira, L.H. Mazo, L.A. Avaca, S.A.S. Machad, Voltametria de onda quadrada. segunda parte: Aplicações, Química Nova, (2004) 790-797.

[111] M. Ates, Review study of electrochemical impedance spectroscopy and equivalent electrical circuits of conducting polymers on carbon surfaces, *Progress in Organic Coatings*, 71 (2011) 1-10.

[112] E.P. Randviir, C.E. Banks, Electrochemical impedance spectroscopy: an overview of bioanalytical applications, *Analytical Methods*, 5 (2013) 1098-1115.

[113] M.A. Panagopoulou, D.V. Stergiou, I.G. Roussis, M.I. Prodromidis, Impedimetric biosensor for the assessment of the clotting activity of rennet, *Analytical Chemistry*, 82 (2010) 8629-8636.

3

Prostate Specific Antigen electrochemical sensor

Publication resulted from the work developed:

Electrochimica Acta

Volume 132, 20 June 2014, Pages 142–150

Novel Prostate Specific Antigen plastic antibody designed with charged binding sites for an improved protein binding and its application in a biosensor of potentiometric transduction

Tânia S.C.R. Rebelo[a, b, c], C. Santos[d, e], J. Costa-Rodrigues[c, f], M.H. Fernandes[c, f], João P. Noronha[b], M. Goreti F. Sales[a]

[a] BioMark/ISEP, School of Engineering of the Polytechnic Institute of Porto, Porto, Portugal
[b] REQUIMTE/FCT, Faculdade de Ciências e Tecnologia da Universidade Nova de Lisboa, Lisboa, Portugal
[c] Laboratory for Bone Metabolism and Regeneration, Faculty of Dental Medicine, University of Porto, Porto, Portugal
[d] Department of Mechanic Engineering, EST Setúbal, Instituto Politécnico de Setúbal, Campus do IPS, Setúbal, Portugal
[e] Technical University of Lisbon, IST, ICEMS, Lisboa, Portugal
[f] MedInUP - Center for Drug Discovery and Innovative Medicines, University of Porto, Porto, Portugal

3.1 Introduction

Until now, PSA biosensors have employed natural-based materials as (bio)recognition element. As explained in chapter 2, the final device could benefit from using synthetic materials instead of naturally-derived species, due to their simple production, low cost and long stability. This could be achieved by

producing artificial antibodies, which in the case of PSA would be named plastic antibodies.

Protein plastic antibodies are typically PIM, obtained by surface imprinting procedures [1]. In this, the polymeric matrix is grown around the protein and the protein extracted afterwards from it, in order to generate the binding site [2].

However, proteins are a complex material to carry out such tailoring processes successfully. These biomolecules may undergo conformational changes quite easily and have multiple charge locations, varying with the specific conformation they exhibit. These critical points under the preparation of PIM may be avoided by using mild conditions, preferably close to those in the native environment of the protein. This includes room temperature polymerization procedures and use of compatible materials. In addition, a way to improve protein binding to the synthetic material is to label the binding site with charged monomers. This procedure was found successful on the preparation of PIM [1], but the effect of the charged labels on this binding site is yet to be proven.

In addition, a biosensor device integrating PIM for PSA detection should be coupled to simple and low cost procedures/apparatus, such as those of the potentiometric kind, one approach that has been proven successful previously [3]. Potentiometric sensors offer the advantage of selectivity, simplicity, being of good overall precision and accuracy [4]. The corresponding devices may be of very low cost when assembled with disposable syringe bodies or micropipette tips. This last approach has only been recently tested for an organic compound [5], and never been applied to monitor complex target analytes, such as proteins.

Considering that the PIM material will be integrated in a biosensor device of electrical nature, it is reasonable to expect that it should be assembled on a compatible and low cost material support of good overall electrical performance.

So, the surface imprinting was made on graphene sheets, a 2D structure of special electrical features and low electrical noise [6]. Its large surface area is also expected to provide high rebinding capacity to the final PIM structure. Protein molecules will be located at the surface of the graphene sheets with high surface-to-volume ratio, thus generating an improved kinetics and accessibility to the generated binding sites and an extended template removal [7]. These features correlated to an improved accessibility of the target species to the binding site, as well as reduced binding times [8]. The use of graphene as support for protein imprint was only most recently reported [9].

Thus, the present work proposes a novel PIM for PSA, supported by graphene and displaying charged labels on the binding site. Two different control materials were also prepared, producing a non-imprinted material (NIM) including charged (C/NIM) or only neutral monomers (N/NIM) around the protein to be imprinted. These materials were used to check the contribution of the polymer chemistry upon the non-specific rebinding of the protein and if the charged label position would enhance the rebinding of the material towards the protein. All the prepared materials were used as ionophores in membranes of conventional solid-contact carbon electrodes and the resulting biosensors evaluated in terms of binding features, calibration slopes, dynamic linear range, limit of detection, effect of pH and selectivity. The best membrane composition was used to prepare micropipette tip-based electrodes of very low detection limit and to analyse serum samples.

3.2 Experimental

3.2.1 Reagents and solutions

De-ionized water (conductivity <0.054 μS/cm at 25 ºC) was employed. All chemicals were of analytical grade and used without further purification.

Graphite (nanopowder <500 nm and mean pore size of 137 Å), potassium permanganate, sulphuric acid 95-97%, hydrogen peroxide 30%, hydrochloric acid 37%, sodium chloride and sodium hydrogen carbonate were obtained from Merck. Human PSA, *N*-ethyl-*N*-(3-dimethylaminopropyl) carbodiimide hydrochloride (EDAC), 4-(2-hydroxyethyl)-1-piperazineethanesulfonic acid (Hepes), trypsin, 2-Aminoethyl methacrylate hydrochloride 90% (AMH), vinyl benzoate (VB), acrylamide (AA), *N*,*N*-methylenebis(acrylamide) (NMAA), creatinine, human hemoglobin, bovine serum albumin (BSA), urea and glucose were obtained from Sigma–Aldrich. Potassium nitrate, benzoyl peroxide (BOP) and tetrahydrofuran (THF) were obtained from Riedel–deHäen. *o*-Nitrophenyloctyl ether (oNPOE), poly(vinylchloride) (PVC) of high molecular weight, and *N*-hydroxysuccinimide (NHS) were obtained from Fluka, and (vinylbenzyl)trimethylammonium chloride 97% (VTA) was purchased to Acros Organics.

Stock solutions of PSA 2.5×10^{4} ng/mL were prepared in Hepes $1\text{x}10^{-4}$ mol/L (pH ~5.2) and less concentrated standard solutions were prepared by suitable dilution in the same buffer. The effect of pH was studied by changing the pH of a 50 mL PSA solution 7 ng/mL. The pH alteration was achieved by little additions of either concentrated hydrochloric acid or saturated sodium hydroxide solution, freshly prepared. Selectivity studies used creatinine (130 mg/L), urea (1900 mg/L), glucose (10.5 g/L), human hemoglobin (150 g/L) and BSA (50 g/L) solutions, prepared in Hepes buffer.

Artificial serum solution was prepared with the following composition: sodium chloride (7.01 g/L), sodium hydrogen carbonate (1.68 g/L) and BSA (30 g/L) [10].

3.2.2 Apparatus

All potentiometric measurements were made in a Crison pH-meter GLP 21 (±0.1 mV sensitivity). The simultaneous reading of multiple potentiometric devices was enabled by a home-made commutation unit with six ways out. The assembly of the potentiometric cell using the solid-contact support was as follows: conductive graphite | PSA selective membrane | buffered solution (Hepes buffer 1×10^{-4} mol/L, pH 5.2, or artificial serum, pH 7.3) || electrolyte solution, KCl |AgCl(s) | Ag. The reference electrode was an Ag/AgCl electrode of double-junction from Crison 5240.

The pH of solutions was measured by a Crison GLP 21 combined glass electrode connected to the above pH meter. An SBS vortex, MVOR 03, was used to grant a good mixing of the reacting solutions. Insoluble materials were suspended in a Sonorex digitec sonicator.

The chemical changes imposed to the materials were controlled by Fourier Transformed Infrared (FTIR) spectra, in Nicolet 6700 FTIR spectrometer coupled to an Attenuated Total Reflectance (ATR) sampling accessory of diamond contact crystal, also from Nicolet. Transmission electron microscopy (TEM) analysis was also conducted over the same materials, in a Hitachi H-9000 AT, operated at 200 kV. Raman spectroscopy studies were also conducted, using a LabRam 300 Jobin Yvon spectrometer, equipped with laser of 50 mW power, operating at 532 nm.

3.2.3 Preparation of graphene oxide

Graphene oxide (GO) was obtained from graphite powder by following the method of Hummers and Offeman [11], and its subsequent modifications described by Shenguang *et al*. [12]. Briefly, 2.0 g of graphite powder, 2.0 g of KNO_3 and 6.0 g of $KMnO_4$ were slowly added to 40 mL of concentrated H_2SO_4 under vigorous stirring at 0 °C. The mixture was then stirred continuously for 1

h, at ambient temperature. After that, 160 mL of water was added to the mixture and the temperature was increased up to 95 °C. The suspension was maintained at this temperature for 15 min and then poured into 240 mL of ultrapure water. After, ~16 mL of H_2O_2 was added into the suspension. The suspension was immediately cooled to room temperature and the solid products were filtered, washed with 5% HCl aqueous solution and water, and dried. The obtained solid was finally dispersed in water to yield a yellow-brown suspension (1 mg/mL). This GO suspension was ultrasonicated for 10 min and then centrifuged for 5 min to remove the unexfoliated graphite oxide particles from it.

3.2.4 Synthesis of protein imprinted material

The overall scheme of synthesis may be found in Figure 3.1. About 80 mL of 1 mg/mL GO solution was mixed with 56 mL of a 50 mg/mL NHS aqueous solution. This solution was placed under continuous magnetic stirring and then 17.2 mL of fresh EDAC aqueous solution (10 mg/mL) were added. This mixture was continuously stirred at room temperature for 30 min. The colloidal GO so obtained started to flocculate and was removed from the solution by filtration, washed with a 1×10^{-4} mol/L Hepes buffer, and allowed to dry in a desiccator under nitrogen atmosphere.

For the preparation of PIM materials, about 1.5 mg of the previous solid was immersed in 50 μL of a 2.5×10^{4} ng/mL PSA solution in Hepes buffer for protein binding. NIM materials were prepared in parallel by replacing the previous PSA solution by only Hepes buffer. Each resulting mixture was continuously stirred at room temperature for 4h, and the solid was separated and washed with Hepes buffer 1×10^{-4} mol/L. Then, 100 μL of a 0.1 g/mL AMH solution prepared in Hepes buffer was added to the solid. The obtained suspension was continually stirred at room temperature for 2 h, and the solid washed with Hepes buffer 1×10^{-4} mol/L.

The next stage consisted on the addition to the solid of 50 μL of VTA solution, $2.9x10^{-6}$ g/mL, 50 μL of VB solution, $6.8x10^{-7}$ g/mL, for the preparation of plastic antibody material with charged binding sites (C/PIM or C/NIM), or 100 μL of a $1.3x10^{-6}$ g/mL AA for the preparation of neutral materials (N/PIM or N/NIM). Both suspensions were continuously stirred at room temperature for 2 h.

The polymerization stage around the protein started by adding to the solid 100 μL of a solution of $3.56x10^{-4}$ g/mL AA (functional monomer), $7.72x10^{-3}$ g/mL NMAA (cross-linker) and $1.2x10^{-3}$ g/mL BOP (radical initiator). The polymerization was carried out at room temperature, for 2 h. The resulting solids were washed again with Hepes buffer $1×10^{-4}$ mol/L. Finally, 50 μL of a 0.5 g/L trypsin solution was added to the solid, and the resulting suspension was kept under continuous stirring, at room temperature, for 2 h. The obtained materials (C/PIM, C/NIM, N/PIM and N/NIM) were centrifuged, washed with Hepes buffer and dried in a desiccator under nitrogen atmosphere.

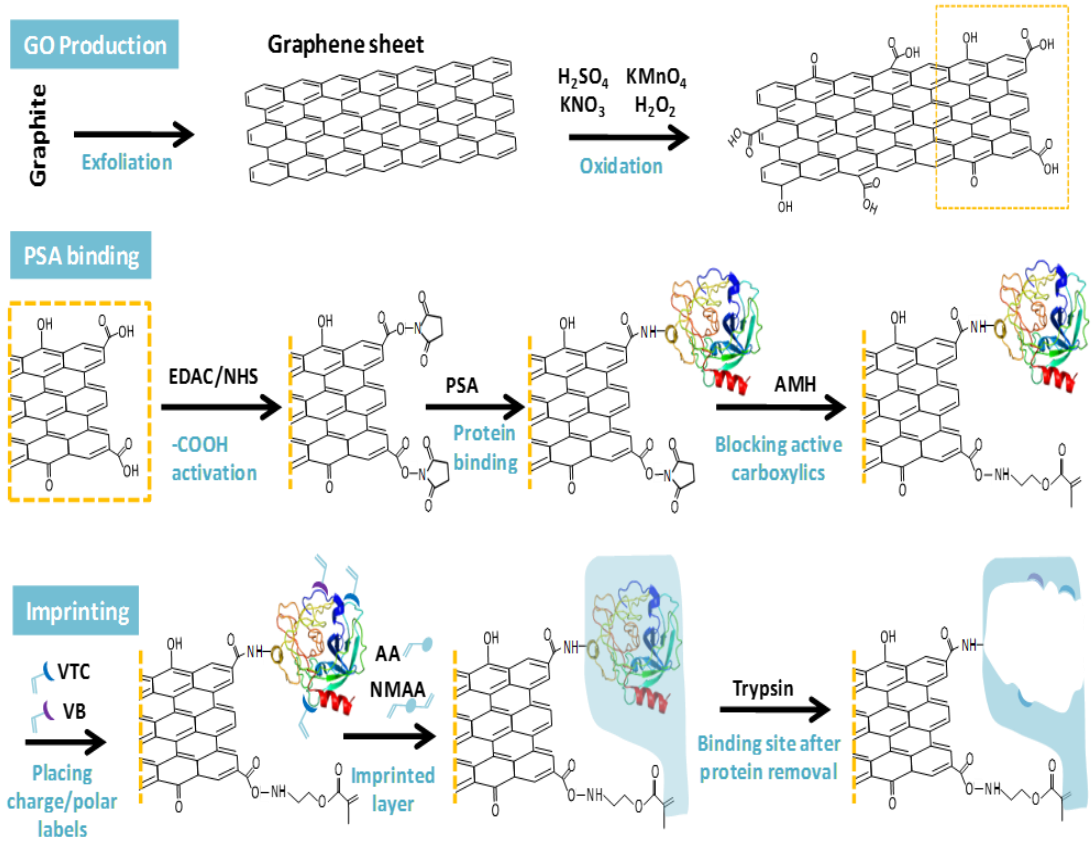

Figure **3.1**: Schematic representation of the synthesis of C/PIM materials (N/PIM, C/NIM, N/NIM are obtained similarly, by omitting specific steps of this scheme).

3.2.5 Assembly of the potentiometric sensors

The selective membranes were prepared by mixing 1 mg of modified graphene material (C/PIM, C/NIM, N/PIM or N/NIM), 33 mg of oNPOE, and 16 mg of PVC (Table 3.1). The mixture was stirred until the PVC was well humidified, and dispersed in 2.0 mL THF. The dispersion was kept uniform by continuous agitation on a magnetic stirrer.

Table **3.1**: Membrane composition of PSA sensors and the corresponding potentiometric features in 1.0×10^{-4} mol/L Hepes buffer.

ISE	Membrane composition			Slope (mV/decade)	LOD		R^2 (n = 3)	Linear concentration range		σ_v (mV)
	Ionophore (mg)	oNFOE (mg)	PVC (mg)		(ng/mL)	(mol/L)		(ng/mL)	(mol/L)	
I	0.90 (C/PIM)	38.9	15.6	-44.16±2.89	<2.0	$<5.83\times10^{-11}$	0.991	2.0–89.0	5.83×10^{-11}–2.62×10^{-9}	0.67
II	0.95 (C/NIM)	30.4	15.6	-24.80±1.91	2.0	5.83×10^{-11}	0.994	2.6–89.0	7.64×10^{-11}–2.62×10^{-9}	0.90
III	0.90 (N/PIM)	35.8	15.6	-35.82±1.21	2.0	5.83×10^{-11}	0.992	2.6–59.4	7.64×10^{-11}–1.75×10^{-9}	1.10
IV	0.85 (N/NIM)	34.8	15.5	-28.25±1.4	3.8	1.11×10^{-10}	0.996	3.8–40.3	1.11×10^{-10}–1.18×10^{-9}	1.15
V	—	34.0	15.5	—	—	—	—	—	5.83×10^{-11}–2.62×10^{-9}	—

LOD: Limit of detection.

The construction of the solid-contact PSA selective electrode was made similarly to that described by Kamel *et al*. in [13]. The electrode body was replaced by using a 10 mL syringe, using the smaller end to pack the conductive material (a mixture of graphite and epoxy resin) and bind the copper electrical wire. The outer graphite layer on top of the syringe was removed to create a small cavity (~1 mm deep), where the selective membrane would be deposited, drop-by-drop. After application of the membrane solution, the membrane was allowed to dry for 24 hours and after conditioned in a solution PSA, 20 ng/mL in Hepes buffer. Due to the instability of PSA, this conditioning was made inside the fridge.

The ISEs prepared with an internal reference solution were constructed by following the procedures described by Almeida *et al*., in [5]. Only the best membrane composition was applied into the electrode bodies made from 1000 µL micropipette tips made of polypropylene. The membrane solution was applied by dipping the tip about 4mm inside the membrane solution. The membrane that entered the tip was allowed to dry for 24 hours. A silver wire covered with a thin layer of AgCl was introduced inside the micropipette body to serve as electrical connection to the inner reference solution. The composition of the inner reference solution was identified after the optimization procedures described later.

3.2.6 Procedures for potentiometric measurements

All potentiometric measurements were carried out at room temperature and in stirred solutions. Emf values of each electrode were measured in solutions with fixed pH 7.3.

Decreasing concentration levels of PSA were obtained by transferring 5 µL of PSA aliquots of PSA $2.5x10^4$ or $2.5x10^3$ ng/mL standard solution to a 75 mL beaker containing 50 µL of artificial serum and 950 µL buffer $1.0x10^{-4}$ mol/L. Potential

readings were recorded after stabilization to ±0.2 mV and emf was plotted as a function of logarithm PSA concentration. Each calibration plot was used for subsequent determination of unknown PSA concentrations. The concentration interval of the calibration was 2.0–124.4 ng/mL or 0.2–12.4 ng/mL for electrodes made with solid-contact or inner reference solution, respectively. The artificial serum with different concentrations of PSA for the evaluation of ISE response was obtained by adding a known amount of PSA (2.5 to 60 ng/mL) to the artificial serum solution.

3.2.7 Binding experiments

Binding constants were calculated by the Sandwich method. For this purpose, the conductive support of the ISE was first coated with NIM membranes, left to dry for 1 hour, and then coated with PIM membranes and let to dry for 24 hours. Before use, the sensors were let stand for 12 hours in a solution of PSA (20 ng/mL) in Hepes buffer, in the fridge. The sensing head of the ISE was then submerged in a solution of 14 µL of PSA (2.5×10^{4} ng/mL), 2.5 mL de serum artificial and 47.5 mL of buffer 1.0×10^{-4} mol/L. The emf was then recorded each 5 mV until full stabilization.

3.2.8 Surface analysis (FTIR, TEM and Raman)

The chemical alteration of the graphene was followed by FTIR analysis. The infrared spectra were collected after background correction. Each spectrum was the average of 32 scans for the same sample. The plot represented wave number, with a range from 600 to 4,000 cm^{-1}, in function of % transmittance. Resolution was set to 4000 (by using Omnic Software).

The TEM analysis was performed for PIM, NIM and oxidized graphene. All these materials were dry, dispersed in ethanol and deposited on a copper grid with a

perforated film prior to microscopic observation. The analysis was done at several sampling points for each material.

Raman spectra were recorded as an extended scan; the laser beam was focused either with 50× or 100× Olympus objective lens and the laser power at the surface of the samples was varied with the aid of a set of neutral density filters (optical densities 0.3, 0.6, 1 and 2).

3.3 Results and discussion

3.3.1 Plastic antibody design

The overall design of the plastic antibody is presented in Figure 3.1. Graphene was the physical support selected to carry out the imprinting process. It consists in a two-dimensional monolayer of carbon atoms where most of all have sp^2 hybridization conjugated system, offering a unique environment for fast electron transport [14]. Graphene was obtained by exfoliating graphite, a process that ended up with the formation of GO. GO contains several functional groups, including hydroxyl (–OH), carbonyl (–C=O), and carboxyl (–COOH) [15].

The next stage was to bind PSA to the GO material, in order to enable its subsequent imprint (Figure 3.1). For this purpose, it was necessary to activate the carboxylic functions within the GO lattice, thus allowing the subsequent binding under mild conditions of any amine group in outer surface of the protein (hard conditions would promote significant changes in the protein conformation, thus leading to a mismatch imprint). This activation was done by the conventional biochemical reaction involving EDAC/NHS transformation [16]. Then, the reaction with PSA was carried out and resulted in the formation of an amide bond that prevented the protein from moving out from the solid support. The carboxylic groups that remained active after the reaction with PSA were blocked by reaction with AMH (Figure 3.1). AMH combined in the same structure a vinyl

group and an amine function: the amine reacted with the activated carboxylic groups and blocked their reactivity, while the vinyl group was expected to participate in the subsequent polymeric reaction leading to imprint, thus ensuring that the imprinted polymer formed around the protein would be covalently attached to the graphene support.

The imprinting stage started by introducing charge/polar labels (C) in the binding site of the imprinted material (C/PIM). This was done by adding to the solution charged/polar monomeric structures: VTA with a positive quaternary ammonium salt and VB with an ester function providing a negative polarity. Both of these contained (as AMH) a vinyl group that would enable their subsequent binding to the imprinted polymeric network. The molar amount of these monomers was controlled to avoid their binding out from the protein surface. VTA was also present in a higher molar amount due to the negative overall net charge of PSA under physiological conditions.

The imprinting around the protein with the charged labels was made by polymerizing AA cross linked by NMAA. The polymerization was initiated by BOP radicals. The imprinted sites were obtained by removing the protein template with trypsin, a protease that digests proteins by destroying peptide bonds. Negative controls of the above process were made by imprinting without template (C/NIM or N/NIM) and without charged labels (N/PIM and N/NIM).

3.3.2 Control of graphene modification

The chemical modification made on GO to establish the protein imprinting was followed by different techniques, namely FTIR, Raman and TEM analysis. The results obtained for C/PIM, N/PIM, C/NIM and N/NIM materials are shown in Figure 3.2, and compared to GO as starting material.

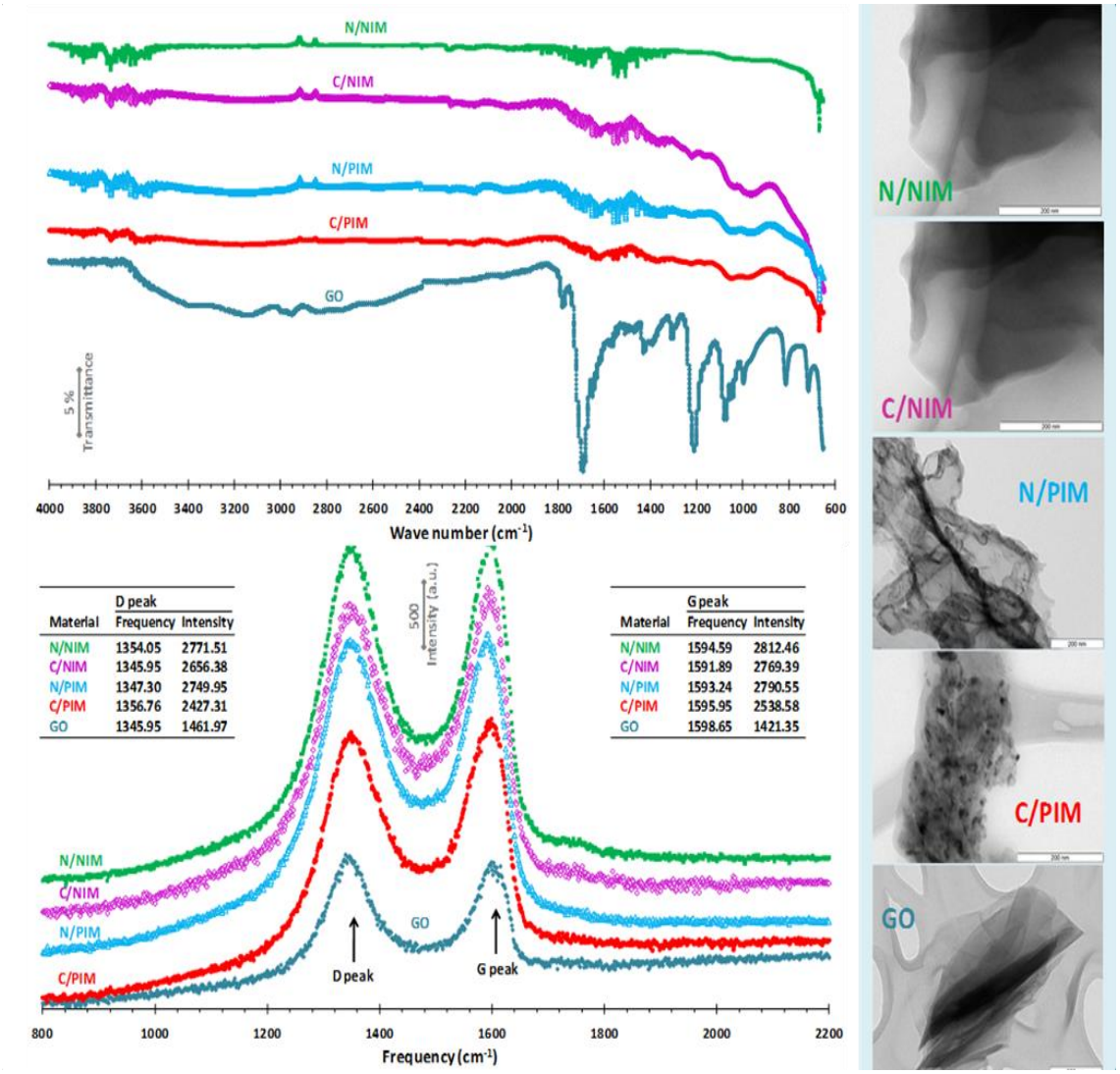

Figure **3.2**: FTIR (top, left) and Raman (bottom, left) spectra and TEM images (right) of all materials (GO is presented as blank control).

The FTIR spectrum of GO (Figure 3.2, top-left) presented a strong absorption peak at ~1700 cm^{-1}, that evidences the presence of the carbonyl group (–C=O). The broad adsorption band between 3700 and 3000 cm^{-1} indicated the presence of carboxylic function (–COOH), as well as the unsaturation between carbon atoms with double bonds and the subsequent sp^2 hybridization of these carbon atoms. The peaks at 1210 and 1070 cm^{-1} are probably accounting the presence of hydroxyl groups (–OH) in the GO due to C–O stretching vibrations. All materials obtained after GO modification showed similar FTIR spectra, with major

depreciation of the significant absorption bands/regions observed in GO. This change in FTIR spectra accounted the presence of the polymeric network around graphene sheets. This similar behaviour was already expected because these materials differed only in the special arrangement of the polymeric network and had roughly the same chemical composition. The only chemical difference within these is that "C" materials include charged monomers, but these are present in very low amount becoming imperceptible under FTIR studies.

The Raman spectra of all materials were dominated by two bands (Figure 3.2, bottom-left). These are the so-called G band, typically associated to the in-phase vibration of the graphite lattice, and the D band, corresponding to the (weak) disorder band from graphite edges [17]. The absolute intensities of G and D peaks in C/PIM, N/PIM, C/NIM and N/NIM were much higher than those in GO and quite similar within this group of materials. This common observation among the modified graphene-based materials resulted from the similar modification made on GO: the presence of the polymeric layer on the graphene sheets. In addition to this increase in peak intensity, the chemical modification of GO changed the intensity ratio D/G band, which reflects the extent of disorder present within the material [18]. The 1.03 ratio observed in GO changed to 0.96 in C/PIM and C/NIM and to 0.99 in N/PIM and N/NIM materials. This change was thus correlated to the polymeric material present in the graphene sheets, also reflecting the presence of charged monomers within the polymer matrix.

The TEM images obtained were not as helpful as Raman in terms of chemical modification of the GO. Graphene-sheets are not "hard" and are very thin, for which they were captured in electron-microscope images in many different positions. Only the imprinted versions of the material showed small black dots coupled to the sheets (Figure 3.2, right), meaning that these dots may be correlated to the binding sites. Such correlation is however difficult to confirm

because the observed material is highly heterogeneous (GO or the other derived materials).

3.3.3 Performance of the Sensors

PSA sensors were prepared with PIM or NIM particles, with or without charged labels, acting as electroactive materials. These materials were dispersed in plasticized PVC and casted over a solid conductive contact made of graphite and epoxy resin. The main analytical features of the devices were obtained by calibrating the electrochemical cell in a range of concentrations of PSA between $5.83x10^{-11}$ and $2.62x10^{-9}$ mol/L (2.0 and 89.0 ng/mL) under static mode of operation. The analytical data extracted from these were calculated according to IUPAC recommendations [19].

The obtained results are presented in Table 3.1. Overall, C/PIM sensor showed the best potentiometric response, with slopes of -44.2 mV/decade and LOD below $5.83x10^{-11}$ mol/L, in agreement with the results depicted in Figure 3.3A. Furthermore, the non-imprinted versions showed smaller sensitivity and showed liner responses for higher concentrations, meaning that the imprinting stage was important to promote a more directed response for PSA. The charged labels were also important, increasing the sensitivity of the response and the reproducibility of the obtained signals, both in imprinted and non-imprinted materials. This result may also account to the increase in perm-selectivity obtained by the presence of charged sites inside the selective membrane, besides suggesting that the labels increased the ability of the material to bind PSA. In general, the time required for the electrodes to reach a steady potential (±0.2 mV) was less than 20 s, even for the highest concentrations tested. The response of the electrodes was fully reversible, a common feature among most potentiometric membranes selective electrodes. The same electrode could be recalibrated several times along one day and several consecutive days, within 2 months (Figure 3.4).

In addition, no significant potential changes in absolute values have been observed over this period. The response was also reproducible along this time, as reflected by the σ_V presented in Table 3.1.

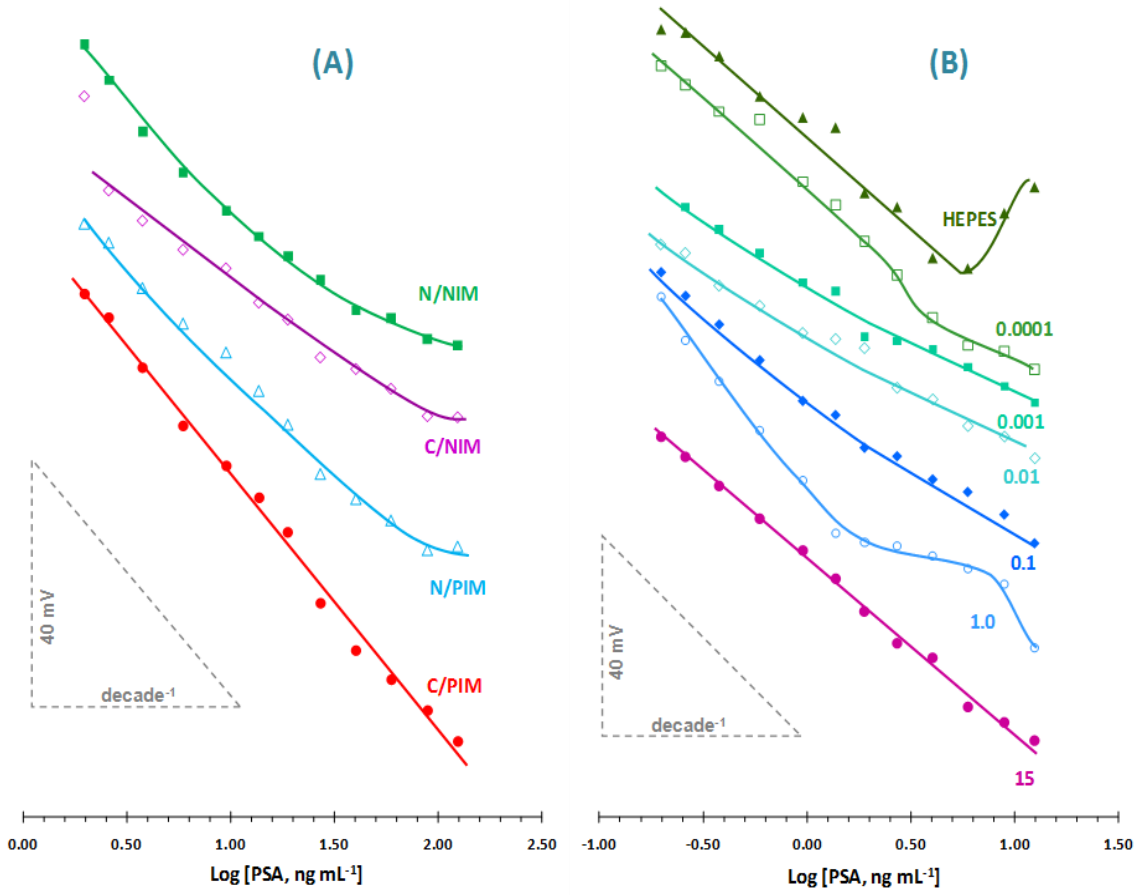

Figure **3.3**: Calibration curves in HEPES buffer of solid contact devices (**A**) prepared with C/PIM, C/NIM, N/PIM and N/NIM materials and of liquid contact devices (**B**) prepared with C/PIM material and inner reference solutions of different PSA concentrations (expressed in nmol/L).

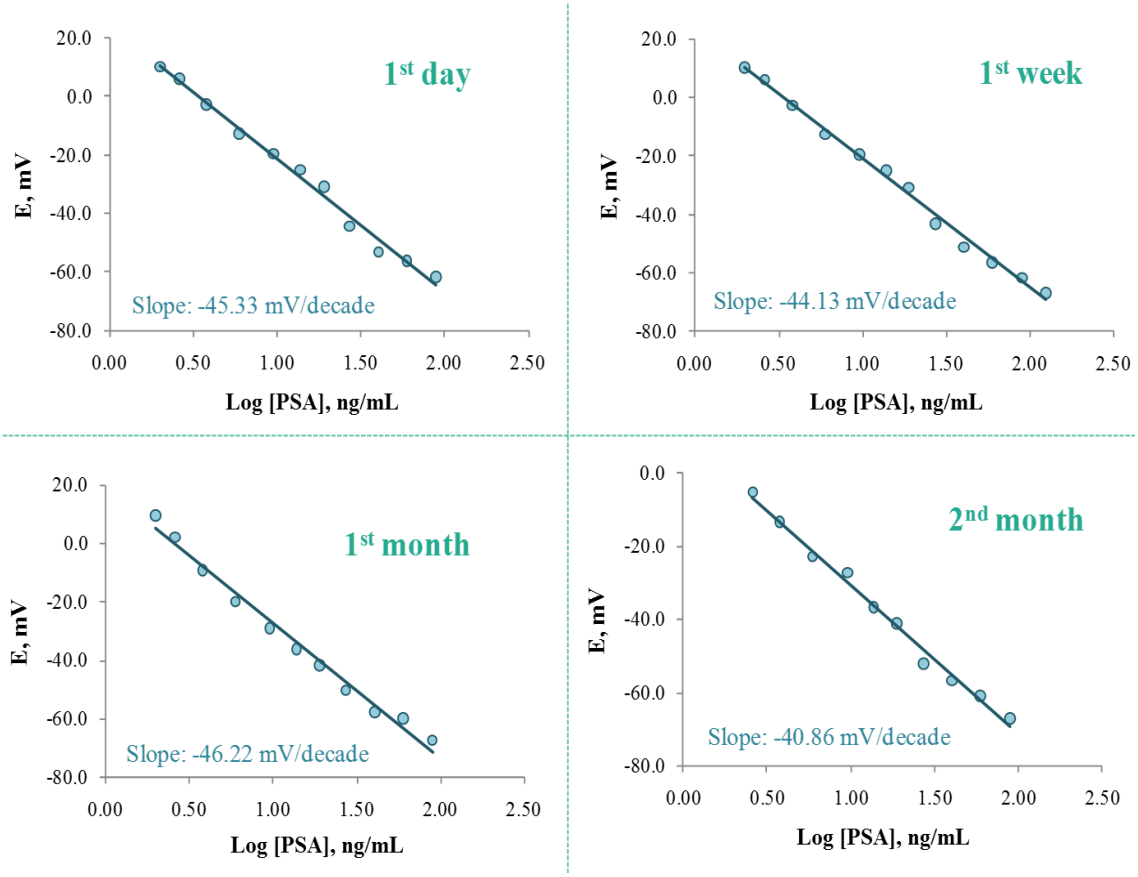

Figure **3.4**: Several calibrations of the C/PIM device measured with the same electrode, under equal background conditions and within time.

The above results were supported by further binding studies, carried out by the sandwich method. For this purpose, membranes of C/PIM and N/PIM materials were casted on top of the corresponding blank membranes, i.e. C/NIM and N/NIM, respectively. The average binding constants so obtained for C/PIM and N/PIM materials were 2.67 and 1.55, respectively, showing the importance of the charged sites within the imprinted layer. These results also suggest that a substantial part of the potentiometric response may arise from a stereochemical recognition of the analyte at the imprinted sites.

3.3.4 Effect of pH

The pH is an important variable for an accurate PSA reading, mostly because the potentiometric sensors detect charged species and PSA is a multiple charged structure, with a net charge that depends on the pH of the reading solution comparing to its isoelectric point [20].

The pH effect on the potentiometric devices was studied by recording Reilley diagrams, plotting the emf variation of a solution of constant PSA concentration with varying pH values. The concentration of PSA in this study was set to 7 ng/mL, and the pH was varied from 12 and 2, by adding saturated NaOH solution (to set the pH up to 12) and small aliquots of concentrated HCl solutions (to decrease slightly the pH, until pH 2). Both C/PIM and N/NIM showed a similar behaviour: emfs varied less than 20 mV within the pH interval 4–11; the emf increased below pH 4, accounting for the intense positive charge in PSA and a possible H^+ interference; and the emf decreased below pH 11, in result of the deprotonation of PSA and its negative net charge.

According to the obtained results, and considering the wide pH range achieved with the above devices, the pH selected for subsequent studies was 7.2. This value is expected to be close or similar to physiological conditions, meaning that any future analytical application would have little or no requirements of pH adjustment.

3.3.5 Sensor selectivity

The selectivity behaviour of potentiometric sensors is typically expressed in potentiometric selectivity coefficients (K^{POT}) [21], and lower values of K^{POT} mean lower interference. The selectivity coefficients were assessed in this work by the matched potential method (MPM) [22], where the PSA concentration was changed from 4 to 10 ng/mL (leading to a 13 mV emf change). The effect of foreign

specifies upon a 4 ng/mL solution of PSA was checked for creatinine, urea, glucose, haemoglobin (human) and bovine serum albumin (BSA). These foreign species were included in this study because they are commonly present in serum and may interfere in readings of PSA in serum samples.

Overall, the addition of small aliquots of solutions of foreign species was unable to change the emf in 13 mV, as requested to calculate the K^{POT}. This was tried out for highly concentrated solutions of interfering species and for concentrations up to their physiological levels. Facing this limitation, instead of calculating the potentiometric selectivity coefficient, tolerance levels were calculated for each foreign species. The concentrations of creatinine, urea, glucose, hemoglobin and BSA tolerated by the devices were 1.3×10^5, 1.9×10^6, 1.1×10^7, 1.5×10^8 and 5.0×10^7 ng/mL. In general, negligible interference was found for the foreign species under study tested up to the previously tolerated concentrations (higher concentrations were not tested due to technical limitations in increasing the foreign species concentration without significantly changing the background concentration in PSA, set to 4 ng/mL due to its high clinical significance).

3.3.6 Liquid contact ISEs

Further optimization of the proposed sensor was tried out by applying the selected C/PIM membrane over the smaller end of a 1000 μL micropipette tip and varying the inner reference solution composition. The concentration of the primary ion in the inner compartment is expected to be set to a low value, in order to generate a net flux of primary ions towards this side of the membrane. The exact concentration required for this purpose must be set by experimental studies.

Thus, several electrodes with different PSA concentrations in the inner electrolyte were constructed. The inner electrolyte was always an Hepes $1x10^{-4}$ mol/L buffer,

with PSA concentrations ranging from $1x10^{-13}$ to $1.53x10^{-8}$ mol/L, or without PSA. The obtained results are presented in Table 3.2 and the corresponding calibrations presented in Figure 3.3B. Overall, the main differences recorded for all conditions tested were slope and linear range, being the best results obtained for the higher PSA concentration tested (which was already sufficiently low for this kind of electrodes). The LOD decreased 10 times, comparing to the solid contact electrodes, meaning that this kind of configuration may be especially attractive for screening vestigial amounts of protein biomarkers.

Table **3.2**: Comparison of PSA sensors with different inner electrolyte solutions.

Characteristics	PSA (mol/L)						Hepes Buffer
	1.53×10^{-8} *I*	**1×10^{-9}** *II*	**1×10^{-10}** *III*	**1×10^{-11}** *IV*	**1×10^{-12}** *V*	**1×10^{-13}** *VI*	— *VII*
Slope (mV/decade)	-34.04±1.24	-50.64±0.38	-31.19±3.57	-23.52±1.30	-23.77±0.85	-35.46±6.04	-34.57±2.75
R^2 (n=3)	0.995	0.991	0.990	0.991	0.992	0.992	0.992
LOD (ng/mL)	0.2	0.2	0.2	0.2	0.2	0.2	0.2
LOD (mol/L)	5.83×10^{-12}	5.83×10^{-12}	5.83×10^{-12}	5.83×10^{-12}	5.83×10^{-12}	5.83×10^{-12}	5.83×10^{-12}
LLLR (ng/mL)	0.2	0.2	0.2	0.2	0.2	0.2	0.2
LLLR (mol/L)	5.83×10^{-12}	5.83×10^{-12}	5.83×10^{-12}	5.83×10^{-12}	5.83×10^{-12}	5.83×10^{-12}	5.83×10^{-12}
ULLR (ng/mL)	12.5	1.9	2.7	12.5	12.5	6.0	6.0
ULLR (mol/L)	3.67×10^{-10}	5.57×10^{-11}	7.99×10^{-11}	3.67×10^{-10}	3.67×10^{-10}	1.75×10^{-10}	1.75×10^{-10}
σ_V (mV)	0.64	0.035	0.093	0.98	0.75	1.56	1.92

LLLR – Lower limit of linear range; ULLR – Upper limit of linear range

3.3.7 Application

C/PIM sensors were used to determine PSA in artificial serum. Blank serum samples were spiked and analyzed for PSA concentrations ranging about 2.6 to 59.4 ng/mL.

The results of the potentiometric analysis conducted in steady state are summarized in Table 3.3. A good agreement was found between added and found amounts of PSA. Overall, recoveries ranged from 96.9 to 106.1% with an average relative standard deviation of 6.8%, suggesting that the proposed sensors may lead to successful results under real applications.

Table **3.3**: Potentiometric determination of PSA in serum using MIP oriented based membrane sensor.

PSA (ng/mL)	Found (ng/mL)	Recovery (%)	Relative error (%)	RSD (%)
59.4	52.0±5.6	96.9±2.6	3.1	10.7
18.9	18.0±0.1	98.1±0.3	1.9	0.8
9.5	9.1±1.1	97.7±5.3	2.3	11.9
5.9	7.3±1.2	111.9±9.0	-11.9	15.9
3.8	4.0±0.3	103.9±5.4	-3.9	7.2
2.6	2.7±0.5	106.1±18.1	-6.1	17.0

3.4 Conclusions

The technique of molecular imprinting over graphene layers produced an inexpensive material that was successfully applied to produce PSA sensors of potentiometric transduction, being the presence of charged labels beneficial for the production of a more sensitive response, extensive to lower PSA concentrations. The use of a liquid contact allowed a decrease in delectability,

although the solid contact devices are more easy to use in routine applications are capable of reading directly PSA concentrations with clinical significance in serum.

The main advantages of these sensors include the simplicity of construction, low detection limits and low manufacturing costs. When compared to methods relying on natural antibodies, the present devices also offer reusability over 2 months. The proposed method is particularly suitable for screening assays carried out in analytical laboratories.

3.5 References

[1] F.T.C. Moreira, R.A.F. Dutra, J.P.C. Noronha, A.E.G. Cass, M.G.F. Sales, Smart Plastic Antibody Material (SPAM) tailored on disposable screen printed electrodes for protein recognition: application to Myoglobin detection, *Biosensors and Bioelectronics*, 45 (2013) 237-244.

[2] F.T.C. Moreira, R.A.F. Dutra, J.P.C. Noronha, M.G.F. Sales, Surface Imprinting approach on screen printed electrodes coated with carboxylated PVC for Myoglobin detection with Electrochemical Transduction, *Procedia Engineerin*, 47 (2012) 865-868.

[3] F.T.C. Moreira, R.A.F. Dutra, J.P.C. Noronha, M.G.F. Sales, Myoglobin-biomimetic electroactive materials made by surface molecular imprinting on silica beads and their use as ionophores in polymeric membranes for potentiometric transduction, *Biosensors and Bioelectronics*, 26 (2011) 4760-4766.

[4] T.S.C.R. Rebelo, S.A.A. Almeida, J.R.L. Guerreiro, M.C.B.S.M. Montenegro, M.G.F. Sales, Trimethoprim-selective electrodes with molecularly imprinted polymers acting as ionophores and potentiometric transduction on graphite solid-contact, *Microchemical Journal*, 98 (2011) 21-28.

[5] S.A.A. Almeidaa, L. Truta, R.B. Queirós, M.C.B.S.M. Montenegro, A.L. Cunha, M.G.F. Sales, Optimizing potentiometric ionophore and electrode design for environmental on-site control of antibiotic drugs: Application to sulfamethoxazole, *Biosensors and Bioelectronics*, 35 (2012) 319-326.

[6] Y. Li, X. Li, C. Dong, J. Qi, X. Han, A graphene oxide-based molecularly imprinted polymer platform for detecting endocrine disrupting chemicals, *Carbon*, 48 (2010) 3427-3433.

[7] Y. Mao, Y. Bao, S. Gan, F. Li, L. Niu, Electrochemical sensor for dopamine based on a novel graphene-molecular imprinted polymers composite recognition element, *Biosensors and Bioelectronics*, 28 (2011) 291-297.

[8] T. Kuila, S. Bose, P. Khanra, A.K. Mishra, N.H. Kim, J.H. Lee, Recent advances in graphene-based biosensors, *Biosensors and Bioelectronics*, 26 (2011) 4637-4648.

[9] J. Luo, S. Jiang, X. Liu, Efficient One-Pot Synthesis of Mussel-Inspired Molecularly Imprinted Polymer Coated Graphene for Protein-Specific Recognition and Fast Separation, *The Journal of Physical Chemistry C*, 117 (2013) 18448-18456.

[10] K.P.G. Ralloff, P. Westh, R.A. Purssell, M. Pudek, Y. Koga, Non-ideality of methanol solution's of artificial serum in the mole fraction range from 5 x 10^{-4} to 5 x 10^{-3} at 25 degrees C, *Fluid phase equilibria*, 207 (2003) 301-317.

[11] W.S. Hummers, R.E. Offeman, Preparation of graphitic oxide, *Journal of the American Chemical Society*, 80 (1958) 1339-1339.

[12] S. Ge, M. Yan, J. Lu, M. Zhang, F. Yu, J. Yu, X. Song, S. Yu, Electrochemical biosensor based on graphene oxide-Au nanoclusters composites for L-cysteine analysis, *Biosensors and Bioelectronics*, 31 (2012) 49-54.

[13] A.H. Kamel, F.T.C. Moreira, S.A.A. Almeida, M.G.F. Sales, Novel potentiometric sensors of molecular imprinted polymers for specific binding of chlormequat, *Electroanalysis*, 20 (2008) 194-202.

[14] N.O. Weiss, H. Zhou, L. Liao, Y. Liu, S. Jiang, Y. Huang, X. Duan, Graphene: An Emerging Electronic Material, *Advanced Materials*, 24 (2012) 5776-5776.

[15] V. Singh, D. Joung, L. Zhai, S. Das, S.I. Khondaker, S. Seal, Graphene based materials: Past, present and future, *Progress in Materials Science*, 56 (2011) 1178-1271.

[16] K. Jiang, L.S. Schadler, R.W. Siegel, X. Zhang, H. Zhang, M. Terrones, Protein immobilization on carbon nanotubes via a two-step process of diimide-activated amidation, *Journal of Materials Chemistry*, 14 (2004) 37-39.

[17] F. Tuinstra, J.L. Koenig, Raman Spectrum of Graphite, *Journal of Chemical Physics*, 53 (1970) 1126.

[18] K.N. Kudin, B. Ozbas, H.C. Schniepp, R.K. Prud'homme, I.A. Aksay, R. Car, Raman Spectra of Graphite Oxide and Functionalized Graphene Sheets, *Nano Letters*, 8 (2007) 36-41.

[19] IUPAC, Analytical Chemistry Division Commission on Analytical Nomenclature, *Pure and Applied Chemistry*, (2000) 1851-2082.

[20] L. Bruun, T. Bjork, H. Lilja, C. Becker, O. Gustafsson, A. Christensson, Percent-free prostate specific antigen is elevated in men on haemodialysis or peritoneal dialysis treatment, *Nephrol Dial Transplant*, 18 (2003) 598-602.

[21] E. Bakker, E. Pretsch, Modern Potentiometry, *Angewandte Chemie-International Edition*, 46 (2007) 5660-5668.

[22] Y. Umezawa, P. Buhlmann, K. Umezawa, K. Tohda, S. Amemiya, Potentiometric selectivity coefficients of ion-selective electrodes Part I. Inorganic cations, *Pure and Applied Chemistry*, 72 (2000) 1851-2082.

4

Annexin A3 electrochemical sensor

Work accepted to journal of Electrochimica Acta:

Protein·Imprinted·Material·electrochemical·sensor·for·determination·of·Annexin·A3·in·biological·samples¶

¶

Tânia·S.C.R.·Rebelo[1,2,3],·Carlos·M.·Pereira[4]*,·M.·Goreti·F.·Sales[1],·João·P.·Noronha[2]·and·Fernando·Silva[4]¶

¶

[1]*BioMark-CINTESIS/ISEP,·Instituto·Superior·de·Engenharia·do·Instituto·Politécnico·do·Porto,·Portugal.*¶

[2]*LAQV,·REQUIMTE,·Departamento·de·Química,·Faculdade·de·Ciências·e·Tecnologia,·Universidade·Nova·de·Lisboa,·Caparica,·Portugal.*¶

[3]*Laboratório·de·Farmacologia·e·Biocompatibilidade·Celular,·Faculdade·de·Medicina·Dentária,·Universidade·do·Porto,·Porto,·Portugal.*¶

[4]*Centro·de·Investigação·em·Química-Linha·4,·Faculdade·de·Ciências·da·Universidade·do·Porto,·Departamento·de·Química·e·Bioquímica,·Porto,·Portugal.*¶

4.1 Introduction

CAF (3,4-dihydroxycinnamic acid) has been successfully employed in the fabrication of electrochemical sensors for the recognition/detection of small biomolecules, but has never been used to generate protein imprinted materials (neither by chemical nor by electrochemical polymerization) [1-5]. Thus, this

work describes the use of CAF to generate highly selective protein imprinted materials for a protein biomarker with reduced non-specific binding, aiming at improving biosensor performance.

This work describes the construction of a novel ANXA3 electrochemical biosensor by electropolymerizing on a screen-printed carbon electrode the monomer CAF, coexisting in solution with the target protein. A systematic investigation and optimization of several analytical parameters leading to the best calibration slopes, widest dynamic linear range, lower limit of detection and higher selectivity, are presented along with the application of the final biosensor to the analysis of spiked urine samples.

4.2 Experimental Procedure

4.2.1 Reagents and solutions

Ultra-pure water (resistivity > 18 MΩ.cm at 25 ºC) was used throughout this work for cleaning and solution preparation. All chemicals were of analytical grade and used without any further purification. CAF, sodium sulfate, potassium phosphate, ammonium chloride, urea and creatinine were purchased from Sigma-Aldrich; ANXA3 (on Human protein) from Abcam; sodium chloride from Panreac; and calcium chloride dehydrate, potassium chloride, potassium ferricyanide ($K_3[Fe(CN)_6]$) and potassium ferrocyanide trihydrate ($K_4[Fe(CN)_6]$) from Merck.

Phosphate buffer solutions (PBS) were prepared and used throughout this work (0.1 M NaH_2PO_4 and 0.1 M Na_2HPO_4, pH 7.2). Stock solutions of ANXA3 (0.2 mg/mL) were prepared in PBS (pH 7.2) and less concentrated standards were prepared by suitable dilution in the buffer solution. Electrochemical assays were performed in the presence of 5.0×10^{-3} mol/L equimolar solution of $K_3[Fe(CN)_6]$ and $K_4[Fe(CN)_6]$ in PBS. Synthetic urine solution was prepared with the following

composition: calcium chloride dihydrate (1.103 g/L), sodium chloride (2.295 g/L), sodium sulfate (2.25 g/L), potassium phosphate (1.40 g/L), potassium chloride (1.60 g/L), ammonium chloride (1.00 g/L), urea (25.0 g/L) and creatinine (1.10 g/L) [6].

4.2.2 Apparatus

The electrochemical measurements were conducted in a PGSTAT302N potentiostat/galvanostat (Metrohm Autolab, the Netherlands), containing an impedance module and controlled by computer with GPES 4.9 software. Carbon screen-printed electrodes (SPEs, 4 mm diameter, DRP-C110) were used as sensor platforms (DropSens, Spain). SPEs were connected to the Autolab by means of a suitable box, also from DropSens.

Atomic force microscopy (AFM) images were recorded using a Molecular Imaging, PicoLe atomic force microscope. The surface topography was measured using a silicon cantilever/tip (App Nano, model ACT) with a resonance frequency between 200 and 400 kHz. Raman spectroscopy studies were also conducted, using a Raman spectrometer from Thermo Unicam, equipped with 10 mW laser operating at 532 nm.

4.2.3. Synthesis of the protein-imprinted layer

The carbon-SPE electrodes were cleaned before modification by cyclic voltammetry, between -0.2 and +1.0 V, with a 100 mV/s scan rate, in a 0.5 mol/L sulfuric acid solution. Cycling procedures were repeated until the resulting voltammogram showed a clean surface (~30 cycles were necessary). The electrodes were then thoroughly rinsed with ultra-pure water and dried under a N_2 stream.

Next, poly(CAF) was obtained by following the procedures described in [2], and the same conditions were applied to produce the imprinted layer. Briefly, about

30 μL of a solution containing 2.0×10^{-4} mol/L of CAF and 5.0×10^{-3} ng/mL ANXA3 in PBS buffer (pH 7.2) were casted over the three-electrode system of the SPE. Electropolymerization was achieved by applying a constant potential of +2.0 V for 30 s. The polymer modified electrode was then thoroughly washed with ultra-pure water, dried under N_2 and incubated overnight in a 1 mol/L H_2SO_4 solution at 45 °C in order to remove the protein [7]. The resulting PIM layer was washed repeatedly with PBS buffer, aiming to remove the remaining protein fragments and H_2SO_4, and finally rinsed with ultra-pure water and dried under N_2. The procedure adopted for the preparation of PIM is described schematically in Figure 4.1.

As a control, a non-imprinted materials (NIM) modified carbon-SPE was also prepared and treated exactly by the same manner, except the absence of ANXA3 in the electropolymerization process.

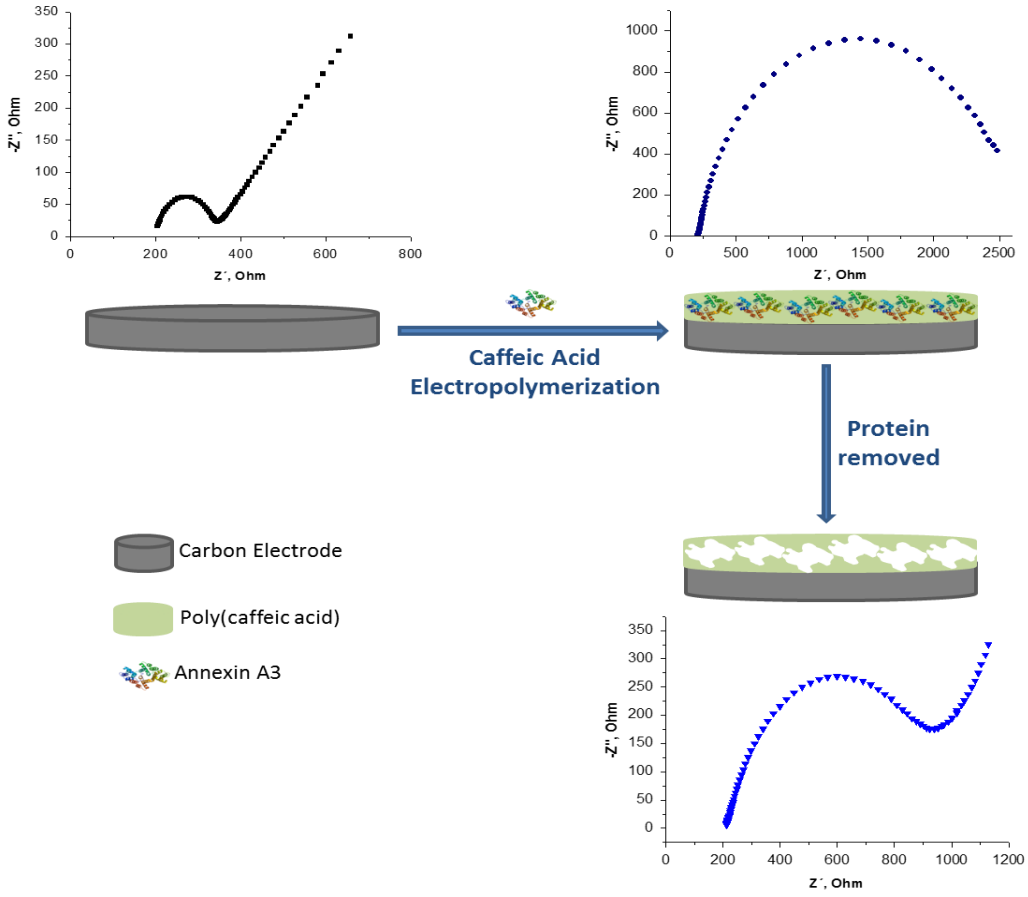

Figure **4.1**: Schematic representation of the synthetic process of PIM.

4.2.4. Electrochemical procedures

SWV measurement were performed in the presence of 5.0×10^{-3} mol/L equimolar $[Fe(CN)_6]^{3-}$ and $[Fe(CN)_6]^{4-}$ solution, prepared in PBS buffer (pH) 7.2. The potentials were changed from -0.5 to 0.6 V, at a frequency of 10 Hz, a step potential of 9.45 mV and an amplitude of 50 mV. All assays were conducted in triplicate.

EIS assays were made in the presence of $[Fe(CN)_6]^{3-/4-}$ redox couple at an open circuit potential of +0.12 V, using a sinusoidal potential perturbation with an amplitude of 0.01 V and the number of frequencies equal to 50, logarithmically distributed over a frequency range of 0.1–100 kHz.

4.2.5 Determination of ANXA3 in synthetic urine

Synthetic urine solutions with different concentrations of ANXA3 were used for the evaluation of sensor response. These solutions were prepared by adding a known amount of ANXA3 (from 0.2 to 20.0 ng/mL) to the synthetic urine solution.

4.3 Results and discussions

4.3.1 Optimization of the experimental conditions for ANXA3 detection

Experiments were carried out using a 0.1 M PBS (pH 7.2), an electrolyte solution close to the physiological conditions. Based in the existing information [2], in order to improve the sensitivity of the sensor, the potential and the deposition time used in electropolymerization process were studied at fixed concentration of CAF (2.0×10^{-4} mol/L). Overall, it was found that the polymerization of CAF is favored by applying a voltage of +2.0 V during 30 s (results not shown), which is in rough agreement with the results found in the literature [2].

Furthermore, the optimization of the concentration ANXA3 used in the construction PIM is a very important factor that influences the biosensor performance, because it dictates the number of rebinding positions that may exist on the sensing layer. Figure 4.2 shows the sensor response obtained for PIM materials obtained with 5.0×10^{-4}, 1.0×10^{-3} or 5.0×10^{-3} ng/mL of ANXA3 in the CAF solution to be electropolymerized. In general, a higher concentration of template improved the sensitivity and widened the linearity range of the biosensor. This was consistent with the existence of a higher number of rebinding sites at the sensory surface. From this point on, the concentration used for producing PIM biosensors was 5.0×10^{-3} ng/mL.

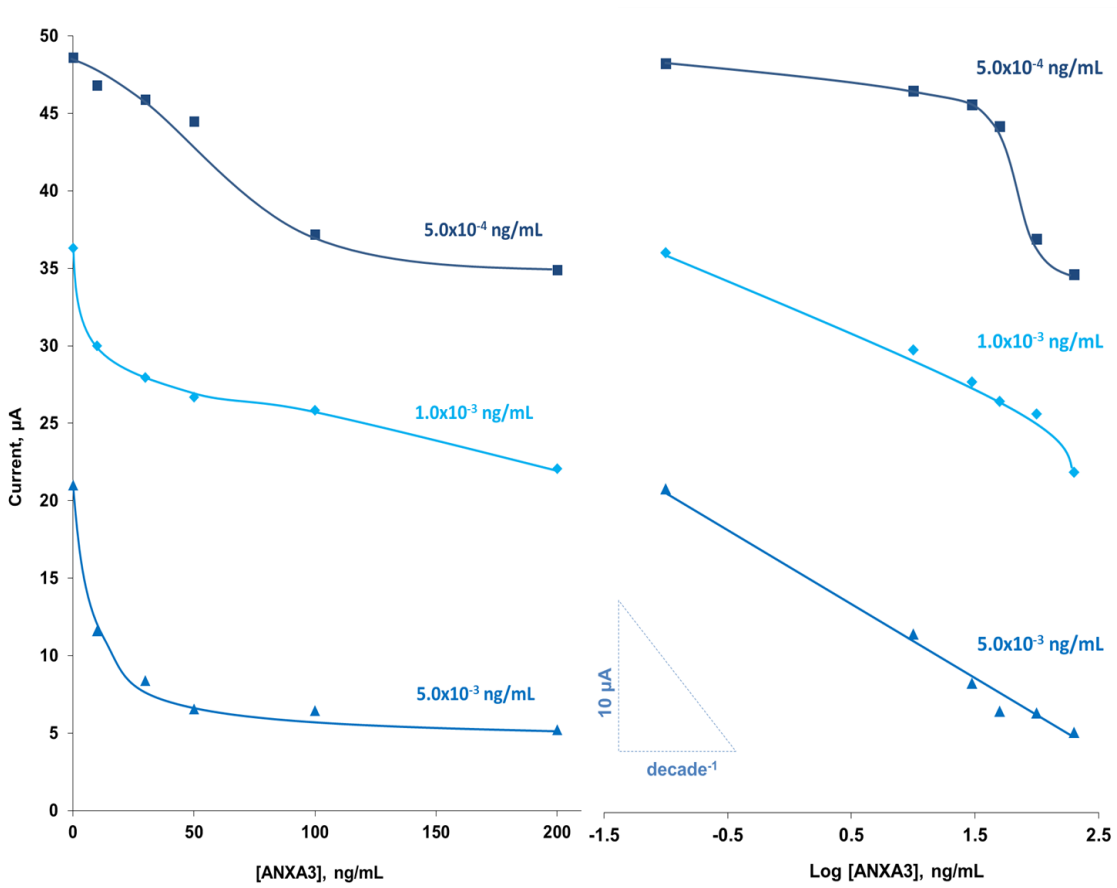

Figure **4.2:** Calibration curves obtained for different concentration the electropolymerization of ANXA3 obtained by SWV measurements in 5.0 mM $[Fe(CN)_6]^{3-}$ and 5.0 mM $[Fe(CN)_6]^{4-}$ in PBS buffer, with range of ANXA3 concentration between 0.1-200 ng/mL.

4.3.2 Optimization of sensor construction

EIS investigations were used to follow the carbon-SPE modification after each chemical step. These can be probed by monitoring the changes in the electron transfer properties of well-known redox systems, such as $[Fe(CN)_6]^{4-}/[Fe(CN)_6]^{3-}$, as shown in Figure 4.3. EIS data was fitted to the Randles equivalent circuit in order to extract the numerical values of the charge transfer resistance. The resulting values are presented in Table 4.1. In the present case the charge transfer resistance is indeed a pseudo-charge transfer resistance that couples the

contribution of the kinetics of electron transfer at the electrode surface and that of the transport of the redox couple within the polymer network.

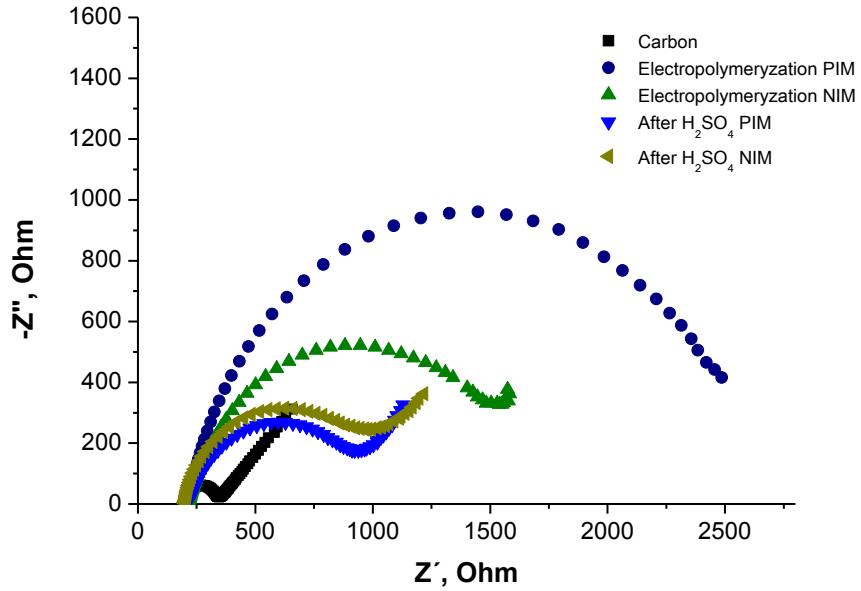

Figure **4.3**: EIS study over the subsequent modification steps of the carbon-SPE in 5.0 mM $[Fe(CN)_6]^{3-}$ and 5.0 mM $[Fe(CN)_6]^{4-}$ in PBS buffer.

Table **4.1**: Fitting parameters extracted from electrochemical impedance data using the Randles type equivalent circuit.

	Carbon	Electropolymerization		After H_2SO_4	
		PIM	NIM	PIM	NIM
R_s (Ω)	201.2	215.0	214.0	213.5	199.3
Q ($\Omega^{-1}s^{-n}$)	2.6×10^{-6}	1.3×10^{-5}	5.1×10^{-5}	4.0×10^{-5}	4.7×10^{-5}
n	0.92	0.87	0.81	0.79	0.86
R_{ct} (Ω)	134.2	2.3×10^{3}	1.3×10^{3}	7.0×10^{2}	7.3×10^{2}
W ($\Omega s^{-1/2}$)	2.8×10^{-3}	2.7×10^{-3}	3.4×10^{-3}	3.0×10^{-3}	2.5×10^{-3}

The EIS data of the PIM assembly (up to the electropolymerization stage) confirmed the modifications made in all stages, displaying an increase in the

resistance to charge transfer, which is consistent with the chemical alterations established in the electrode surface and the electrical charge of the redox probe used to follow the biosensor construction and performance.

As expected, the values of R_s are constant in the different studies, mainly because this parameter is related with the electrical features of the solution, which are almost the same in the different experiments.

Q and n are the adjustment parameters of constant phase elements (CPE) and they are used when the circuit does not fit to capacity. The n is an adimensional adjusting parameter, which reflects the deviation from ideality. When n=1 it means that a pure capacity behavior is observed, while when $1 > n > 0.8$ the behavior corresponds to a non-ideal capacitive electrode.

Q value is related with C_{dl} and reflects changes in the charges at the electrode surface. PIMs and NIMs Q values do not show any consistent change, what is probably connected to the complex polymeric film design and the large number of experimental variables. In this work, Q values are always higher than carbon-SPE and NIM Q values slightly higher than PIM Q values.

W evidences changes of electroactive species diffusion into electrode surface. It is possible to consider that values are keeping constant along all the process.

Regarding R_{ct}, it can be said that the polymeric layer assembled on the surface does not display conductive features, as the resistance to charge transfer increases after polymerization. Most probably, the polymerization was hindered by the presence of the target protein, because the NIM sensory layers displayed slightly higher resistances compared to PIM, thereby confirming higher polymeric yields in the absence of the protein.

The protein was removed in the final stage of the PIM assembly. This was done by surface treatment with H_2SO_4, which promoted a decrease in the charge

transfer resistance. This decrease was consistent with a successful removal of ANXA3 from the imprinted polymer layer leaving vacant holes in the polymeric structure that facilitated the redox probe access to the electrode surface, thus decreasing the pseudo-charge transfer resistance.

In general, the NIM material displayed a similar behavior compared to the PIM. An increase in the charge transfer resistance was observed after CAF electropolymerization, but the absence of ANXA3 within the poly(CAF) layer yielded lower charge resistance values. After treatment with H_2SO_4, the charge transfer resistance decreased, indicating that small fractions of the polymer weekly attached to the electrode surface were removed. The absolute charge transfer resistance of the NIM was however higher than the PIM, thereby corroborating with the formation of cavity binding sites on the later electrode material.

4.3.3 Surface characterization morphological by AFM and Raman

AFM was used to investigate the morphology of the electrode surface before and after the electropolymerization process. The images collected are shown in Figure 4.4.

The top image shows the typical morphology of a clean carbon electrode surface, displaying the surface roughness typical of the carbon ink films used in the fabrication of SPEs carbon electrodes. The root mean square (RMS) surface roughness is 32.9 nm (Figure 4.4, top). After CAF electropolymerization, the RMS value decreased to 20.6 nm (Figure 4.4, middle) which can be interpreted as the leveling of the electrode surface by the formation of the polymeric network. Finally, after removal of the protein, the RMS surface roughness increased to 29.7 nm (Figure 4.4, bottom), indicating that ANXA3 removal from the polymeric network induced an increase in film roughness. Coupling the AFM data with the

EIS data obtained for both NIM and PIM, such roughness increase was related to the exit of the template protein and the leaching of small fragments of polymer weekly attached to the poly(CAF) structure.

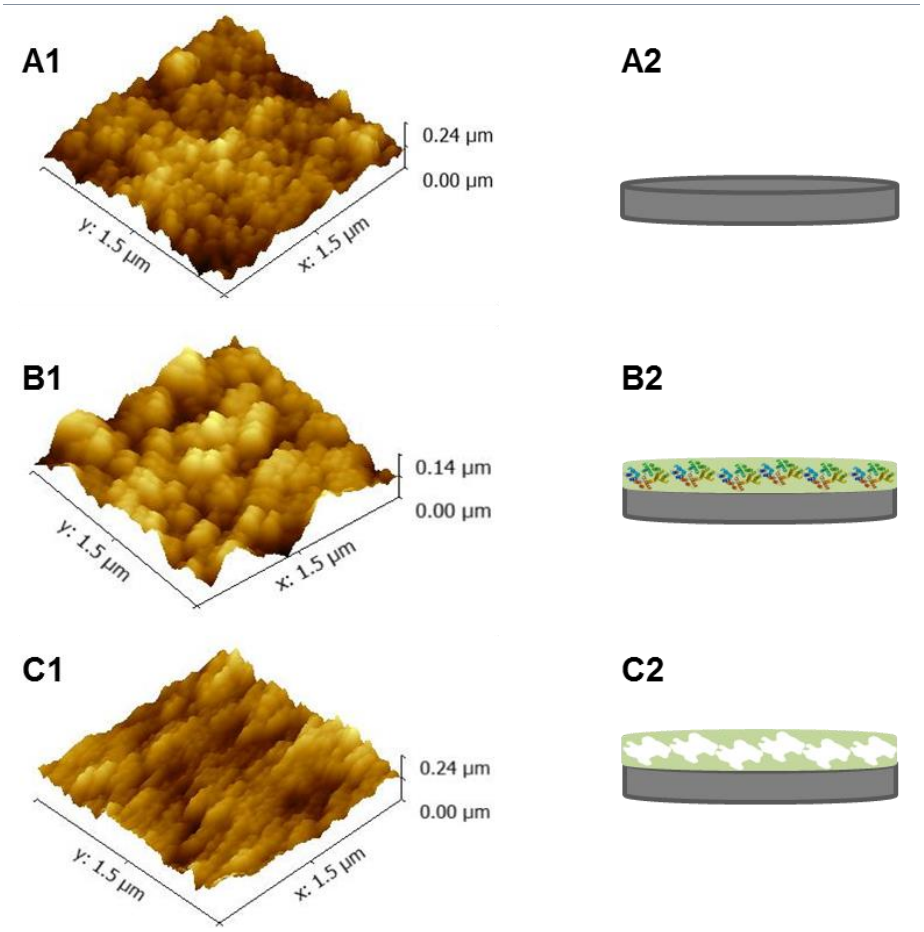

Figure **4.4**: AFM images in 3D for the different modification of surface SPE-PIM electrode. **A** - Carbon surface, **B** - CAF electropolymerization and **C** - Protein removal; **1** - AFM images and **2** - Diagram electrode.

The different stages of the SPE modification were also followed by Raman Spectroscopy. The resulting Raman spectra are shown in Figure 4.5, corresponding to the blank (carbon ink screen printed electrode), the imprinted material before the protein removal (PIM with protein) and after protein removal (PIM with protein removed). As expected, the Raman spectra of all materials showed three main peaks, typically recognized by G, D and 2D.

In the blank electrode surface, (i) the G band was located at 1569 cm^{-1}, corresponding to the stretching vibration of any pair of sp^2 bonds, either in chains or in rings; (ii) the D band was centered at 1320 cm^{-1}, corresponding to the collective breathing mode of sp^2 sites in six-member graphitic rings; and (iii) the 2D band at 2725 cm^{-1} was assigned to the overtone of the D band.

Regarding the Raman spectra of PIM and NIM materials, the most important information involved the changes in G and D band peak ratios [8]. In general, the ratio of Raman signal of G/D peaks was altered in all stages of chemical modification, as indicated in Table 4.2. The relative intensity of the D peak decreased with significance (compared to G), when poly(CAF) and protein were present on the SPE (to lower values than those of the blank). In addition, the presence of the protein within the polymer matrix was highlighted by intense 2D peak absorption, of unique profile when compared to the other materials. The D peak was after augmented once the protein was removed. Overall, such D/G peak ratio changes confirmed the occurrence of chemical alterations on the working electrode. These peak ratio changes were coupled by changes in Raman shift (Table 4.2) also consistent with such chemical alterations.

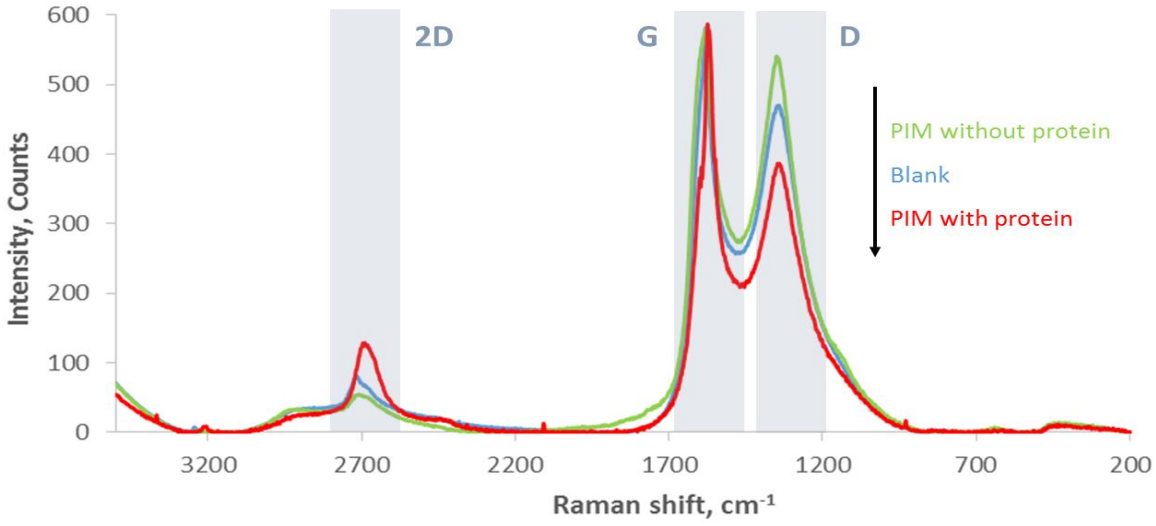

Figure **4.5**: Raman Spectroscopy of the blank-SPE, PIM with protein and PIM without protein.

Table **4.2**: Values extracted from Raman spectra of the blank-SPE, PIM with protein and PIM without protein.

	Raman Intensity (Counts)			**Raman Shift (cm^{-1})**			**Peak ratio**	
	2D Peak	**G Peak**	**D Peak**	**2D Peak**	**G Peak**	**D Peak**	I_D/I_G	I_{2D}/I_G
Blank	73	575	462	2725	1569	1320	0.80	0.13
PIM without protein	56	575	537	2735	1569	1343	0.93	0.10
PIM with protein	126	575	382	2681	1569	1335	0.66	0.22

4.3.4 Analytical performance of ANXA3 biosensor

The fabricated biosensors were applied to the quantification of ANXA3 using SWV as analytical technique. This technique offered the advantages of high sensitivity to surface-confined electrode reactions, along with suitable detection capabilities and fast data acquisition.

The calibration curve obtained is shown in Figure 4.6 for the concentration range between 0.050 and 200 ng/mL. As can be seen, the binding of ANXA3 to the available sites on the polymeric network lead to a decrease in the typical anodic peak current of the $[Fe(CN)_6]^{4-}/[Fe(CN)_6]^{3-}$ redox probe with the increasing ANXA3 concentration in solution. Furthermore, a linear pattern against Log[ANXA3] was observed for concentrations ranging from 0.1 to 200 ng/mL, with a correlation coefficient 0.9968, as shown in the inset of Figure 4.6.

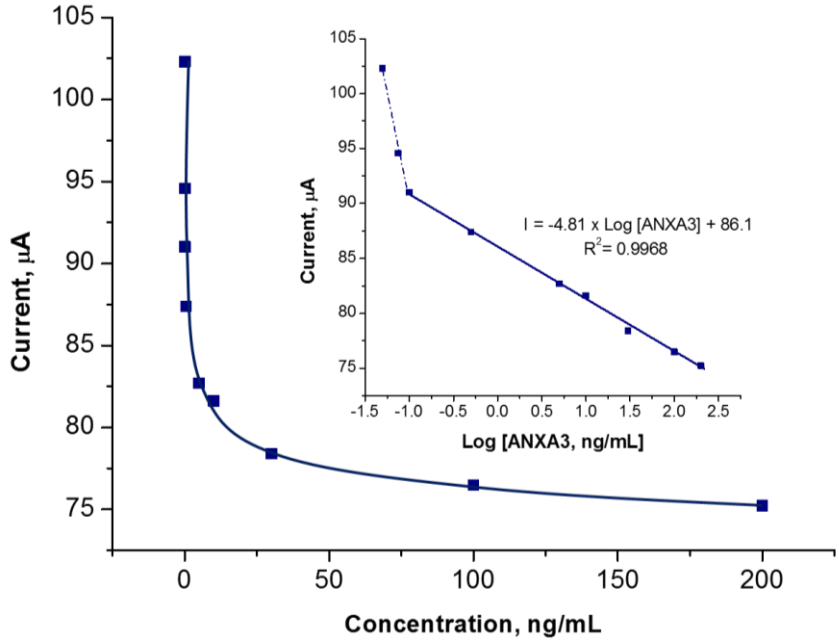

Figure **4.6**: Calibration curve obtained of PIM based carbon-SPE biosensor obtained by SWV measurements in 5.0 mM $[Fe(CN)_6]^{3-}$ and 5.0 mM $[Fe(CN)_6]^{4-}$ in PBS buffer. **Inset**: Linear calibration plot obtained for Annexin A3.

The limit of detection (LOD) was 0.095 ng/mL and it was estimated by the intersection section of the two linear parts of the response function [9]. The LOD obtained in this work for the detection of ANXA3 was of the same order of magnitude of that obtained by other electrochemical device described in the literature [10] but using a more complex analytical methodology, making use of an antibody as (bio)recognition element.

The NIM sensor displayed an inconsistent response over the concentration range of the calibration curve used for the PIM electrode (Figure 4.7), indicating that in this case the interaction between the protein and polymer was random and uncontrolled. In addition, such behavior confirmed that the binding event on the PIM surface was mainly regulated by the binding sites formed upon the imprinting process.

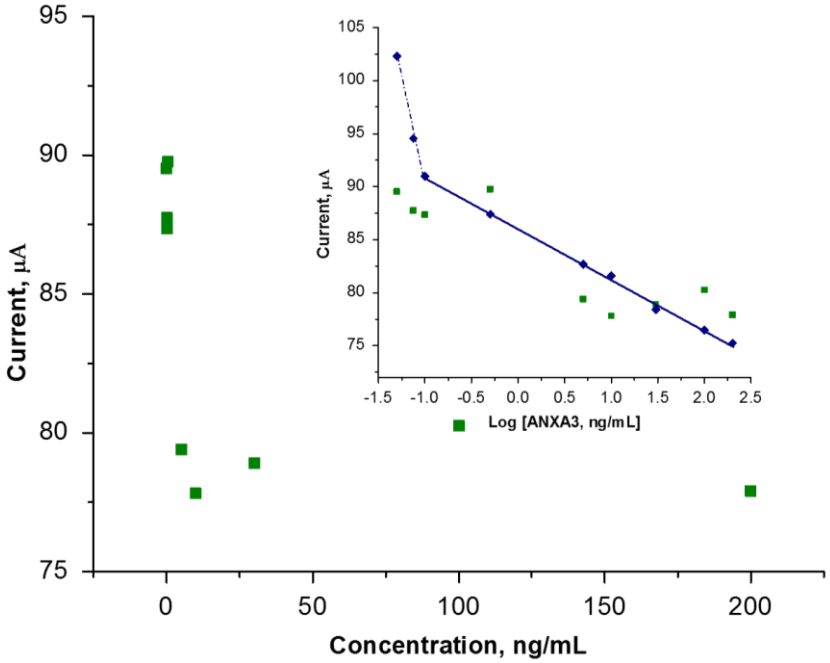

Figure **4.7**: Calibration curve obtained of NIM based carbon-SPE biosensor obtained by SWV measurements in 5.0 mM $[Fe(CN)_6]^{3-}$ and 5.0 mM $[Fe(CN)_6]^{4-}$ in PBS buffer. **Inset**: Linear calibration plot obtained for Annexin A3. For comparison, the linear calibration plot obtained with PIM was also included in the inset of the figure.

4.3.5 Selectivity study and electrode stability

The selectivity of the sensor is of great importance for a successful analytical application. Herein, the interfering species tested were selected among those that may be found in the biological fluids, such as creatinine (1.10 g/L) and urea (25 g/L) [6].

The interference study was carried out by comparing the linear range and the LODs obtained in the absence and in the presence of creatinine and urea and the results were summarized in Table 4.3 The results obtained indicate that the LODs obtained for ANXA3 in the presence of the interfering species are greater (up to 0.098 ng/mL for urea and 0.099 ng/mL for creatinine), linear ranges narrower (from 0.1 to 100 ng/mL for urea and 0.1 to 50 ng/mL for creatinine), when

compared with the ones in the absence of that interfering species. Still, these alterations do not have a large effect for diagnostic purposes, since ANXA3 is physiologically present in the biological fluids at around 2 ng/mL [11].

Table **4.3**: Analytical performance of the ANXA3 biosensor in the presence of the interfering species used in the study.

Interferences	Linear range (ng/mL)	LOD (ng/mL)
Creatinine	0.1 - 50	0.099
Urea	0.1 - 100	0.098
----	0.1 - 200	0.095

The biosensor offered a stable response within time and could be re-used for ~3 times. Reusing was possible after cleaning with H_2SO_4 over night at 45 °C and subsequent washing with PBS and ultra-pure water. Such limitation of ~3 times reuse was a consequence of the destruction of the carbon layer deposited on the commercial SPE. No evidences were found about alterations on the PIM layer, but the device was destroyed after that and could not be used for electrical readings. In these conditions, the biosensor response had an average relative standard deviation of 3% compared to the first use.

4.3.6 Application

The PIM sensor was applied in the determination of ANXA3 in artificial urine samples. For this purpose, blank samples of synthetic urine were spiked with ANXA3 in order to obtain concentrations ranging from 0.2 to 20.0 ng/mL. The results obtained for three concentration levels of ANXA3 were summarized in Table 4.4.

Table **4.4**: Determination of ANXA3 in urine samples.

Sample	ANXA3 added (ng/mL)	ANXA3 Found (ng/mL)	Recovery (%)	Relative error (%)
1	0.2	0.18±0.05	110.4±26.3	+9.5
2	1.5	1.63±0.36	92.2±2.99	-8.5
3	20.0	20.81±5.69	96.1±12.9	-4.1

A good agreement was obtained between added and found amounts of ANXA3. In the presence of 1.10 g/L and 25.0 g/L of creatinine and urea, respectively, the overall recoveries ranged from 92.2 to 110.4%, with an average relative error of 7.4%, suggesting that the proposed sensor may have successful results under real applications.

4.4 Conclusions

The technique of molecular imprinting over the surface of a SPE produced a simple and low cost electrochemical biosensor, for the determination of ANXA3 in urine. The biosensor was obtained by simple electropolymerization of CAF in the presence of ANXA3 on carbon-SPEs.

The biosensor presented high analytical performance features, such as large concentration linear range (0.10 to 200 ng/mL), low LODs (0.095 ng/mL), and high selectivity, with a performance similar to analogous immunosensor devices. The biosensor was successfully applied to the analysis of ANXA3 in synthetic urine samples. The proposed detection methodology can be particularly suitable for screening assays carried out in analytical laboratories.

4.5 References

[1] H. Filik, A.A. Avan, S. Aydar, G. Çetintaş, Determination of Acetaminophen in the Presence of Ascorbic Acid Using a Glassy Carbon

Electrode Modified with Poly(Caffeic acid), *International Journal of Electrochemical Science*, 9 (2014) 148-160.

[2] W. Ren, H.Q. Luo, N.B. Li, Electrochemical Behavior of Epinephrine at a Glassy Carbon Electrode Modified by Electrodeposited Films of Caffeic Acid, *Sensors*, 6 (2006) 80-89.

[3] W. Ren, H.Q. Luo, N.B. Li, Simultaneous voltammetric measurement of ascorbic acid, epinephrine and uric acid at a glassy carbon electrode modified with caffeic acid, *Biosensors and Bioelectronics*, 21 (2006) 1086-1092.

[4] N.B. Li, W. Ren, H.Q. Luo, Caffeic Acid-Modified Glassy Carbon Electrode for the Simultaneous Determination of Epinephrine and Dopamine, *Electroanalysis*, 19 (2007) 1496-1502.

[5] P. T. Lee, K. R. Ward, K. Tschulik, G. Chapman, R.G. Compton, Electrochemical Detection of Glutathione Using a Poly(caffeic acid) Nanocarbon Composite Modified Electrode, *Electroanalysis*, 26 (2014) 366-373.

[6] C.J. Collins, A. Berduque, D.W.M. Arrigan, Electrochemically Modulated Liquid−Liquid Extraction of Ionized Drugs under Physiological Conditions, *Analytical Chemistry*, 80 (2008) 8102-8108.

[7] X. Kan, Z. Xing, A. Zhu, Z. Zhao, G. Xu, C. Li, H. Zhou, Molecularly imprinted polymers based electrochemical sensor for bovine hemoglobin recognition, *Sensors and Actuators B: Chemical*, 168 (2012) 395-401.

[8] H. S. Hsu, P. Y. Chung, J. H. Zhang, S. J. Sun, H. Chou, H. C. Su, C. H. Lee, J. Chen and J. C. A. Huang, Observation of bias-dependent low field positive magneto-resistance in Co-doped amorphous carbon films, *Applied Physics Letters*, 97 (2010) 032503.

[9] R.P. Buck, E. Lindner, Recommendations for nomenclature of ion-selective electrodes (IUPAC Recommendations 1994), *Pure and Applied Chemistry*, 66 (1994) 2527-2536.

[10] Y.J. Kim, M.M. Rahman, J.J. Lee, Ultrasensitive and label-free detection of annexin A3 based on quartz crystal microbalance, *Sensors and Actuators B: Chemical*, 177 (2013) 172-177.

[11] M. Schostak, G.P. Schwall, S. Poznanovic, K. Groebe, M. Mueller, D. Messinger, K. Miller, H. Krause, A. Pelzer, W. Horninger, H. Klocker, J.

Hennenlotter, S. Feyerabend, A. Stenzl, A. Schrattenholz, Annexin A3 in Urine: A Highly Specific Noninvasive Marker for Prostate Cancer Early Detection, *Journal of Urology*, 181 (2009) 343-353.

5

Microseminoprotein-Beta electrochemical sensor

Publication resulted from the work developed:

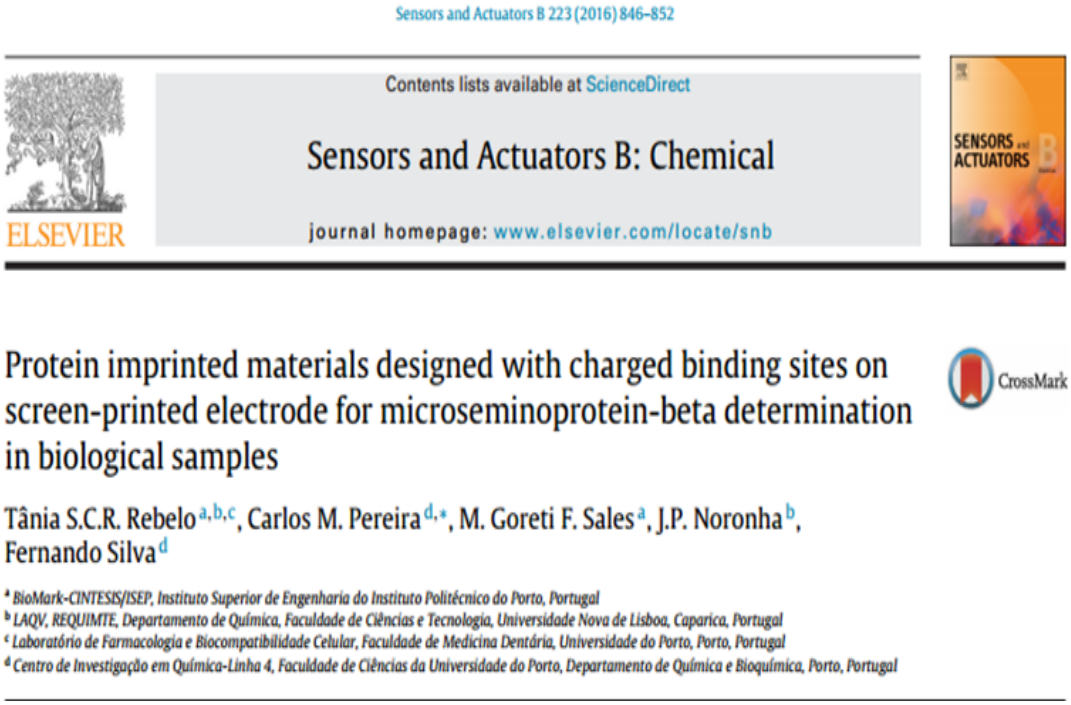

Sensors and Actuators B 223 (2016) 846–852

Contents lists available at ScienceDirect

Sensors and Actuators B: Chemical

journal homepage: www.elsevier.com/locate/snb

Protein imprinted materials designed with charged binding sites on screen-printed electrode for microseminoprotein-beta determination in biological samples

Tânia S.C.R. Rebelo[a,b,c], Carlos M. Pereira[d,*], M. Goreti F. Sales[a], J.P. Noronha[b], Fernando Silva[d]

[a] BioMark-CINTESIS/ISEP, Instituto Superior de Engenharia do Instituto Politécnico do Porto, Portugal
[b] LAQV, REQUIMTE, Departamento de Química, Faculdade de Ciências e Tecnologia, Universidade Nova de Lisboa, Caparica, Portugal
[c] Laboratório de Farmacologia e Biocompatibilidade Celular, Faculdade de Medicina Dentária, Universidade do Porto, Porto, Portugal
[d] Centro de Investigação em Química-Linha 4, Faculdade de Ciências da Universidade do Porto, Departamento de Química e Bioquímica, Porto, Portugal

5.1 Introduction

After the successful application of CAF to create a protein-imprinted layer for a PCa biomarker (in chapter 4), it was important to understand if this material would be suitable for tracking another biomarker. The overall process was simple and more appropriate to up-scaling procedures than batch-based approaches. Furthermore, and as explained earlier, CAF has been employed in the fabrication of electrochemical sensors for recognition and detection of some biomolecules [1-

5] offering good biocompatibility properties and simple procedures for the immobilization of biomolecules.

In addition, the use of charged labels around the imprinted binding sites was found a suitable approach to enhance both sensitivity and linearity of a protein biosensors (in chapter 3). When the binding site bears opposite charges of those prevailing at the outer surface of the protein, the template will be attracted to its binding position by complementary charge arrangement.

Thus, this work proposes a novel PIM material for MSMB, using poly(CAF) material as imprinted layer on screen-printed carbon electrodes and having dopamine as added charged labels to the binding site. Overall, the construction of an electrochemical biosensor was based on the electropolymerization of CAF in the presence of MSMB that was surrounded by dopamine, aiming to increase its site specificity. Dopamine was introduced as a charged monomer able to self-organize around the protein and creating, in this way, binding sites that would increase the specificity of imprinted cavities towards MSMB. This approach has been established by following a systematic investigation of several analytical parameters of interest, such as sensitivity, dynamic linear range, limit of detection and selectivity, in order to evaluate the performance of the MSMB electrochemical biosensor for PCa screening.

5.2 Experimental Procedure

5.2.1 Reagents and solutions

Ultra-pure water (resistivity > 18 MΩ.cm at 25 °C) was used throughout the work for cleaning and solution preparation. All chemicals were of analytical grade and used without any further purification. CAF, sodium sulfate, potassium phosphate, ammonium chloride, urea, creatinine, BSA and 3-hydroxytyramine (dopamine) were purchased from Sigma-Aldrich; MSMB from OriGene; sodium

chloride from Panreac; sodium hydrogen carbonate, calcium chloride dehydrate, potassium chloride, potassium ferricyanide ($K_3[Fe(CN)_6]$) and potassium ferrocyanide trihydrate ($K_4[Fe(CN)_6]$) from Merck.

5.2.2 Solutions

PBS solution of pH 7.2 (0.1 M NaH_2PO_4 and 0.1 M Na_2HPO_4) were used in this work. Stock solutions of MSMB (0.2 mg/mL) were prepared in PBS (pH 7.2) and less concentrated standards were prepared by suitable dilution in PBS buffer solution. Electrochemical assays were performed in the presence of 5.0×10^{-3} mol/L $K_3[Fe(CN)_6]$ and $K_4[Fe(CN)_6]$ in PBS.

The artificial urine solution had the following composition: calcium chloride dihydrate (1.103 g/L), sodium chloride (2.295 g/L), sodium sulfate (2.25 g/L), potassium phosphate (1.40 g/L), potassium chloride (1.60 g/L), ammonium chloride (1.00 g/L), urea (25.0 g/L) and creatinine (1.10 g/L) [6]. Artificial serum solution was prepared with the following composition: sodium chloride (7.01 g/L), sodium hydrogen carbonate (1.68 g/L) and BSA (30 g/L) [7].

5.2.3 Apparatus

The electrochemical measurements were conducted in a PGSTAT302N potentiostat/galvanostat from Metrohm Autolab, containing a FRA impedimetric module and controlled by computer with GPES 4.9 software. SPEs had carbon working electrodes with 4 mm diameter (DRP-C110) and were from DropSens (Spain). SPEs were connected to the Autolab by means of a suitable box, also from DropSens.

5.2.4 Synthesis of PIM on carbon support

Before modification, the carbon-SPE electrodes were electrochemically cleaned by cycling the potential from -0.2 V to +1.0 V, at a 100 mV/s scan-rate, in a 0.5

mol/L sulfuric acid solution. Cycling procedures were repeated until the resulting voltammograms were reproducible (~30 cycles were necessary). The electrodes were then thoroughly rinsed with ultra-pure water and dried under N_2 atmosphere.

Next, the imprinted layer of poly(CAF) was assembled on the cleaned carbon surface, where the electropolymerization of CAF was achieved by adapting the procedure described in reference [3]. PIM materials were obtained by casting over the three-electrode system of the SPE 30 μL of a solution containing 2.0×10^{-4} mol/L CAF and 5.0×10^{-3} ng/mL MSMB, in PBS buffer (pH 7.2). Electropolymerization was conducted by applying a constant potential of +2.0 V for 30 s. The polymer modified electrode was then thoroughly washed with ultra-pure water, dried under N_2 and incubated overnight in a 1 mol/L H_2SO_4 solution, at 45 °C, in order to remove the protein [8]. The resulting PIM layer was washed with PBS buffer for several times, aiming to remove the remaining protein fragments and H_2SO_4, and finally rinsed with ultra-pure water and dried under N_2.

The preparation of the PIM material with charged-binding sites (C/PIM) was identical to the PIM, being the only difference the addition of dopamine to the synthetic process. Dopamine was introduced as a charged monomer, labelling the binding site around the protein. Thus, for this purpose, 30 μL of a solution containing 5.0×10^{-3} mg/mL of MSMB and 5.0×10^{-2} mg/mL dopamine in PBS buffer (pH 7.2) was incubated overnight in fridge at 4 °C. After that, 5 μL a solution with 2.0×10^{-4} mol/L of CAF was added to the previous solution. After homogenization, the resulting solution was ready to be casted on the SPE electrodes and to follow similar electropolymerization procedures.

The schematic representation of the overall procedure adopted for the preparation of PIM and C/PIM materials is described in Figure 5.1. As control,

non-imprinted sensing layers were prepared in parallel, by excluding from procedure both protein and charged monomers (NIM) or only charged monomers (C/NIM).

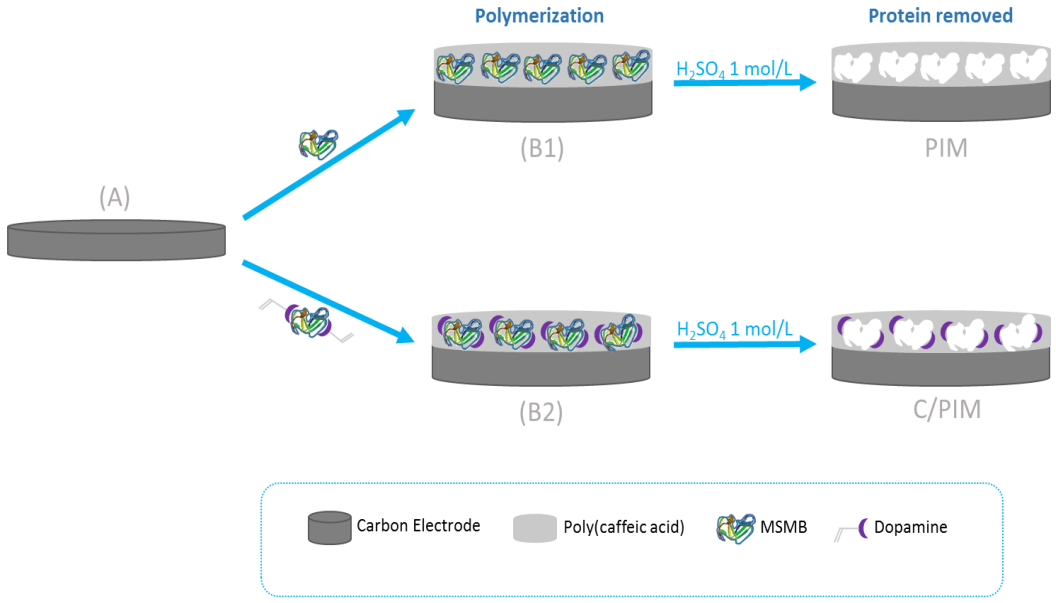

Figure **5.1**: Schematic representation of the synthetic process of PIM and C/PIM. **A**: Carbon working electrode of the SPE; **B1**: Poly(CAF) layer with entrapped template; **B2**: Poly(CAF) layer with template holding electrostatic interactions with dopamine.

5.2.5 Electrochemical procedures

SWV and EIS measurements were conducted in triplicate and a redox probe solution containing 5.0×10^{-3} mol/L $[Fe(CN)_6]^{3-}$ and 5.0×10^{-3} mol/L $[Fe(CN)_6]^{4-}$, and prepared in PBS buffer of pH 7.2, was used. In SWV, a potential window from –0.5 to 0.6 V, was used at a frequency of 10 Hz, a step potential of 10 mV and amplitude of 50 mV. EIS was performed at open circuit potential (~0.12 V), using a sinusoidal potential perturbation with an amplitude of 0.1 mV and the number of frequencies equal to 50, logarithmically distributed over a frequency range of 0.1–100 kHz.

Calibration curves plotted the peak current values obtained from SWV measurements against the logarithm of MSMB concentration (ranging from 0.1 to 200 ng/mL, in PBS buffer, pH 7.2).

All experiments were carried out using a 0.1 M PBS pH 7.2, an electrolyte solution close to the physiological conditions.

5.2.6 Determination of MSMB in synthetic urine and artificial serum

Synthetic urine and artificial serum solutions with different concentrations of MSMB were used for the evaluation of sensor response. These were prepared by adding a known amount of MSMB (from 0.2 to 20.0 ng/mL) to the synthetic urine or to the artificial serum solution.

5.3 Results and discussions

5.3.1 Imprinting stage

The studies carried out in chapter 4 indicated that the polymerization of CAF was favored by applying +2.0 V for 30 s. These conditions were tested for a fixed concentration of 2.0×10^{-4} mol/L CAF, having or not MSMB, in a concentration of 5×10^{-3} ng/mL.

Charged labels (C) were further introduced in the binding sites of the imprinted material (C/PIM). This was done during the imprinting stage by adding dopamine to the solution. Dopamine had an amine group that was positively charged at the working pH. The selection of Dopamine accounted the fact that MSMB (isoelectric point of 5.6) had a negative overall net charge at pH 7.2 and under physiological conditions. In addition, dopamine also contained two hydroxyl groups linked to a benzene aromatic ring, which were capable of

participating in the polymerization of CAF, thereby allowing their covalent bonding to the polymeric network.

The imprinted sites were obtained by removing the protein template with 1 mol/L H_2SO_4 solution at 45 °C, incubated overnight. The selection of an acidic solution and temperature above 45 °C contributed to the denaturation of the protein, thereby helping the protein removal from the corresponding imprinted position through its denaturation.

5.3.2 Control of the surface modification by impedance measurement

EIS studies were used to follow the carbon-SPE modification after each chemical change. These can be probed by monitoring the changes in the electron transfer properties of redox systems, such as $[Fe(CN)_6]^{4-}/[Fe(CN)_6]^{3-}$, as shown in Figure 5.2. Data was fitted to the Randles equivalent circuit, in order to extract the numerical values of the R_{ct} that change significantly along the chemical modification of the surface. The obtained values are displayed in Tables 5.1 and 5.2.

The overall behavior was similar to that presented in the previous chapter, having R_{ct} dominated the greater changes. In general, the obtained results clearly showed an increase in the R_{ct} after polymerization. This increase was visible both for PIM and C/PIM, due to the modifications made on the electrode surface. In general, the presence of polymer/protein hindered the access of the redox probe ($[Fe(CN)_6]^{4-}/[Fe(CN)_6]^{3-}$) to the surface, thereby limiting the charge transfer process (at the electrode surface). It is noteworthy that the increase in R_{ct} was greater in the case of C/PIM, where the polymerization was performed in presence of dopamine. In addition, the significant difference between the pairs

PIM–NIM and C/PIM–C/NIM accounted the presence of MSMB entrapped within the polymeric matrix.

In the final step of the PIM and C/PIM synthesis, after the protein removal with H_2SO_4, a decrease in the charge transfer resistance was observed, suggesting that MSMB was successfully extracted from the polymer. In addition, NIM and C/NIM also shifted to similar values of the imprinted-based materials, thereby confirming that such change in R_{ct} resulted from the leaching to smaller polymeric fragments or unreacted species that were adsorbed on the surface.

In the same way, an increase in the R_{ct} was observed for the NIM and C/NIM electrode after the eletropolymerization of CAF in absence of MSMB. After, the treatment of the electrode surface with H_2SO_4, the EIS profiles obtained were similar to the PIM and C/PIM electrodes, indicating the removal of a small fraction of polymer attached to the electrode surface.

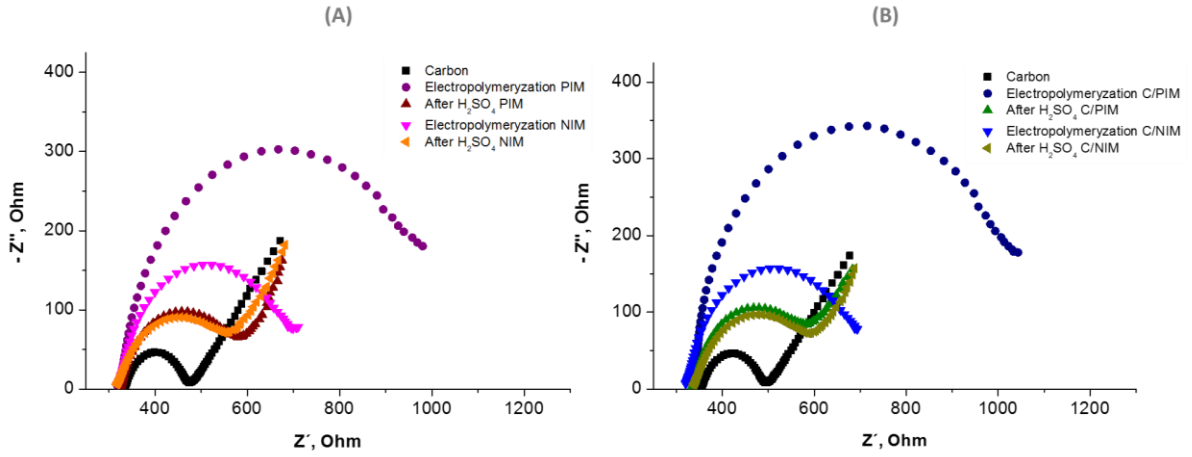

Figure **5.2**: EIS data over the subsequent modification steps of the carbon-SPE, in 5.0 mM $[Fe(CN)_6]^{3-}$ and 5.0 mM $[Fe(CN)_6]^{4-}$, in PBS buffer. **A**: Materials without oriented charges (PIM and NIM) and **B**: Materials with charged binding sites (C/PIM and C/NIM).

Table **5.1**: Fitting parameters extracted from electrochemical impedance data using the Randles type equivalent circuit for PIM-NIM.

Parameters	Carbon	Electropolymerization		After H_2SO_4	
		PIM	NIM	PIM	NIM
R_S (Ω)	331.0	340.0	334.0	334.0	319.0
Q ($\Omega^{-1}s^{-n}$)	7×10^{-5}	2×10^{-5}	4×10^{-5}	1×10^{-5}	6×10^{-5}
n	0.86	0.92	0.81	0.71	0.80
R_{ct} (Ω)	150.0	582.0	481.0	202.4	274.4
W ($\Omega s^{-1/2}$)	6×10^{-3}	6×10^{-3}	6×10^{-3}	6×10^{-3}	6×10^{-3}

Table **5.2**: Fitting parameters extracted from electrochemical impedance data using the Randles type equivalent circuit for C/PIM-C/NIM.

Parameters	Carbon	Electropolimerization		After H_2SO_4	
		C/PIM	C/NIM	C/PIM	C/NIM
R_S (Ω)	331.0	343.0	336.0	327.0	345.0
Q ($\Omega^{-1}s^{-n}$)	7×10^{-5}	3×10^{-5}	2×10^{-5}	8×10^{-5}	9×10^{-5}
n	0.86	0.87	0.85	0.79	0.71
R_{ct} (Ω)	150.0	640.0	542.0	191.9	266.6
W ($\Omega s^{-1/2}$)	6×10^{-3}	6×10^{-3}	6×10^{-3}	6×10^{-3}	6×10^{-3}

5.3.3 Performance of the sensors

The main analytical features of the MSMB sensors were prepared without and with charged labels (PIM or C/PIM) were evaluated by SWV.

The calibrations curves obtained are shown in Figure 5.3 and plotte peak current as function of MSMB logarithm concentration (between 0.050 and 200 ng/mL). MSMB binding was revealed by a decrease in the typical anodic peak current of the $[Fe(CN)_6]^{4-}/[Fe(CN)_6]^{3-}$ redox probe. Higher MSMB concentrations yielded

smaller current peaks. As shown in Figure 5.3, it is found that the calibration curves for PIM and C/PIM followed a linear pattern versus Log[MSMB], respectively, from 0.1 to 200 ng/mL and 0.5 to 100 ng/mL, with a correlation coefficient of 0.9939 and 0.9945. The limit of detection (LOD) was 0.090 ng/mL for PIM and 0.12 ng/mL for C/PIM, which were estimated by the intersection of the two linear parts of the response function [9].

In general, the calibration curves obtained indicated that the charged labels around the protein improved the sensitivity (from -6.67 to -7.59 μA/decade [MSMB, ng/mL]), but decreased the detection capability of the device. Thus, the best sensor material prepared form MSMB detection was PIM, containing only poly(CAF) and yielding sensors of wider working range and lower LOD.

The NIM and C/NIM sensors displayed an inconsistent response over the concentration range under study (Figure 5.3). These results indicated that the interaction between the protein and polymer was random and uncontrolled, and evidenced that the response of the imprinted material was mainly controlled by the interaction of MSMB with its binding site.

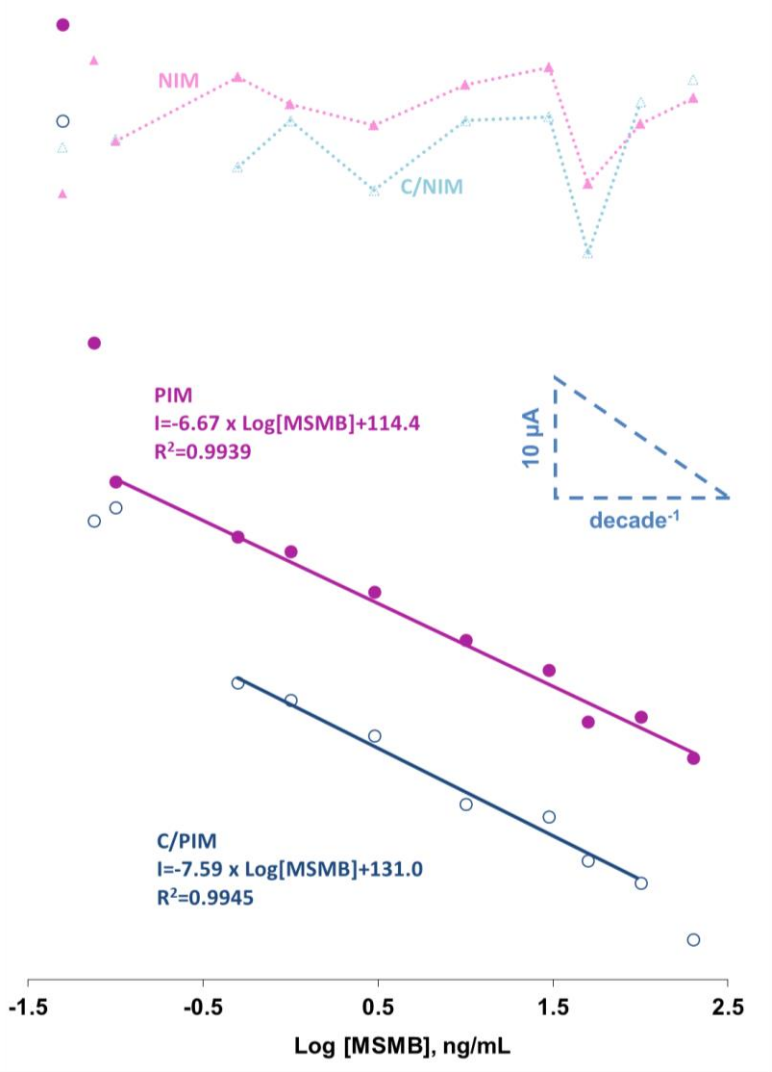

Figure **5.3**: Calibration curves of PIM, C/PIM, NIM and C/NIM based carbon-SPE biosensors obtained by SWV measurements in 5.0 mM $[Fe(CN)_6]^{3-}$ and 5.0 mM $[Fe(CN)_6]^{4-}$ PBS buffer.

5.3.4 Selectivity study and electrode stability

The selectivity of the sensor is very important for a successful analytical application, where the sensory surface is exposed to many species that are present in biological fluids, such as urine and serum, and that may interfere with the analytical data. Therefore, instead of studying the individual effect of each interfering species on the performance of the electrodes, the global effect of the sample matrix was evaluated by calibrating the devices in such matrix. Synthetic

biological fluids were selected for this purpose, containing a similar composition to that expected in nature.

Thus, the selectivity study was carried out by comparing the linear ranges, slopes and the LODs obtained through the calibration curves of PIM and C/PIM sensors in artificial serum and artificial urine. The obtained results are resumed in Table 5.3. The results obtained showed that the PIM sensor in contact with biological fluids decreased its sensitivity (-5.50 μA/decade in serum; -6.38 μA/decade in urine), increased LODs (0.10 ng/mL serum; 0.18 ng/mL urine) and linear concentration range was narrower (0.5-200 ng/mL), while the C/PIM sensor increased sensitivity (-7.95 μA/decade serum; -13.52 μA/decade urine), decreased LODs (0.084 ng/mL serum; 0.079 ng/mL urine) and kept the linear concentration range (0.5-100 ng/mL).

Still, once average values of MSMB present in the serum under normal physiological conditions are around 12 ng/mL, any of sensors is capable of measuring concentrations of MSMB down to 0.5 ng/mL, and detect the decreasing of MSMB concentrations due to prostate cancer related processes [10].

In terms of signal stability, both PIM and C/PIM devices offered a stable response and could be re-used a few times (≈3 times), as indicated in Figure 5.4. The behavior is similar to that obtained with protein-imprinted materials relying on poly(CAF), for which the same cleaning approach was taken here: cleaning with H_2SO_4 for 12 h at 45 °C and subsequent washing with PBS and ultra-pure water. In these conditions, the biosensor response has an average relative standard deviation of 5% in terms of absolute current.

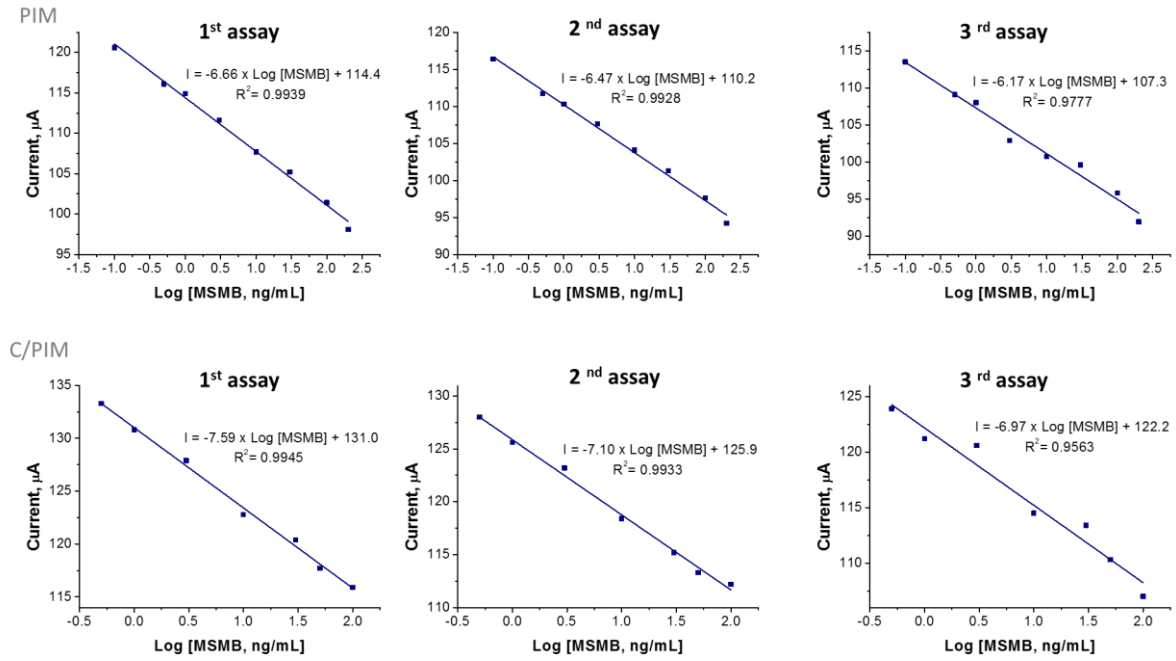

Figure **5.4**: Calibration curves displaying the effect of reused PIM and C/PIM carbon-SPE biosensors obtained by SWV measurements in 5.0 mM $[Fe(CN)_6]^{3-}$ and 5.0 mM $[Fe(CN)_6]^{4-}$ PBS buffer.

As discussed previously, PIM showed better characteristics than C/PIM when calibrated in PBS, but worse analytical features when calibrated in synthetic biological medium. Thus, it seems that charged rebinding sites are clearly contributing to the selectivity of the device, while also improving its sensitivity.

Thus, for application purposes, the C/PIM devices contained the best sensory materials, displaying improved sensitivity, selectivity and LOD. The quality of its linearity features was also better, as expressed by the squared correlation coefficients (Table 5.3), with a minimum value of 0.994. The C/PIM was therefore chosen to proceed with the application of the sensors to the analysis of MSMB in biological fluids.

Table **5.3**: Calibration features of the biosensors in the PBS, serum and urine artificial.

Characteristics	PIM			C/PIM		
	PBS	Serum	Urine	PBS	Serum	Urine
Slope (μA/decade)	-6.67	-5.50	-6.38	-7.29	-7.97	-13.52
LOD (ng/mL)	0.090	0.100	0.180	0.120	0.084	0.079
R^2	0.994	0.991	0.991	0.995	0.994	0.999
Linear concentration range (ng/mL)	0.1-200	0.5-200	0.5-200	0.5-100	0.5-100	0.5-100

5.3.5 Application

The C/PIM biosensor was used for the determination of MSMB in artificial urine and serum samples. Blank samples of synthetic urine and serum were spiked with MSMB in order to obtain concentrations ranging from 0.2 to 20.0 ng/mL. The results obtained for four concentration levels tested within this range are summarized in Table 5.4.

For samples 2, 3 and 4 in serum, the recoveries ranged from 92.8 to 104.1 % with an average relative error of 4.9 %; in urine the recoveries ranged from 91.5 to 104.9 % with an average relative error of 5.7 %, these results suggesting that the proposed sensor may have success in real applications. Sample 1, in serum and urine, has weaker recoveries and high relative errors, but this is due to the little concentration used.

Table **5.4**: Determination of MSMB in serum and urine samples.

Sample	MSMB (ng/mL)	Serum			Urine		
		Found (ng/mL)	Recovery (%)	Relative error (%)	Found (ng/mL)	Recovery (%)	Relative error (%)
1	0.2	0.17±0.05	114.6±19.4	12.8	0.22± 0.05	90.0±18.3	-11.1
2	1.0	1.1±0.11	92.8±9.2	-7.8	1.1± 0.13	91.5±9.1	-9.2
3	3.0	2.9±0.10	104.1±3.7	4.0	2.9± 0.19	104.9±7.9	+4.7
4	20.0	19.4±0.89	103.0±3.8	3.0	20.6± 1.1	97.0±7.0	-3.1

5.4 Conclusions

Once more, the molecular imprinting technique was successfully applied over the surface of a carbon-SPE to produce a simple and low cost electrochemical sensor for the determination of MSMB in biological fluids. The presence of charged labels in the rebinding site enabled the synthesis of a more selective and sensitive device. The (bio)recognition element of the biosensor was prepared by electropolymerizing CAF in the presence of MSMB and dopamine (C/PIM).

In general, the C/PIM biosensor showed simplicity in design, short measuring time, reusability, low limit of detection and good selectivity. This biosensor was successfully applied to the analysis of MSMB in serum and urine artificial samples. In a near future this can be a valuable alternative method for screening MSMB in point-of-care or for coupling this device to a multiplex reading involving a panel of relevant biomarkers in PCa.

5.5 References

[1] H. Filik, A.A. Avan, S. Aydar, G. Çetintaş, Determination of Acetaminophen in the Presence of Ascorbic Acid Using a Glassy Carbon Electrode Modified with Poly(Caffeic acid), *International Journal of Electrochemical Science*, 9 (2014) 148-160.

[2] W. Ren, H.Q. Luo, N.B. Li, Simultaneous voltammetric measurement of ascorbic acid, epinephrine and uric acid at a glassy carbon electrode modified with caffeic acid, *Biosensors and Bioelectronics*, 21 (2006) 1086-1092.

[3] W. Ren, H.Q. Luo, N.B. Li, Electrochemical Behavior of Epinephrine at a Glassy Carbon Electrode Modified by Electrodeposited Films of Caffeic Acid, *Sensors*, 6 (2006) 80-89.

[4] N.B. Li, W. Ren, H.Q. Luo, Caffeic Acid-Modified Glassy Carbon Electrode for the Simultaneous Determination of Epinephrine and Dopamine, *Electroanalysis*, 19 (2007) 1496-1502.

[5] P. T. Lee, K. R. Ward, K. Tschulik, G. Chapman, R.G. Compton, Electrochemical Detection of Glutathione Using a Poly(caffeic acid) Nanocarbon Composite Modified Electrode, *Electroanalysis*, 26 (2014) 366-373.

[6] C.J. Collins, A. Berduque, D.W.M. Arrigan, Electrochemically Modulated Liquid−Liquid Extraction of Ionized Drugs under Physiological Conditions, *Analytical Chemistry*, 80 (2008) 8102-8108.

[7] K.P.G. Ralloff, P. Westh, R.A. Purssell, M. Pudek, Y. Koga, Non-ideality of methanol solution's of artificial serum in the mole fraction range from 5 x 10^{-4} to 5 x 10^{-3} at 25 degrees C, *Fluid phase equilibria*, 207 (2003) 301-317.

[8] X. Kan, Z. Xing, A. Zhu, Z. Zhao, G. Xu, C. Li, H. Zhou, Molecularly imprinted polymers based electrochemical sensor for bovine hemoglobin recognition, *Sensors and Actuators B: Chemical*, 168 (2012) 395-401.

[9] R.P. Buck, E. Lindner, Recommendations for nomenclature of ion-selective electrodes (IUPAC Recommendations 1994), *Pure and Applied Chemistry*, 66 (1994) 2527-2536.

[10] C. Valtonen-André, C. Sävblom, P. Fernlund, H. Lilja, A. Giwercman, Å. Lundwall, Beta-Microseminoprotein in Serum Correlates With the Levels in Seminal Plasma of Young, Healthy Males, *Journal of Andrology*, 29 (2008) 330-337.

6

Sarcosine electrochemical sensor

Publication resulted from the work developed:

Analytica Chimica Acta 850 (2014) 26–32

Contents lists available at ScienceDirect

Analytica Chimica Acta

journal homepage: www.elsevier.com/locate/aca

Sarcosine oxidase composite screen-printed electrode for sarcosine determination in biological samples

Tânia S.C.R. Rebelo [a,b,c], Carlos M. Pereira [d,*], M.Goreti F. Sales [a], João P. Noronha [b], J. Costa-Rodrigues [c], Fernando Silva [d], M.H. Fernandes [c]

[a] BioMark/ISEP, Instituto Superior de Engenharia do Instituto Politécnico do Porto, Portugal
[b] REQUIMTE/FCT, Faculdade de Ciências e Tecnologia da Universidade Nova de Lisboa, Portugal
[c] Laboratório de Farmacologia e Biocompatibilidade Celular, Faculdade de Medicina Dentária, Universidade do Porto, Porto, Portugal
[d] Centro de Investigação em Química-Linha 4, Faculdade de Ciências da Universidade do Porto, Departamento de Química e Bioquímica, Porto, Portugal

6.1 Introduction

The direct determination of SAR may be difficult, but its indirect quantification can be achieved by the reaction between SAR and SOX, which catalyses the oxidative demethylation of SAR to glycine, formaldehyde, and hydrogen peroxide. The methods commonly used for the indirect determination of SAR are colorimetry [1, 2], fluorimetry [3] and electrochemical sensors with immobilization of the enzyme on the electrode surface [4-8]. The enzyme immobilization is a promising choice, due to the intrinsic advantages associated with their high catalytic activity and enzyme specificity for their substrates. The

electrode surfaces can usually be mass produced, stored and used as required and in some cases re-used decreasing the cost of the detection process.

In this work, we describe the construction of a novel SAR biosensor based on the covalent immobilization of SOX, using EDAC and NHS, on the surface of the carbon-SPE. The selectivity of the electrochemical biosensor was improved by covering the electrode surface with Nafion. Nafion is used due to its film hydrophobicity and enzyme-favored environment as well as to enhance selectivity of the sensor by electrostatic repulsion of unwanted species [9, 10].

The catalyzed oxidation of SAR, mediated by SOX, has as final products not only glycine and formaldehyde but also H_2O_2 (Eq. 6.1). This last one will permit indirect detection of SAR through its electrochemical detection (Eq. 6.2).

$$\textbf{Sarcosine} + H_2O + O_2 \xrightarrow{SOX} \textbf{Formaldehyde} + \textbf{Glycine} + H_2O_2 \qquad \text{Eq. } \mathbf{6.1}$$

$$H_2O_2 \xrightarrow{0.6V} O_2 + 2H^+ + 2e^- \qquad \text{Eq. } \mathbf{6.2}$$

For this purpose, this work presents a systematic investigation study of several experimental parameters. Calibration slopes, dynamic linear range, LOD, and selectivity were investigated to evaluate the performance of the SAR biosensor for PCa fast and non-invasive screening.

6.2 Experimental Procedure

6.2.1 Reagents and solutions

SOX from *Bacillus sp* (lyophilized powder, 25-50 units/mg), EDAC, Nafion® 117 solution, glutaraldehyde (50 %), sodium sulfate, potassium phosphate,

ammonium chloride, urea and creatinine were purchased from Sigma-Aldrich. NHS was obtained from Fluka; sodium chloride from Panreac; and calcium chloride dihydrate and potassium chloride were obtained from Merck. All chemicals were of analytical grade and used without further purification.

PBS buffer solutions of pH 7.2 were used in this work, prepared with 0.1 M $NaHPO_4$ and 0.1 M Na_2PO_4. Stock solutions of SAR ($1x10^{-3}$ M) were prepared in PBS (pH 7.2) and less concentrated standards were prepared by suitable dilution in the buffer solution. Synthetic urine solution used herein had the following composition: calcium chloride dihydrate (1.103 g/L), sodium chloride (2.295 g/L), sodium sulfate (2.25 g/L), potassium phosphate (1.40 g/L), potassium chloride (1.60 g/L), ammonium chloride (1.00 g/L), urea (25.0 g/L) and creatinine (1.10 g/L) [11]. Ultra-pure water (resistivity > 18 MΩ.cm at 25 ºC) was used throughout.

6.2.2 Apparatus

The electrochemical measurements were carried out using a potentiostat/galvanostat Autolab Eco Chemie PSTAT10 interfaced to a computer with GPES 4.9 software analysis. Carbon-SPEs of 4 mm diameter (DRP-C110) were used as electrochemical cell, being purchased from DropSens (Spain). SPEs were connected to the Autolab by means of a suitable DropSens adaptor box.

Atomic force microscopy (AFM) images were recorded using a Molecular Imaging, PicoLe atomic force microscope. The surface topography was measured using a silicon cantilever/tip (App Nano, model ACT) with a resonance frequency between 200 and 400 kHz. FTIR measurements were performed using a Thermo Scientific Smart iTR Nicolet iS10, coupled to a SAGA smart accessory, also from Thermo Scientific.Raman spectroscopy studies were also conducted, using a Raman spectrometer from Thermo Unicam, equipped with 10 mW laser operating at 532 nm.

6.2.3 Sarcosine Oxidase Immobilization

Aiming to choose the best electrode material and the best SOX immobilization procedure, a preliminary study was carried out first using gold and carbon-SPE. The results obtained with the gold working electrodes were not satisfactory (the voltammograms were not stable, showing high signal interference and leading to higher LOD and reduced linearity). Thus the gold-SPEs were discarded in the early stages of this work.

SPEs with working electrode of carbon and or carbon nanotubes were further tested, using different conditions of SOX immobilization, with the purpose of increasing enzyme stability and biosensor sensitivity. A summary of the different biosensor configurations studied in this work is presented in Table 6.1.

In this chapter, different immobilization procedures of SOX on the surface of the working electrodes are described. The cleaning and oxidation of the surface of the electrodes was achieved after 30 CV cycles from -0.2 to +1.0 V (scan rate: 100 mV/s) in 0.5 M sulfuric acid. This procedure also ensured that the carboxylic acid groups remained on the surface. The electrodes were then thoroughly rinsed with ultra-pure water and dried under N_2.

For sensors # 1, 2, 8, 9 and 10 (Table 6.1), –COOH groups were activated by covering the working electrode surface with 5 μL of a NHS/EDAC solution (10 mM in PBS) for 6 h at room temperature. The reaction of NHS and EDAC at the electrode surface lead to the formation of stable ester surface groups, giving rise to carbon activated surface. The excess of EDAC and NHS was removed by washing the chip with PBS [6]. The –COOH groups present in the electrode surfaces of the sensors # 3, 4, 5, 6 and 7 were not activated.

Table **6.1**: Different procedures used in the modification of the electrodes surfaces.

Sensor #	Working electrode	–COOH activation	Nanoparticles	SOX Immobilization
1	Carbon	NHS/EDAC	____	SOX
2	Carbon Nanotubes	NHS/EDAC	____	SOX
3	Carbon	____	____	SOX + Glutaraldehyde
4	Carbon Nanotubes	____	____	SOX + Glutaraldehyde
5	Carbon	____	Au	SOX + Glutaraldehyde
6	Carbon Nanotubes	____	Au	SOX + Glutaraldehyde
7	Carbon	____	____	SOX + Nafion
8	Carbon	NHS/EDAC	____	SOX + Nafion
9	Carbon	NHS/EDAC	____	SOX+ (SOX + Nafion)
10	Carbon	NHS/EDAC	ZnO	SOX + Nafion

In the following step, gold (Au) or zinc oxide (ZnO) nanoparticles were used to modify the electrode surface by complete evaporation of aqueous nanoparticle solutions (5 μL): sensors # 5 and 6 were modified with gold nanoparticles (≈0.5 nm), synthesized by following the protocol of Chirea *et al.* [12], and sensor # 10 was modified by ZnO (≈200 nm) nanoparticles, synthesized by using the protocol of Jezequel *et al.* [13]. The electrode surface was washed with PBS to remove exceeding and non-adsorbed nanoparticles, and dried under N_2.

The last step of the modification process consisted in the immobilization of SOX on the electrode surface by using the different immobilization procedures described in Table 6.1. The electrode surface of sensors # 1, 2 and 9 were modified by casting 5 μL of SOX solution (1 mg/mL in PBS) on the surface of the carbon

electrode, kept at 4 °C for 20 h (# 1 and 2) or 6 h (# 9); sensors # 3, 4, 5 and 6 were modified by casting 5 μL of a mixture of a solution containing 1 mg SOX in 20 μL PBS and 20 μL 10 % glutaraldehyde, kept at 4 °C for 20 h [4]; finally, sensors # 7, 8, 9 and 10 were modified by dissolving 1 mg of SOX in a mixture of 20 μL of PBS and 20 μL of Nafion 2.5% [8], and casting 5 μL of this solution onto the surface of the electrodes at 4 °C for 20 h. All electrodes were washed with PBS after and dried under N_2.

6.2.4 Electrochemical measurements/optimization

The sensitivity of SAR biosensor was tested by measuring current as function of the applied potential for different solutions with increasing amounts of SAR. Initially 30 μL SAR solution (ranging from $5x10^{-6}$ to $3x10^{-1}$ mM, in 0.1 M PBS of pH 7.2) was placed at the surface of the sensors and a potential scan was applied using a potential range of -1.5 to 0.9 V.

EIS assays were made with redox couple $[Fe(CN)_6]^{3-/4-}$ at open circuit potential (~0.12 V), using a sinusoidal potential perturbation with an amplitude of 0.01 V and the number of frequencies equal to 50, logarithmically distributed over a frequency range of 0.1–100 kHz.

6.2.5 Determination of sarcosine in synthetic urine

Synthetic urine solution with different concentrations of SAR was used for the evaluation sensor # 9. This solution was prepared by adding a known amount of SAR (15 to 65 nM) to the synthetic urine solution.

6.3 Results and discussions

6.3.1 Optimization of the experimental condition for sarcosine detection

Experiments were carried out using a 0.1 M PBS pH 7.2 as electrolyte solution since it is close to the physiological conditions. In addition, this pH value is within the pH range where SOX has maximum stability (from 7 to 10 in 0.1 M PBS) [14].

The sensitivity of SAR biosensor was tested by measuring the current as function of the applied potential (cyclic voltammograms) in the potential range from -1.5 to 0.9 V for the different solutions (5 μL) with increasing concentrations of SAR. The SAR concentration range tested was from 0.5 to 100 μM. The cyclic voltammogram obtained in the absence of SAR was used as the baseline in this work.

The optimization of the potential value that corresponds to the maximum current obtained due to H_2O_2 oxidation produced by the catalytic decomposition of SAR by SOX (Eq.s 6.1 and 6.2) was made, to achieve the lowest detection limit and to minimize the interference from other species present in solution. As an example, the current due to the oxidation of H_2O_2 for the different concentration of SAR was measured for 3 different potentials (0.1, 0.4 and 0.6V) using sensor # 9, as shown Figure 6.1. The current values (n=3) were corrected to eliminate the baseline contribution. After analysis of Figure 6.1, it was observed that, the steady state current response increased with increasing concentration of SAR for the three potentials studied, with the potential of 0.6 V leading to the highest current values. Thus, a potential of +0.6 V was selected for further studies, because an increased sensitivity of the SAR determination was expected.

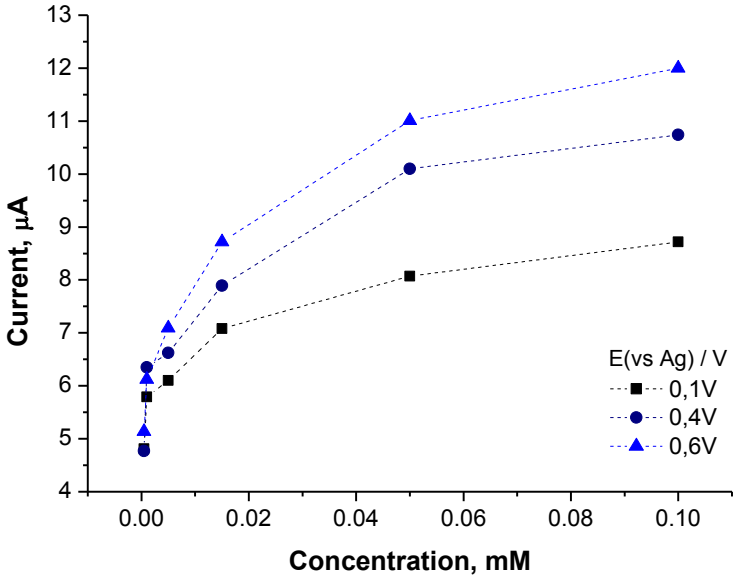

Figure **6.1**: Calibration curves obtained at different potential values using sensor # **9**.

The optimization of the effect of SOX concentration on the performance of the SAR biosensor was also performed and the results obtained are represented in Figure 6.2. Increasing the concentration of SOX has the inconvenience of increasing the cost of the analysis furthermore, from the analysis of data, the maximum current obtained is around 20% less than the current obtained using 1 mg/mL of SOX. In addition, the current for the lowest SAR concentration tested in this evaluation (1 µM) significantly decreases, reducing the linear range of the biosensor response. This may be due to steric effects impairing the interaction between SAR and SOX molecules.

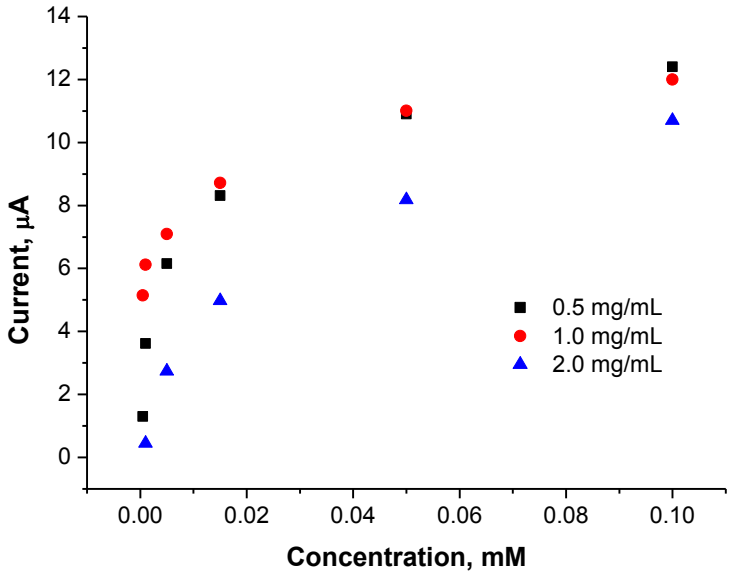

Figure **6.2**: Calibration curves obtained for different concentrations of immobilized SOX (0.5, 1.0 and 2.0 mg/mL).

Reducing the concentration of SOX to a 0.5 mg/mL level did not change the maximum current obtained, however, the current for the lowest SAR concentration tested in this evaluation (1 μM) was lower than that obtained at 1.0 mg/mL SOX, reducing the linear range of the biosensor response. For these reasons, 1.0 mg/mL of enzyme solution was selected for studies related to the performance of the biosensor (Figure 6.3).

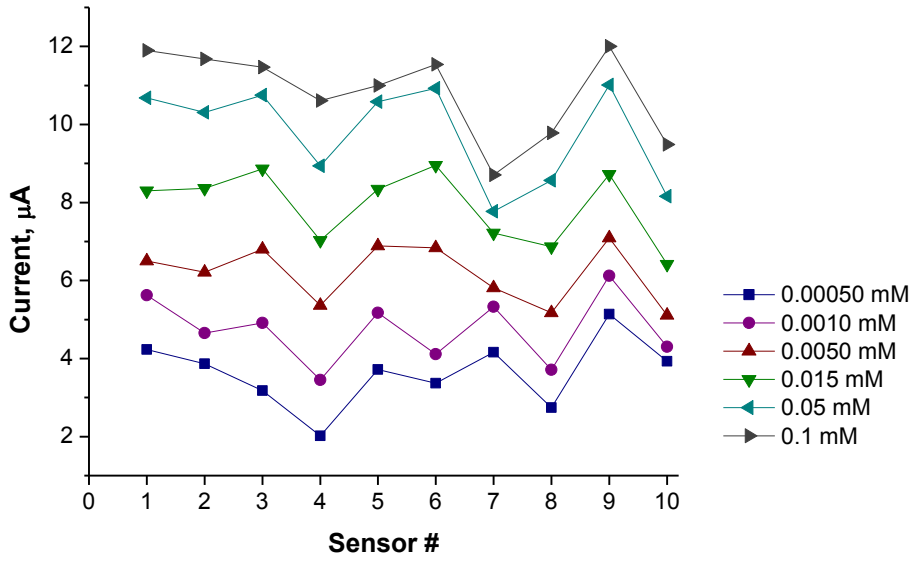

Figure **6.3**: Analytical response of the chips fabricated in this work for the increasing concentrations values of SAR (concentration values indicated in the plot, expressed in mM).

6.3.2 Optimization of sensor construction method

For the selection of the best sensor fabricated in this work, all sensors were used to measure solutions with different SAR concentrations and the results are presented in Figure 6.3. As can be seen in this figure, sensor # 9 was selected as the best sensor because it presented the highest current values for the same concentration value.

The overall process for the immobilization of SOX on the SPE surface established for sensor # 9 is described in Figure 6.4. The first step shows the oxidation of the carbon surface, which ensured a homogeneous electrode surface among the different electrodes and that carboxylic acid groups were available at the electrode surface. These groups were then activated via addition of an EDAC/NHS solution, yielding unstable ester groups that would readily react with any available amine function. In the following step, the enzyme was

covalently bond to the surface, by casting the SOX solution and allowing the amine groups on the outer surface of the enzyme to react with the unstable ester groups at the surface and form an amide bond. Finally, a mixture of Nafion and SOX was added in order to entrap the enzyme under a favorable environment where the electrochemical features were simultaneously enhanced.

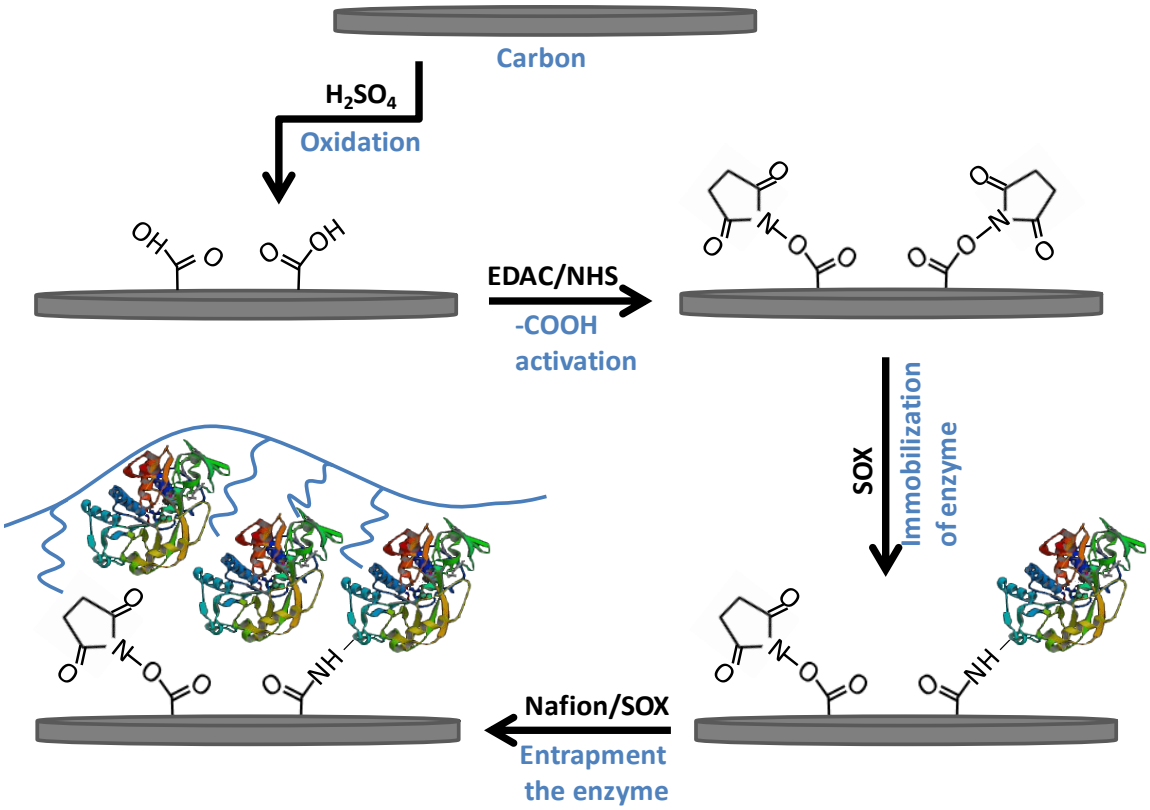

Figure **6.4**: Scheme of the immobilization process of SOX on SPE surface for sensor # **9**.

EIS studies were used to follow the carbon-SPE modification after each chemical change. As in the previous studies, this was done by monitoring the changes in the electron transfer properties of $[Fe(CN)_6]^{4-}/[Fe(CN)_6]^{3-}$ (Figure 6.5).

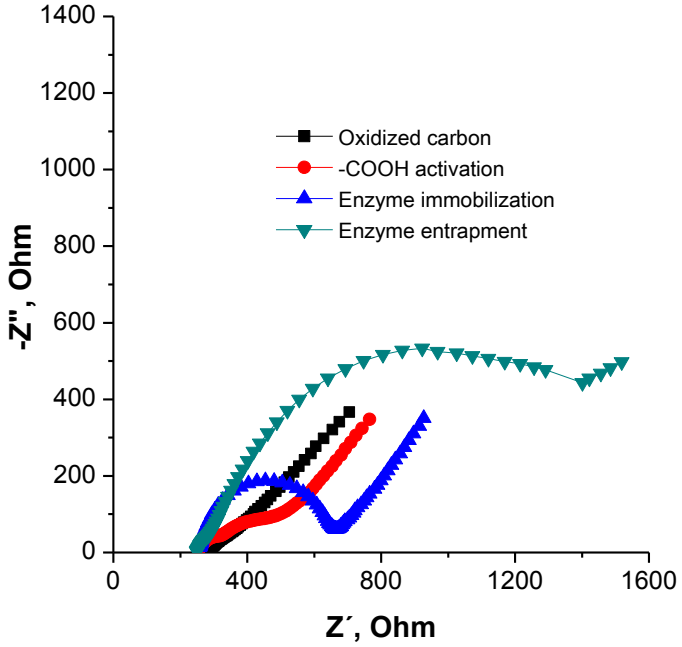

Figure **6.5**: EIS study over the subsequent modification steps of the carbon-SPE in 5.0 mM $[Fe(CN)_6]^{3-}$ and 5.0 mM $[Fe(CN)_6]^{4-}$ in PBS buffer.

Results in Figure 6.5 clearly show an increase in the R_{ct} when the several sensor layers were built. This reflected the introduction of negative charges at the electrode surface and the hindered transport of $[Fe(CN)_6]^{4-}/[Fe(CN)_6]^{3-}$ ions towards the electrode surface, after the entrapment of the enzyme (this corresponded to the highest increase in R_{ct}).

The C_{dl} reflects the changes of the surface electrode and the alteration of the surface charges (when the surface oxidation is made), the formation of a film on the surface after adsorption of the enzyme and an increase of the capacity due to the increase of charged species close to the surface during the enzyme entrapment.

The EIS data was fitted to the Randles equivalent circuit, in order to extract the numerical values of the R_{ct} and those values are displayed in Table 6.2.

Table **6.2**: Fitting parameters extracted from electrochemical impedance data using the Randles equivalent circuit.

Parameter	**Oxidation carbon**	**COOH activation**	**Immobilization of enzyme**	**Entrapment the enzyme**
R_S (Ω)	270	259	262	253
C (μF)	6.32	4.91	1.76	16.95
R_{ct} (Ω)	40.5	128.5	368	716
W (Ω $s^{-1/2}$)	$4.16x10^{-3}$	$2.50x10^{-3}$	$2.52x10^{-3}$	$1.53x10^{-3}$

6.3.3 Surface characterization morphological by AFM, Raman and FTIR

AFM was used to investigate the morphology of the electrode surface before and along the enzyme immobilization process. The images collected are shown in Figure 6.6. The top image shows the typical morphology of a clean carbon electrode surface, showing the surface roughness typical of the carbon ink films used in the fabrication of carbon-SPEs.

The RMS surface roughness initially obtained after the oxidation of the carbon at the electrode surface was 27.4 nm (Figure 6.6, top) and decreased to 22.1 nm after the activation step of the carboxylic acid groups (Figure 6.6, middle). After the last step of the modification procedure, the immobilization and entrapment of enzyme, the RMS value decreased to 12.9 nm (Figure 6.6, bottom), indicating that the materials deposition during the successive steps contributed to the decrease the surface roughness. This could be used as an indication of the success of the immobilization steps.

The chemical modifications made to the carbon electrode were also followed by Raman Spectroscopy. This study was applied to the following stages of SPE preparation: Blank, EDAC/NHS, SOX and Nafion/SOX. As may be seen in Figure 6.7A, the relative intensities of the typical G and D peaks of the carbon matrix

changed significantly in all stages of chemical modification. These relative intensity variations accounted, among others, changes in the ratio of sp^2 and sp^3 carbon hybridization in each stage of the sensor development, therefore confirming the occurrence of chemical changes at the working electrode.

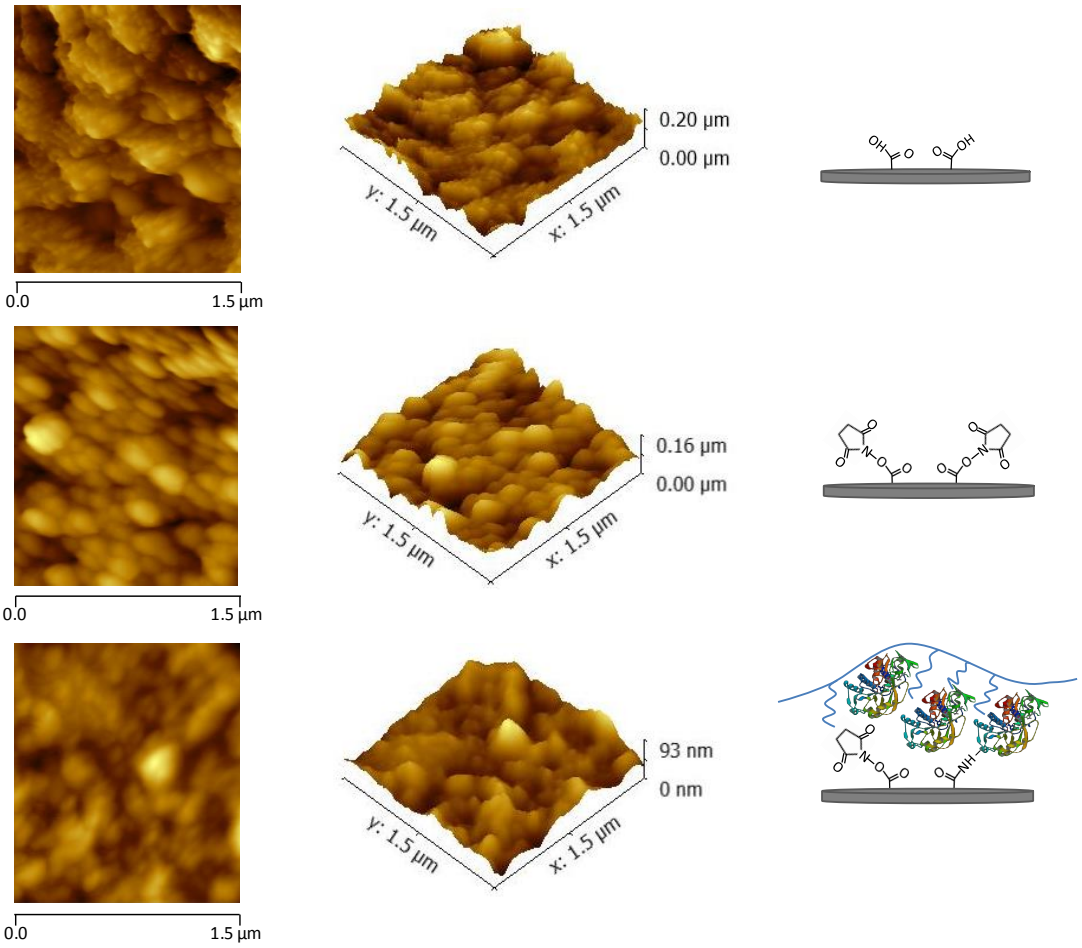

Figure **6.6**: AFM images in 2D (left) and 3D (right) for the different modification of surface SPE electrode.

The FTIR study was applied to the same materials as in Raman spectroscopy, and the corresponding spectra are shown in Figure 6.7B. As expected, the carbon matrix of the blank SPEs saturated the infrared signal, decreasing the overall sensitivity of the technique to identify dominant chemical functions arising from the chemical modification. Only the presence of Nafion was indeed perceptible

above the carbon matrix. The corresponding spectra displayed two strong absorption peaks, at 1153 and 1219 cm^{-1}, typically assigned to the symmetric and asymmetric stretching of $–CF_2$ groups, respectively [15].

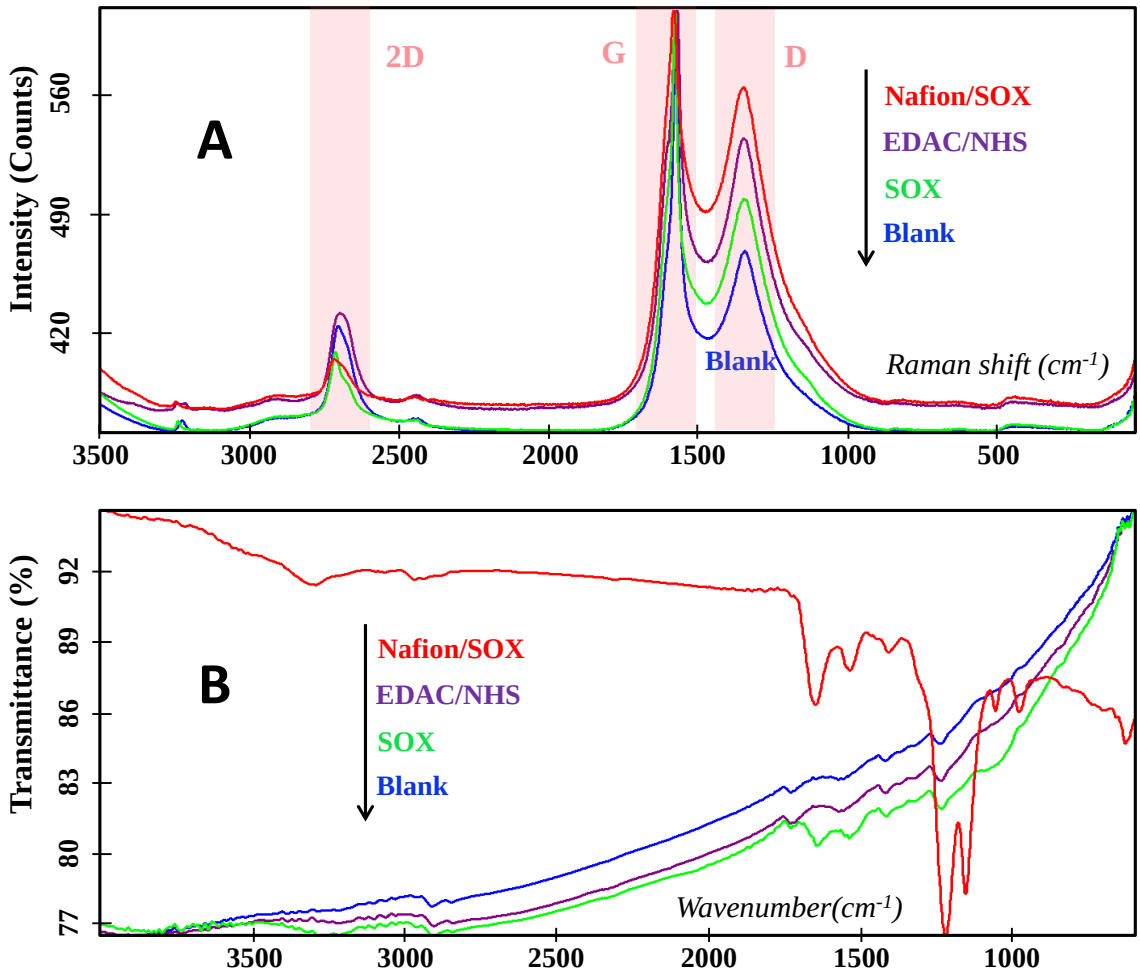

Figure **6.7**: Raman Spectroscopy (**A**) and FTIR (**B**) spectra of blank carbon-SPEs, and SPEs subsequently modified with EDAC/NHS, SOX and Nafion/SOX.

6.3.4 Evaluation of sarcosine biosensor

After the modification of the electrode surface, the analytical features of the optimum biosensor were evaluated. For this purpose, the hydrogen peroxide generated from the oxidation of SAR at the electrode surface (E = 0.6 V) was measured as a function of the SAR concentration. The calibration curve obtained

is shown in Figure 6.8 for a SAR concentration range between 5.0 nM to 0.3 mM. As can be seen in the figure, a saturation of the analytical signal is observed for concentration values greater than 0.1 μM, which is characteristic of the enzymatic systems [16]. Furthermore, a linear relationship was obtained for SAR concentrations ranging from 10 nM to 0.1 μM, with a correlation coefficient 0.9966, as shown in the inset of Figure 6.8.

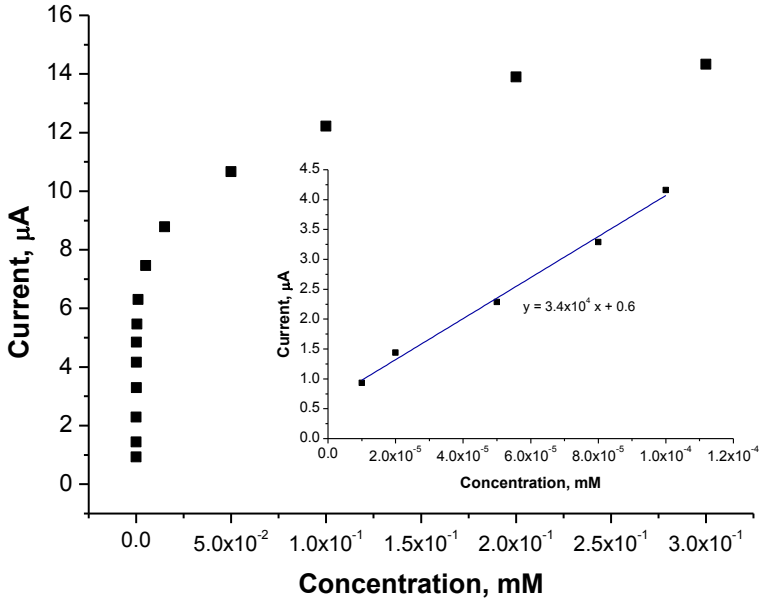

Figure **6.8**: Calibration curve obtained for SAR in the concentration range used. **Inset**: Linear calibration plot obtained for SAR.

The LOD was calculated according to the international recommendations [17, 18] and using a signal-to-noise ratio of 3. An LOD of 16 nM was obtained for the proposed quantification methodology. The LOD obtained in this work is about one order of magnitude lower than the LOD found in the literature for the electrochemical detection of creatinine [5-7]. Comparing to the devices described in the literature for the detection of SAR, a much higher value was published for the electrochemical device (28 μM) [8] and a similar value was found for the

optical sensor (5 nM) [2]. However it is important to mention that the optical sensor operated at 37 °C, required sample pre-treatment and could not be reused.

6.3.5 Selectivity study and electrode stability

Species that coexist with SAR in the biological fluids, such as creatinine and/or urea [7], can interfere in the detection of this molecule [19]. The interference study was carried out by comparing the LODs obtained in absence and in the presence of creatinine 1.10 g/L and urea 25 g/L [11] and the results obtained are resumed in Table 6.3. The LODs were estimated from calibration curves obtained in the same linear region. The results indicated that the LODs obtained for SAR in the presence of the interfering species tested were greater than the ones obtained for SAR in the absence of the interfering compounds, which could be explained by the increasing standard deviation of the baseline (blank solution + interfering × g/L).

Table **6.3**: Analytical features of calibrations made in the presence/absence of interfering species.

Interfering compound	Standard deviation of the blank (μA)	LOD (mM)
Urea	0.585	9.52×10^{-5}
Creatinine	0.283	6.53×10^{-5}
—	0.183	1.59×10^{-5}

The storage of a biosensor that employs biological material is an important parameter, because the immobilized enzyme on the electrode surface can lose activity. In this work, the biosensor was stored at 4 °C and under this condition the biosensor could be reused several times (≈10) with stable results within a period of 60 days. After this period of time, the biosensor performance decreased significantly. When comparing the results obtained for different biosensors

prepared using the same immobilization procedure, an average relative standard deviation of 2 % was found.

6.3.6 Application

Sensor #9 was applied in the determination of SAR in artificial urine samples. For this purpose, blank samples of synthetic urine were spiked with SAR in order to obtain concentration values ranging from 15 to 65 nM. The results obtained for the three concentration values are summarized in Table 6.4.

Table **6.4**: Determination of SAR in urine samples.

Sample	SAR (mM)	Found (mM)	Recovery (%)	Relative error (%)
1	1.50×10^{-5}	$1.82\text{x}10^{-5}\pm3.56\text{x}10^{-6}$	120.9±23.7	-21.0
2	6.50×10^{-5}	$6.75\text{x}10^{-5}\pm4.05\text{x}10^{-6}$	103.8±6.23	-3.8
3	9.00×10^{-5}	$8.50\text{x}10^{-5}\pm3.24\text{x}10^{-6}$	94.4±3.60	5.6

For samples 2 and 3, recoveries were 103.8 % and 94.4 %, respectively, corresponding to relative standard deviation errors below 6 %. For sample 1, a relative error of 21 % was obtained, which can be explained by the fact that the concentration of SAR in the urine sample is very close to the LOD of the methodology, increasing the error in the determination of SAR.

6.4 Conclusions

In this study, a simple and low cost electrochemical enzymatic biosensor for the determination of SAR in urine has been developed, based on the covalent immobilization of SOX, using EDAC and NHS, on the surface of the screen-printed carbon electrode. The biosensor presented high analytical performance features, such as large concentration linear range (10 to 100 nM), low detection

limit (16 nM) and large storage stability (60 days). The biosensor was successfully applied to the analysis of SAR in synthetic urine samples.

The proposed detection methodology can be particularly suitable for screening assays carried out in analytical laboratories.

6.5 References

[1] C.S. Pundir, N. Chauhan, G. Kumari, Vandana, Immobilization of *Arthrobacter* sarcosine oxidase onto alkylamine and arylamine glass and its application in serum sarcosine determination, *Indian Journal of Biotechnology*, 10 (2011) 219-223.

[2] J. Lan, W. Xu, Q. Wan, X. Zhang, J. Lin, J. Chen, J. Chen, Colorimetric determination of sarcosine in urine samples of prostatic carcinoma by mimic enzyme palladium nanoparticles, *Analytica Chimica Acta*, 825 (2014) 63-68.

[3] C. Burton, S. Gamagedara, Y. Ma, A novel enzymatic technique for determination of sarcosine in urine samples, *Analytical Methods*, 4 (2012) 141-146.

[4] A. Ramanavicius, Amperometric biosensor for the determination of creatine, *Analytical and Bioanalytical Chemistry*, 387 (2007) 1899-1906.

[5] S. Yadav, R. Devi, P. Bhar, S. Singhla, C.S. Pundir, Immobilization of creatininase, creatinase and sarcosine oxidase on iron oxide nanoparticles/chitosan-g-polyaniline modified Pt electrode for detection of creatinine, *Enzyme and Microbial Technology*, 50 (2012) 247-254.

[6] S. Yadav, A. Kumar, C.S. Pundir, Amperometric creatinine biosensor based on covalently coimmobilized enzymes onto carboxylated multiwalled carbon nanotubes/polyaniline composite film, *Analytical Biochemistry*, 419 (2011) 277-283.

[7] C.H. Chen, M.S. Lin, A novel structural specific creatinine sensing scheme for the determination of the urine creatinine, *Biosensors and Bioelectronics*, 31 (2012) 90-94.

[8] P. Kotzian, N.W. Beyene, L.F. Llano, H. Moderegger, P. Tunón-Blanco, K. Kalcher, K. Vytras, Amperometric determination of sarcosine with sarcosine oxidase entrapped with nafion on manganese dioxide-modified

screen-printed electrodes, *Scientific papers of the University of Pardubice. Serie A. Faculty of Chemical Technology*, 8 (2002) 93-101.

[9] L. Mao, F. Xu, Q. Xu, L. Jin, Miniaturized Amperometric Biosensor Based on Xanthine Oxidase for Monitoring Hypoxanthine in Cell Culture Media, *Analytical Biochemistry*, 292 (2001) 94-101.

[10] A.C. Torres, M.E. Ghica, C.A. Brett, Design of a new hypoxanthine biosensor: xanthine oxidase modified carbon film and multi-walled carbon nanotube/carbon film electrodes, *Analytical and Bioanalytical Chemistry*, 405 (2013) 3813-3822.

[11] C.J. Collins, A. Berduque, D.W.M. Arrigan, Electrochemically Modulated Liquid−Liquid Extraction of Ionized Drugs under Physiological Conditions, *Analytical Chemistry*, 80 (2008) 8102-8108.

[12] M. Chirea, E.M. Pereira, C.M. Pereira, F. Silva, Synthesis of poly-Lysine/Gold nanoparticle films and their electrocatalytic properties, *Biointerface Research in Applied Chemistry*, 1 (2011) 119-126.

[13] D. Jezequel, J. Guenot, N. Jouini, F. Fievet, Submicrometer zinc oxide particles: Elaboration in polyol medium and morphological characteritics, *Journal of Materials Research*, 10 (1994) 77-83.

[14] Y. Matsuda, H. Hoshika, Y. Inouye, S. Ikuta, K. Matsuura, S. Nakamura, Purification and Characterization of Sarcosine Oxidase of Bacillus Origin, *Chemical and pharmaceutical bulletin*, 35 (1987) 711-717.

[15] L. Grosmaire, S. Castagnoni, P. Huguet, P. Sistat, M. Boucher, P. Bouchard, P. Bébin, S. Deabate, Probing proton dissociation in ionic polymers by means of in situ ATR-FTIR spectroscopy, *Physical Chemistry Chemical Physics*, 10 (2008) 1577-1583.

[16] C.R. Ispas, G. Crivat, S. Andreescu, Review: Recent Developments in Enzyme-Based Biosensors for Biomedical Analysis, *Analytical Letters*, 45 (2012) 168-186.

[17] C. Analytical Methods, Recommendations for the definition, estimation and use of the detection limit, *Analyst*, 112 (1987) 199-204.

[18] J. Mocak, A.M. Bond, S. Mithell, G. Scollary, A statistical overview of standard (IUPAC and ACS) and new procedures for determining the limits of detection and quantification: Application to voltammetric and

stripping techniques (Technical Report), *Pure and Applied Chemistry*, 69 (1997) 297-328.

[19] Y. Jiang, X. Cheng, C. Wang, Y. Ma, Quantitative Determination of Sarcosine and Related Compounds in Urinary Samples by Liquid Chromatography with Tandem Mass Spectrometry, *Analytical Chemistry*, 82 (2010) 9022-9027.

7

Testing the Variability of PSA Expression by Different Human Prostate Cancer Cell Lines

Work submitted to journal of Current Topics in Medicinal Chemistry:

Materials Science and Engineering C 59 (2016) 1069–1078

Contents lists available at ScienceDirect

Materials Science and Engineering C

journal homepage: www.elsevier.com/locate/msec

Testing the variability of PSA expression by different human prostate cancer cell lines by means of a new potentiometric device employing molecularly antibody assembled on graphene surface

Tânia S.C.R. Rebelo [a,b,c], João P. Noronha [b], Marco Galésio [b], Hugo Santos [b], Mário Diniz [b], M. Goreti F. Sales [a], Maria H. Fernandes [c], João Costa-Rodrigues [c,d,*]

[a] BioMark-CINTESIS/ISEP, Instituto Superior de Engenharia do Instituto Politécnico do Porto, Portugal
[b] LAQV, REQUIMTE, Departamento de Química, Faculdade de Ciências e Tecnologia, Universidade Nova de Lisboa, Caparica, Portugal
[c] Laboratory for Bone Metabolism and Regeneration, Faculdade de Medicina Dentária, Universidade do Porto, Porto, Portugal
[d] ESTSP – Escola Superior de Tecnologia da Saúde do Porto, Instituto Politécnico do Porto, Portugal

7.1 Introduction

PSA is a protein produced mainly by the prostate. In healthy men almost all is released to semen, being only a small fraction present in blood. However, an increase of PSA levels in blood can be a consequence of the presence of PCa, but also the result of some physiological or pathological modifications such as, prostatitis, urinary tract infection, and BPH. Moreover, some other tissues are also capable of its synthesis which can origin problems to detect when PSA presence is due or not to PCa [1, 2]. Due to this significant variability, it is

important to have accurate and reliable methods for PSA detection within a broad range of protein concentrations, in biological fluids with complex composition. And from this result the need to test these methods in cell lines.

There are two different ways to test these methods in cell lines, *in vitro* and *in vivo*. *In vitro* models are the simplest, in these models monitoring all variables is easier because some interfering species, present in *in vivo* models, can be avoided. Although, even in *in vitro* models, PSA expression can vary with chemical composition of cellular medium this work brings an important achievement once our method obtained good results in all tested mediums.

The application of an electrochemical biosensor for screening PSA in real context making use of an artificial antibody may yield significant advantages when compared to the natural ones [3]. This biosensor, described herein in chapter 3, was already tested to determine PSA levels in artificial serum, with recoveries ≥ 96.9% and relative errors of ~6.8%. These results suggested that the sensor may have successful results under real applications [3].

In this context, the aim of this study was to test the effectiveness of the electrochemical biosensor in screening PSA in complex biological environments, such as the culture medium from several prostate cell lines, cultured in a variety of experimental conditions (different culture periods and media composition), thus with an expected wide range of PSA, in the presence of different concentrations of many other metabolites. The tested prostate cell lines included the cancer cell lines LNCaP (positive for androgen receptors) and PC3 (negative for androgen receptors) and the non-cancerous prostate cell line PNT2. In parallel, human skin fibroblasts were used as a non-prostatic control. Validation of the results was performed by assessing PSA levels in the same media samples by the conventional ELISA assay. MALDI-TOF mass spectrometry was also used to identify the protein.

7.2 Materials and Methods

7.2.1 Setup of the electrochemical biosensor

The construction of the solid-contact PSA electrode (schematized in figure 7.1) and the electrochemical biosensor were built as described previously on chapter 3.

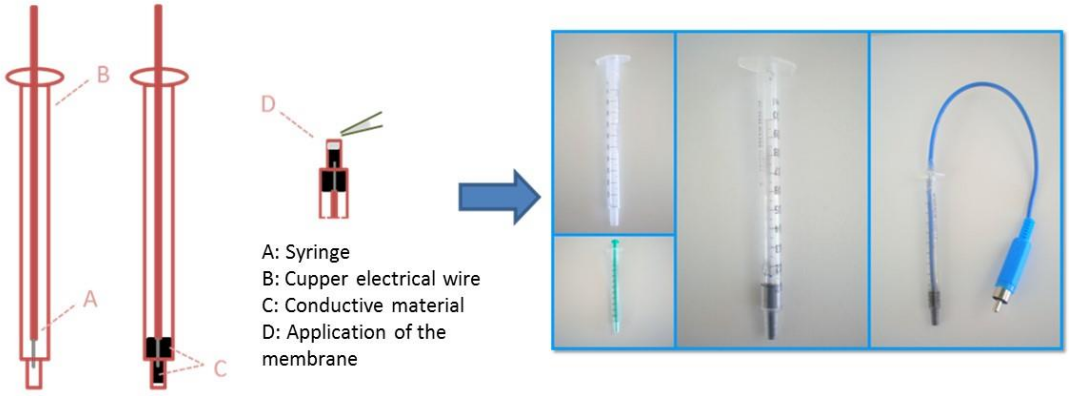

Figure **7.1**: Schematic representation of the assembly of the conductive support (left) and the picture of the several integrant parts final device (right).

7.2.2 Cell cultures. Characterization of the cell behavior

The prostate cell lines LNCaP, PC3 and PNT2 were purchased from ATCC. Human gingival fibroblasts (FB) were obtained from explants collected from healthy donors with 25–35 years old, after informed consent. Cells were cultured in 100 mm culture plates and were maintained in standard culture conditions, i.e., α-minimal essential medium (α-MEM) supplemented with 10% fetal bovine serum (FBS), 2.5 μg/mL fungizone and penicillin-streptomycin (100 IU/mL and 10 g/mL, respectively). Cells were incubated in a humidified atmosphere with 5% CO_2 in air, at 37 °C, and culture medium was changed twice a week. At 70–80% confluence, adherent cells were enzymatically released with a solution of 0.05% trypsin in 0.25% ethylenediamine tetraacetic acid (EDTA).

The cells were seeded (10^4 cells/cm^2) in culture plates, and were incubated for 2, 7 and 14 days, without any further medium change. Cell cultures were performed in four culture media with different compositions: (*i*) α-MEM with 10% FBS, (*ii*) α-MEM with 30% FBS, (*iii*) RPMI 1640 with 10% FBS, and (*iv*) RPMI 1640 with 30% FBS. All culture media were supplemented with 2.5 μg/mL fungizone and penicillin-streptomycin (100 IU/mL and 10 μg/mL, respectively). In parallel, the four tested culture media were incubated under the experimental conditions described above, but in the absence of any cell type, and were used as a negative control.

Cultures were characterized for DNA content throughout the culture time, as a measure of cell proliferation. Further, at day 14, the cell layer was analyzed for several prostate markers by RT-PCR. At the end of each culture period, the medium was collected, centrifuged at 400 g for 10 minutes, aliquoted and frozen for subsequent analysis of PSA levels.

7.2.2.1 Total RNA extraction and qPCR analysis

RNA isolation was performed with RNeasy® Mini Kit (QIAGEN) according to manufacturer's instructions. Quantification of RNA was conducted at 260 nm. cDNA synthesis was performed using the DyNAmo cDNA synthesis kit (Finnzymthes, Finland) and random hexamers according to the manufacturer's instructions. Each cDNA template (~1.5 ng) was amplified with the DyNAmo Flash SYBR green qPCR kit (Finnzymes) on a Rotor-Gene thermocycler (Qiagen), according to the manufacturer's instructions. Validation of the reactions was performed by the presence of a single peak in the melt curve analysis. Cells were assessed for the expression of the housekeeping genes beta-glucuronidase (GUSB) and proteasome subunit beta type-6 (PSMB6), and the prostate associated markers PSA, Kallikrein-2 (KLK2), Kallikrein-4 (KLK4), Prostate Carcinoma Tumor Antigen-1 (PCTA1), Prostate Stem Cell Antigen (PSCA),

Prostein, Prostate-Specific Membrane Antigen (PSMA), Protein-glutamine gamma-glutamyltransferase 4 (TGM4) and Prostate Leucine Zipper (PrLZ) [4, 5]. In addition, LNCaP cells were also characterized regarding the expression of p53, androgen receptor (AR) and FKBP52 [6-8]. Primers used are listed in table 7.1. qPCR results were analyzed using the standard curve analysis method. Briefly, the number of cycles required for the fluorescent signal to cross the threshold and exceed the background level, defined as cycle threshold (CT), was converted in relative expression levels, with the slope and the Y intersect extracted from the standard curve and applying the equation 10 (Y intersect−CT/slope) [9]. The values obtained were normalized with the values obtained for both housekeeping genes.

Table **7.1**: Primers used in RT-PCR analysis of cell cultures.

Gene	5′ Primer	3′ Primer
GUSB	TGCAGCGGTCTGTACTTCTG	CCTTGACAGAGATCTGGTAAT
PSMB6	GCCGGCTACCTTACTACCTG	AAACTGCACGGCCATGATA
PSA	ACCAGAGGAGTTCTTGACCCCAA	CCCCAGAATCACCCGAGCAG
KLK2	GGTGGCTGTGTACAGTCATGG	TGTCTTCAGGCTCAAACAGGTT
KLK4	GGCACTGGTCATGGAAAACGA	TCAAGACTGTGCAGGCCCAGCC
PCTA1	CGTAGTGTTCTTTGGACACG	CTACCAGCTCCTTACTTCCAG
PSCA	TGCTTGCCCTGTTGATGGCA	CCAGAGCAGCAGGCCGAGTGC
Prostein	CCTTCACGCTGTTTTACACG	CTACGCTGAGTATTTGGCCAAG

Table **7.2**: Primers used in RT-PCR analysis of cell cultures (cont.).

Gene	5′ Primer	3′ Primer
PSMA	CCAGGTTCGAGGAGGGATGGT	GCTACTTCACTCAAAGTATCTG
TGM4	CATCATTGCGGAAATTGTGG	CTACTTGGTTGATGAGAACAA
PrLZ	GTAGAGAGATGGACTTATATG	TCACAGGCTCTCCTGTGTCTT

7.2.2.2 DNA content

DNA content was quantified as a measure of cell proliferation. DNA was analyzed by the PicoGreen DNA quantification assay (*Quant-iT™ PicoGreen®* dsDNA Assay Kit, Molecular Probes Inc., Eugene), according to manufacturer´s instructions. At each culture time, cultures were treated with Triton X-100 (0.1%) (Sigma) and fluorescence was measured on an Elisa plate reader (Synergy HT, Biotek) at wavelengths of 480 and 520 nm, excitation and emission respectively, and corrected for fluorescence of reagent blanks. The amount of DNA was calculated by extrapolating a standard curve obtained by running the assay with the given DNA standards, and is expressed as ng/mL.

7.2.3 PSA levels in the culture media

PSA levels were quantified in the culture medium from the cell cultures maintained in all tested conditions, and collected after 2, 7 and 14 days of culture. Quantification was performed with the Biosensor and with a commercial ELISA kit. Results were normalized to the DNA content of the cell layer.

7.2.3.1 Electrochemical Biosensor

Calibration plots were used to determine the PSA concentrations in the several culture media and cell lines. For this purpose, decreasing concentration levels of PSA were obtained by transferring 5 μL of PSA aliquots of PSA 2.5 $x10^4$ ng/mL standard solution to a 75 mL beaker containing 375 μL of each tested medium and 620 μL Hepes buffer $1.0x10^{-4}$ mol/L. Potential readings were recorded after stabilization to ±0.2 mV and emf was plotted as a function of the logarithm of the PSA concentration. After calibration, the diluted samples (375 μL of sample and 625 μL buffer) were analyzed. All potentiometric measurements were carried out at room temperature and in stirred solutions of pH 7.3.

7.2.3.2 ELISA assay

The same samples used to quantify PSA levels with the biosensor were assessed by ELISA, with a commercial ELISA kit (CanAg PSA EIA), according to the manufacturer's instructions. The minimum dose of PSA detectable by the kit was 0.1 ng/mL. The concentration of PSA in each sample was determined at 405 nm in an ELISA plate reader (Synergy HT, Biotek).

7.2.3.3 Statistical analysis

Results are expressed as the mean ± standard deviation. Groups of data were evaluated using a two-way analysis of variance (ANOVA). Statistical differences between controls and experimental conditions were assessed by Bonferroni's method. Values of $p \leq 0.05$ were considered significant.

7.2.4 PSA identification by MALDI-TOF mass spectrometry

7.2.4.1 In solution digestion of proteins

MALDI-TOF mass spectrometry (MS) analysis was performed on all tested culture medium samples. However, the presence of PSA was only detected on

the samples from 14-day LNCaP cell cultures. Sample treatment followed essentially López-Ferrer [10] and Santos [11] with minor modifications. Briefly, protein samples were ressuspended in 12.5 mM ammonium bicarbonate solution (NH_4HCO_3) and mixed using a vortex for one minute followed by adding 2 µL of 110 mM dithiothreitol (DTT) in 12.5 mM NH_4HCO_3 (Sigma, Germany) as reduction step of protein disulfide bonds. Then, samples were sonicated in a sonoreactor UTR200, from Dr. Hielsher (Teltow, Switzerland) for one min. at 50% amplitude and continuous mode. After cooling to room temperature, it was added 600 mM iodoacetamide (IAA) (Sigma, Germany) in 12.5 mM NH_4HCO_3, for alkylation, and again sonicated in the sonoreactor (1 min.; 50% amplitude; continuous mode). The sample solutions were diluted in 72 µL of NH_4HCO_3. Then, 4 µL of trypsin sequencing grade (Sigma, Germany) (0.025 mg/ml in 25 µL of 12.5 mM NH_4HCO_3) were added to each sample and incubated overnight (37 °C) with trypsin for digestion. Afterwards, 2 µL of formic acid (50% v/v) (Fluka, Germany) were added to each sample to stop enzyme activity and mixed using the vortex.

7.2.4.2 Intact Protein by MALDI-MS

7.2.4.2.1 Sample clean-up

To improve data quality, prior to MALDI-TOF-MS intact protein analysis, the sample was purified and concentrated using ZipTip$_{C4}$ pipette tips. The protocol for ZipTip$_{C4}$ sample preparation was adapted from manufacturer's guidelines. The micropipette was set to 10 µL and ZipTip$_{C4}$ equilibration step was performed, first by aspirating and dispense a solution 50% methanol and 0.1% TFA in MilliQ water (3 cycles), and then by aspirating and dispense the washing solution, 0.1% TFA in MilliQ water (3 cycles). After ZipTip equilibration the protein binding step was carried out by aspiration and dispense of the sample (10 cycles in 50 µL of sample), followed by a washing step with 0.1% TFA in MilliQ water (5 cycles).

Sample elution was accomplished by aspirating and dispensing 10 µL of a solution 75% methanol 0.1 % TFA in MilliQ water that was previously added to a clean vial (5 cycles).

7.2.4.2.2 MALDI-TOF-MS analysis

Prior to MALDI-TOF-MS analysis the sample was mixed with an equal volume of the MALDI matrix solution 10 mg/mL α-Cyano-4-hydroxycinnamic acid (α–CHCA) in trifluoroacetic acid 0.1% (v/v) and acetonitrile 50% (v/v). An aliquot of the sample/matrix solution (0.5 µL) was hand-spotted onto the MALDI sample plate and the sample was allowed to dry at room temperature. Intact protein data was obtained using a ABI 4700 Proteomics Analyzer with time-of-flight (TOF)/TOF optics (Applied Biosystems, Foster City, USA) equipped with a 355-nm Nd:YAG laser and the laser intensity was set just above the threshold for ion production. Laser shots of 600 per spectrum were used to acquire spectra within a mass range of 10 to 50 kDa. Spectra were acquired in the linear positive ion mode with a 20 kV acceleration voltage, 16 kV grid voltages and a delay time of 240 ns. All the mass spectra were processed using Data Explorer™ software, version 4.5 (Applied Biosystems, USA). MS acquisition data was calibrated externally using the ProteoMass Protein MALDI-MS Calibration Kit (MSCAL2) from Sigma as mass calibration standard for MALDI-TOF-MS.

7.2.4.2.3 *Data analysis and database searching*

All data were processed using DataExplorer 4.5 software from Applied Biosystems. Peptide Mass Fingerprint (PMF) data were used to search for candidate proteins using the MASCOT database search (http://www.matrixscience.com) engine. SwissProt database was selected by default for all Mascot searches. NCBInr database was used each time no significant identification was obtained with SwissProt. Database searches were,

by default, performed with no taxonomy restriction and allowing up to a maximum peptide mass tolerance of 100 ppm. The number of allowed missed cleavages for trypsin was set to one. Carbamidomethylation of cysteine and methionine oxidation were selected as fixed and variable modifications, respectively. In order to provide accurate results, protein identification was considered positive for MASCOT protein scores higher than 56 ($p<0.05$), that presents a minimum of 4 peptides matching.

7.3 Results

7.3.1 Characterization of the cell cultures

7.3.1.1 Cell proliferation

The different cell types were stained for cytoplasm and nucleus with hematoxylin and eosin, respectively, and were visualized under a light microscope (Figure. 7.2A). It was observed that the cells displayed a uniform distribution in the wells and revealed the morphology and pattern of cell growth expected for each tested cell type.

Figure 7.2B shows the DNA content of the cell cultures in the different experimental conditions. Cells proliferated throughout the culture time in the tested culture conditions. The fibroblast cell cultures presented a higher proliferation in α-MEM (with slightly higher values in the medium with 30% FBS). The prostate cell lines showed a higher growth rate during the first week. LNCaP cells presented higher DNA values in α-MEM and RPMI containing 10% FBS. PC3 cells showed a slight preference for RPMI media and, α-MEM and RPMI containing 30% FBS yielded slightly increased DNA values. Regarding PNT2 cells, values were only somewhat higher in RPMI, and the percentage of FBS did not affect the cell behavior.

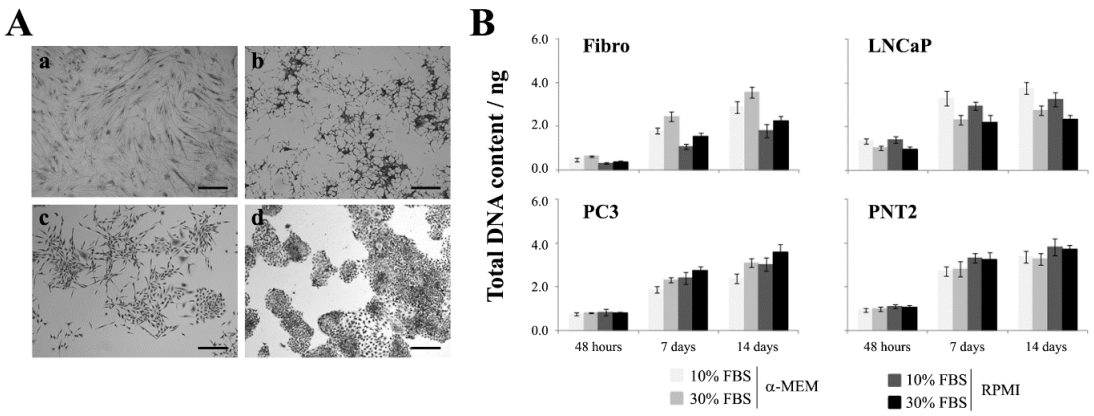

Figure **7.2**: Cellular characterization of cell cultures. **A** – Cellular morphology at 7 days of culture, after hematoxylin/eosin staining method. Cell lines images: **a** – human skin fibroblasts, **b** – LNCaP, **c** – PC3 and **d** – PNT2. Bar represents 300 μm. **B** – Cell proliferation, assessed by total DNA quantification, of cell cultures maintained in different culture media for 14 days.

7.3.1.2 Expression of prostate genes

Cell cultures were assessed for the expression of several genes reported to be specifically or preferentially expressed by normal and malignant prostate cells, namely, PSA, KLK2, KLK4, PCTA1, PSCA, Prostein, PSMA, TGM4 and PrLZ. Results are presented in Figure 7.3A.

Fibroblasts did not reveal the expression of any analyzed genes. The prostate cancer cell line LNCaP expressed all the tested genes, with responses globally higher or similar, when grown in α-MEM, compared to those achieved with RPMI. PSA gene presented the highest expression values, particularly in α-MEM supplemented with 10% FBS. A similar behavior was observed for KLK2 gene. In the case of PC3 cell line, no expression was observed for PSA, KLK2 and PSMA. Furthermore, PSCA expression was not detected when cells were grown in α-MEM, and when cells were maintained in RPMI, they did not reveal the expression of Prostein. The non-cancerous cell line PNT2 did not express PSA, KLK2 and KLK4, but the expression of the remaining genes was observed.

Following, LNCaP cells were analyzed for the expression of several genes known to be involved in the regulation of PSA expression, namely, p53, AR and FKBP52 (Figure 7.3B).

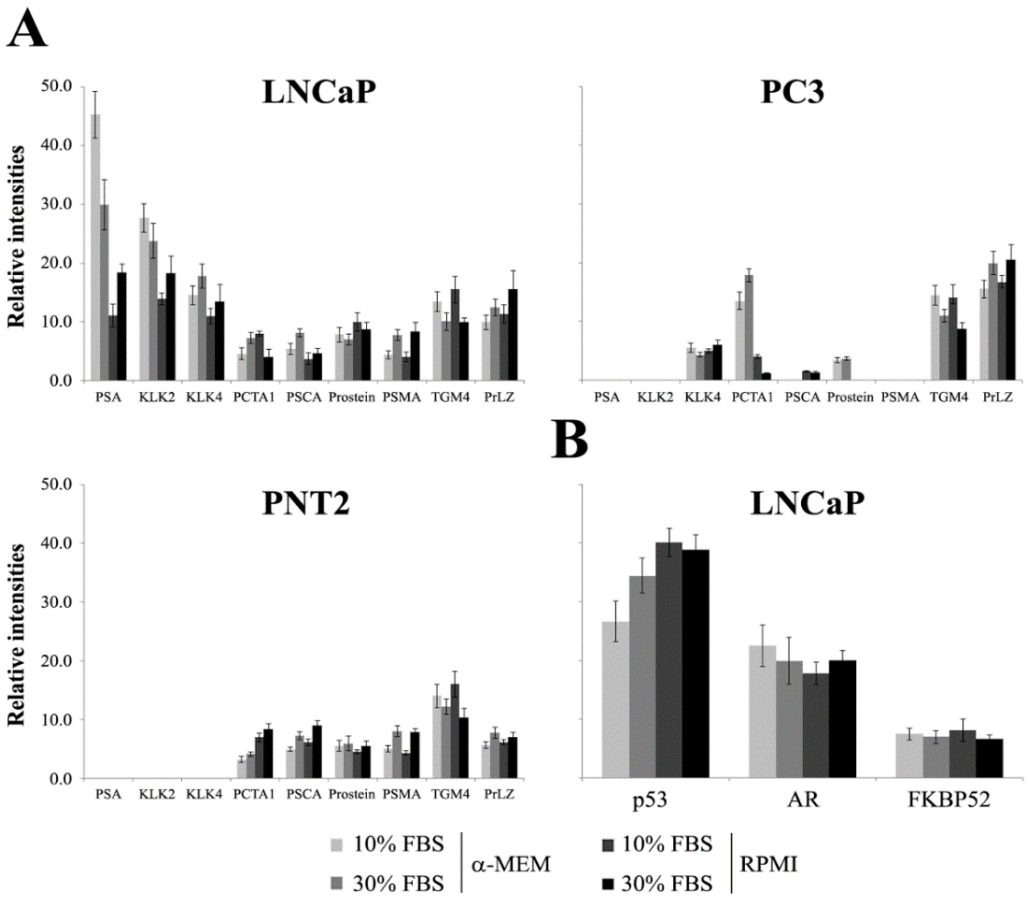

Figure **7.3**: qPCR analysis of cell cultures. **A** – PSA, KLK2, KLK4, PCTA, PSCA, Prostein, PSMA, TGM4 and PrLZ expression by LNCaP, PC3 and PNT2 cell lines. **B** – p53, AR and FKBP52 expression by LNCaP cell line.

It was observed that p53 expression was higher in cultures performed in RPMI, and the lowest value was achieved in α-MEM supplemented with 10% FBS. AR and FKBP52 expression was similar in all the tested conditions, though the expression values were lower for the latter gene.

7.3.2 PSA levels in the culture medium

7.3.2.1 Biosensor

Calibration curves were performed in a range of PSA concentrations 2.0 to 89.0 ng/mL. The sensor showed a good potentiometric response, with a slope of -44.16 mV/decade and a limit of detection (LOD) of 2.0 ng/mL, in agreement with the data depicted in Figure 7.4. A negative control of non-imprinted polymer (NIP) was moreover prepared by following the same steps. In general, the time required for the electrodes to make a steady potential (±0.2 mV) was always less than 20 s, even for the highest concentrations tested.

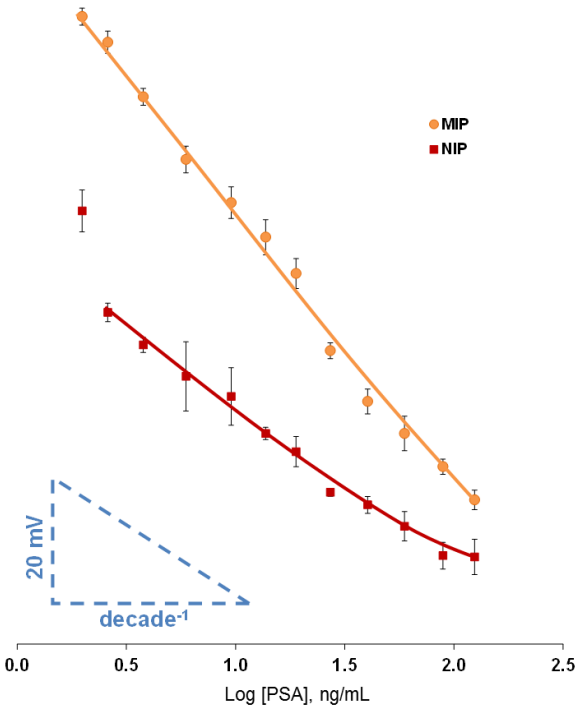

Biosensor	MIP	NIP
Slope (mV/decade)	-44.16 ± 2.89	-24.80 ± 1.91
R^2 (n=3)	0.991	0.994
LOD (ng/mL)	2.0	2.6
Linear range (ng/mL)	2.0 – 89.0	2.6 – 89.0

Figure **7.4**: Potentiometric response of PSA selective electrodes prepared with imprinted and non-imprinted materials (ranging from 2.0 to 89.0 ng/mL, in 1×10^{-4} mol/L Hepes buffer).

The quantification of PSA levels by potentiometry was performed in the culture medium collected from the cell cultures. Only LNCaP cell line was able to produce detectable amounts of PSA. Levels were higher at day 14 in all conditions, and the highest values were found in α-MEM, especially with 10% FBS. In the RPMI medium, the presence of 30% FBS induced a greater production of PSA. The biosensor was unable to quantify PSA levels at day 2 for all culture media, nor at day 7 in RPMI medium. The results are shown in Table 7.2.

7.3.2.2 ELISA assay

The quantification of PSA was carried out in the same samples used for the analysis with the biosensor. Also, PSA was only detected in the culture medium from the LNCaP cell line. The pattern of PSA production in the different culture media was similar to that described for the quantification with the biosensor. Results are shown also in Table 7.2.

Table **7.3**: Quantification of PSA in culture media.

Culture		Biosensor		ELISA		F-test		t-test	
media	**time**	**PSA (ng/mL)***	**RSD**	**PSA (ng/mL)***	**RSD**	**calculated**	**critical**	**calculated**	**critical**
α-MEM 10%	7 days	17.86±2.17	12.15	16.19±1.65	10.19	1.73	19.3	1.16	2.36
	14 days	206.93±7.97	3.85	196.91±15.56	7.90	3.81	5.79	1.32	2.36
α-MEM 30%	7 days	12.40±0.90	7.26	14.01±1.17	8.35	1.69	5.79	2.32	2.36
	14 days	74.75±2.54	3.40	94.86±8.58	9.04	11.41	5.79	3.97	4.30
RPMI 10%	14 days	9.35±2.0	21.40	11.54±1.45	12.56	1.90	5.79	1.67	2.36
RPMI 30%	14 days	29.83±1.73	5.80	33.83±4.84	14.31	7.83	5.79	1.39	4.30

RSD – Relative Standard Deviation; * Results were normalized to the corresponding DNA content of the cell layer

7.3.2.3 Data correlation

Quantification of PSA levels by the biosensor and by the ELISA assay revealed similar concentrations, with recoveries ranging from 72.07 to 110.36%. The obtained results are summarized in Table 7.3.

Table **7.4**: Data correlation between the biosensor and the ELISA analysis.

Culture media	Culture time	Error %	Recovery %
α-MEM 10% FBS	7 days	10.36	110.36
	14 days	5.09	105.09
α-MEM 30% FBS	7 days	-11.5	88.50
	14 days	-21.2	78.80
RPMI 10% FBS	14 days	-27.93	72.07
RPMI 30% FBS	14 days	-11.83	88.17

7.3.3 PSA identification by MALDI-TOF mass spectrometry

Samples were also analyzed by MALDI-TOF and compared with a PSA protein standard solution, in order to have information about potential changes in the size/composition of PSA in the different experimental conditions, Figure 7.5. PSA was only detected in the samples collected from LNCaP cell line, at day 14. The protein appeared in a sharp peak corresponding to $[M+H]^+$ at 33440 Da. $[M+H]^{2+}$ was also observed at 16690 Da. In order to confirm the identity of PSA, the identification by peptide mass fingerprinting (PMF) was performed. Positive

identification was achieved with a score of 70 and sequence coverage of 26% corresponding to 8 peptide matches.

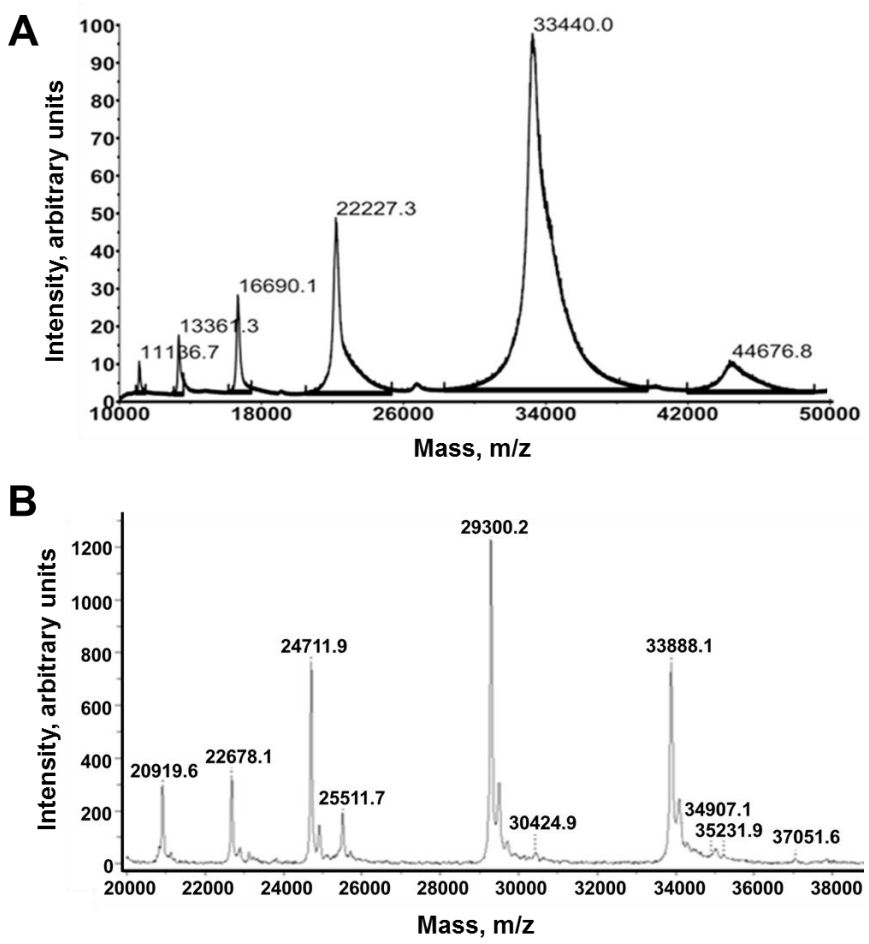

Figure **7.5**: MALDI-TOF MS analysis of the (**A**) PSA from LNCaP cell culture and (**B**) standard PSA in solution.

7.4 Discussion

The PCa is a public health problem, which can reduce the quality of life and even lead to the death of the patients [12]. However, if detected early it can be treated and even cured. PSA is a protein that has been used for the screening of PCa and monitoring patients after therapy, being considered an important biomarker for this pathology [13].

For this purpose, a PSA electrochemical biosensor was developed (chapter 3 of this thesis) and reported to present a good response in the determination of PSA levels in non-biological fluids with a simple composition [3]. In addition to the observed high sensitivity/selectivity, this methodology presented a significantly lower price of analysis than the currently used ELISA technique, which makes it a potentially useful routine tool for PCa diagnosis.

Despite its recognized potential as a PCa biomarker, PSA expression is not only confined to prostate cancer cells. In fact, normal prostate cells have the ability to produce low levels of this protein, and also it is reported that some non-prostatic cancer cells may express PSA [14]. Moreover, the synthesis and secretion of PSA is under a complex regulation, which responds to many different exogenous stimuli, being significantly affected by the cellular metabolic context [14, 15].

Taking this into account, in this study, the effectiveness of PSA quantification by the biosensor was assessed in culture media from human prostate cell lines, as representative of biological complex environments. For that, two prostate cancer and one non-cancerous prostate cell lines were cultured in different conditions, which are expected to modulate the PSA expression and, thus, to create a wide range of PSA concentrations in environments with different complex compositions. Cells were maintained in two different but widely used culture media (α-MEM and RPMI), that present significantly different composition, especially in the proportions of the standard amino acids. In order to create more pronounced differences in the culture media composition, the concentration of fetal bovine serum (FBS), was also changed, being tested at a final concentration of 10% and 30% of FBS. In parallel, human gingival fibroblasts were used as a non-cancerous, non-prostatic control.

Regarding cell viability/proliferation in the different culture condition, it was observed that cell cultures presented different behaviors during the 14-day

culture period. For fibroblasts, the culture medium that elicited a higher cellular growth was α-MEM supplemented with 30% FBS. It is important to note that α-MEM is one of the most widely used culture medium for this cell type [16, 17], although there also studies conducted in DMEM [18, 19] or RPMI [20, 21]. In the case of prostate cell lines, studies are usually performed in RPMI [22, 23]. In line with this, PC3 and PNT2 revealed a somehow higher growth in this medium. PNT2 behavior was not significantly affected by the different concentrations of FBS, while PC3 viability/proliferation was increased in the presence of 30% FBS. LNCaP cell line exhibited a slightly higher cellular response in α-MEM. In addition, in both culture media, the presence of 10% FBS seemed to promote a higher cell viability/proliferation of LNCaP cells. This differential behavior observed in the presence of culture media with different compositions is in line with the known specific needs of each cell line, when maintained in culture [24].

Also, cells were assessed by qPCR for the expression of different prostate marker genes, namely, PSA, KLK2, KLK4, PCTA1 PSCA, Prostein, PSMA, TGM4 and PrLZ [4, 5]. KLK2 and KLK4 are two members of the kallikrein protein family that are thought to be important for the activation of several prostate zymogens, including pro-PSA [25, 26]. PCTA1, also known as galectin-8, is over expressed by PCa cells. Its main function is thought to be related to cell adhesion and growth regulation [27]. PSCA, Prostein, TGM4 and PrLZ are proteins that are related with prostate cancer progression and metastatic behavior [28-31]. PSMA seems to be important for angiogenesis regulation during prostate cancer development [32]. It was observed that all the markers were expressed by at least LNCaP cells, although with evident differences between them. Furthermore, the medium composition had a significant effect on the express of the genes by the different cell types. None of the markers were expressed by the fibroblasts. PSA was only expressed by LNCaP cells, which is in agreement with previously

published reports [4, 33] and its expression was significantly modulated by the culture media composition. Interestingly, KLK2 and, in a lesser extent, KLK4 (which was also expressed by PC3 cell line, at low levels) revealed a similar culture media-dependent expression pattern, which is in line with their proposed role in pro-PSA activation [25, 26]. PCTA1 was expressed differentially by the three prostate cell lines. Generally, LNCaP and, particularly, PC3 cells revealed high expression values when maintained in α-MEM supplemented with 30% FBS. PNT2 revealed a higher cell response in RPMI in the presence of 30% FBS. Up to our knowledge, this is the first time that PCTA1 expression is observed in PNT2 cell line [4]. Regarding PSCA expression, a similar pattern was observed for LNCaP and PNT2 cells. However, in the case of PC3, only a residual expression was found in cell cultures conducted in RPMI supplemented with 30% FBS. Although there are studies that point to the expression of PSCA in the three tested cell lines [4], others did not observe its expression by PC3 cell line. The gene coding for Prostein was expressed by LNCaP and PNT2 cells, as reported previously [4] and also at low levels by PC3 cell line, though in this case it was only observed when cells were cultured in α-MEM. A residual Prostein expression by PC3 was observed by others [34], although there are also reports that point for an inability of this cell line to express that gene [4]. PSMA was only expressed by LNCaP and PNT2 cells, while TGM4 and PrLZ were expressed by all the tested cell lines. Taken together, since the different culture conditions elicited significant differences in the expression levels of several genes in all tested cell lines, the effect that the metabolic environment has in gene expression may account for some apparent contradictions with previously published data and even among the literature. Furthermore, it reinforces the importance that culture media composition may have in the cell response observed in this kind of analysis.

PSA production is known to be under a complex network of regulatory mechanisms [35, 36]. In this context, the expression by LNCaP of some important modulatory proteins, namely p53, AR and FKBP52 [6-8], in the different culture conditions was also investigated. p53 is a transcription factor encoded by a tumor suppressor gene that inhibits the expression of different prostate cancer biomarkers, including PSA [6]. AR is the intracellular receptor of androgen molecules, and its activation promotes the expression of PSA [7]. FKBP52 is a cochaperone that functions as a positive modulator of AR [8]. It was observed that p53 expression inversely correlated with the expression profile observed for PSA, which is in line with the proposed negative role of p53 in the expression of PSA [6]. Regarding AR and FKBP52, no significant differences were observed in the different tested conditions. Although androgen appear as key players in the regulation of PSA expression [7, 8, 37], no hormonal treatment was performed in cell cultures, which might help to explain the observed results.

The production of PSA was analyzed by a recently developed electrochemical biosensor [3]. It was observed that PSA was only detected in culture media from LNCaP cell line, which increased with the culture period. The relative production of PSA was higher in α-MEM supplemented with 10% FBS. A similar behavior was observed for RPMI, although in this case the values were significantly lower. The ability that human PCa cell lines, and, more precisely, LNCaP cell line, have to express PSA is far from being elucidated. This appears to be strongly affected by the culture conditions and culture time, which reflects the high variability of PSA production values found in literature. Even when the media composition is similar, significant differences are reported. For instance, it was observed that PSA concentration on LNCaP cell line culture medium (RPMI supplemented with 10% FBS) ranges between 0.1-110 ng/mL [6, 37-39]. This apparent heterogeneity of responses is in agreement with what happens in vivo, since both

acute and chronic stimuli (ex: neuropeptides and androgens, respectively) may modulate PSA expression [40, 41]. Moreover, PSA production and secretion appears to be regulated by complex mechanisms, which are affected not only by growth factors and hormones, but also by cellular interactions with the extracellular matrix [33, 38]. Taken together, it is noteworthy to highlight that although LNCaP produced PSA in all tested conditions, the culture media composition and the concentration of FBS markedly affected this ability, which demonstrates that PSA expression is strongly modulated by the cellular environment. Also, although the production of the protein increased with the culture period, this increase was particularly evident during the second week of culture, which coincided with a period of a lower proliferation rate. This suggests that cell density and, consequently, the establishment of proper cell-to-cell contacts may play an important role in the ability of prostate cancer cells to produce PSA. Regarding PC3 cell cultures, the absence of PSA expression is in line with previous studies [42].

Results showed that the PSA levels measured with the biosensor were in line with those obtained by the ELISA method. The accuracy and precision of the data was assessed by *t-Student* and Fisher tests, respectively. Considering as null hypothesis that the two methods agree, an unpaired single-tail test for 5% level of significance gave calculated *F-values* almost always below the tabulated one (Table 7.2), therefore accepting the null hypothesis for most samples observed. Samples outside this validation showed RSD values of the biosensor were much lower than the ones obtained by the ELISA method, meaning that the biosensor proposed herein is displaying a much better analytical performance than the ELISA itself. The calculated t value used the same assumptions, using homoscedastic or heteroscedastic populations (according to the F test) and confirmed for all cases the null hypothesis.

Despite the complexity of the samples, the biosensor was able to detect with selectivity and sensitivity the presence of PSA. The utilization of the biosensor presents several advantages when compared with the traditional immunoassays and, specifically, ELISA assays, such as its inexpensiveness, simplicity of construction, high robustness and easy miniaturization. This method appears to be particularly suitable for screening assays carried out in analytical laboratories. The detection limit and the linear response were significantly lower than the cut-off value for PSA levels (2.0 vs 4.0 ng/mL, respectively), which supports its potential application as a diagnosis tool for PCa. In order to confirm this potential, an assay with different biological samples from healthy individuals and from those with PCa is required. This study is now underway.

In order to evaluate if the PSA produced in the different experimental conditions presented some composition changes, like proteolytic cleavages or post-translational changes, the samples were analyzed by MALDI-TOF MS. The digested PSA was analyzed by PMF search, using the MASCOT search engine, for putative identification of the protein, resulting in unambiguous PSA identification. In addition, the results from intact protein analysis revealed that PSA (from LNCaP cell line) appeared as a uniform population of molecules with about 33.400 Da, which corresponded to the full-length PSA molecular ion. The observed peak corresponding to a mass of 16.690 Da may correspond to the PSA molecular ion with double charge. However, the MALDI-TOF analysis of the standard PSA showed a main peak corresponding to a mass of 29.300 Da followed by other prominent peaks that corresponds to 24.712 Da and 33.888 Da which are compatible with findings from Végvári *et al*. [43]. In fact, these results may be explained by the fact that PSA can occur in three major isoforms and it was suggested that these isoforms may appear upon translation of alternative hKLK3 transcripts [44].

In conclusion, PSA is not expressed equally by the different prostate cell lines. Besides the individual ability of the cell lines to produce the protein, the cellular environment is a key modulator of the PSA expression. The recently developed PSA electrochemical biosensor based/employing on molecularly imprinted polymers was able to specifically detect PSA in the samples, with values similar to those achieved by a commercial ELISA kit, and in levels well below the upper cut-off values for PCa. Thus, the tested biosensor may be regarded as a potentially useful diagnostic tool for PCa, due to the advantages that it offers when compared with the current assays employed in PSA quantification.

7.5 References

[1] J.C. Chen, C.L. Ho, H.W. Tsai, T.S. Tzai, H.S. Liu, N.H. Chow, W.H. Yang, H.-L. Cheng, Immunohistochemical Detection of Prostate-specific Antigen Expression in Primary Urothelial Carcinoma of the Urinary Bladder, *Anticancer Research*, 28 (2008) 4149-4154.

[2] J. You, P. Cozzi, B. Walsh, M. Willcox, J. Kearsley, P. Russell, Y. Li, Innovative biomarkers for prostate cancer early diagnosis and progression, *Critical Reviews in Oncology Hematology*, 73 (2010) 10-22.

[3] T.S.C.R. Rebelo, C. Santos, J. Costa-Rodrigues, M.H. Fernandes, J.P. Noronha, M.G.F. Sales, Novel Prostate Specific Antigen plastic antibody designed with charged binding sites for an improved protein binding and its application in a biosensor of potentiometric transduction, *Electrochimica Acta*, 132 (2014) 142-150.

[4] B. Carlsson, O. Forsberg, M. Bengtsson, T.H. Tötterman, M. Essand, Characterization of human prostate and breast cancer cell lines for experimental T cell-based immunotherapy, *The Prostate*, 67 (2007) 389-395.

[5] A.B. Reed, D.J. Parekh, Biomarkers for prostate cancer detection, *Expert Review of Anticancer Therapy*, 10 (2010) 103-114.

[6] V.K. Gurova, W.O. Roklin, I.V. Krivokrysenko, M.P. Chumakov, B.M. Cohen, E. Feinstein, V.A. Gudkov, Expression of prostate specific antigen (PSA) is negatively regulated by p53, *Oncogene*, 21 (2002) 153-157.

[7] H. Yin, H. Radomska, D. Tenen, J. Glass, Down regulation of PSA by C/EBPa is associated with loss of AR expression and inhibition of PSA promoter activity in the LNCaP cell Line, *BMC Cancer*, 6 (2006) 1-14.

[8] J.T. De Leon, A. Iwai, C. Feau, Y. Garcia, H.A. Balsiger, C.L. Storer, R.M. Suro, K.M. Garza, S. Lee, Y. Sang Kim, Y. Chen, Y.M. Ning, D.L. Riggs, R.J. Fletterick, R.K. Guy, J.B. Trepel, L.M. Neckers, M.B. Cox, Targeting the regulation of androgen receptor signaling by the heat shock protein 90 cochaperone FKBP52 in prostate cancer cells, *Proceedings of the National Academy of Sciences*, 108 (2011) 11878-11883.

[9] M.L. Wong, J.F. Medrano, Real-time PCR for mRNA quantitation, *Biotechniques*, 39 (2005) 75-85.

[10] D. López-Ferrer, J.L. Capelo, J. Vázquez, Ultra Fast Trypsin Digestion of Proteins by High Intensity Focused Ultrasound, *Journal of Proteome Research*, 4 (2005) 1569-1574.

[11] H.M. Santos, C. Mota, C. Lodeiro, I. Moura, I. Isaac, J.L. Capelo, An improved clean sonoreactor-based method for protein identification by mass spectrometry-based techniques, *Talanta*, 77 (2008) 870-875.

[12] World Health Organization (WHO), www.who.int/mediacentre/factsheets/fs297/en, accessed in September 2010.

[13] J. Hernández, I.M. Thompson, Prostate-specific antigen: A review of the validation of the most commonly used cancer biomarker, *Cancer*, 101 (2004) 894-904.

[14] Z. Nosratollah, O. Habib, A. Behrangh, Association between steroid hormone receptors and PSA gene expression in breast cancer cell lines, *African Journal of Biotechnology*, 4 (2005) 1415-1420.

[15] I. Giusti, V. Dolo, Extracellular Vesicles in Prostate Cancer: New Future Clinical Strategies?, *BioMed Research International*, 2014 (2014) 14.

[16] J.H. Park, Y.-K. Lee, K.-M. Kim, K.-N. Kim, Transformation of Electrodeposited Calcium Phosphate Coatings in Simulated Body Fluid and in Culture Medium, *Key Engineering Materials*, 284-286 (2005) 473-476.

[17] T.G. Heaney, Inhibition of Attachment of Human Gingival Fibroblast-Like Cells in Vitro by Saliva and Salivary-Sulfated Glycoprotein in the Presence of Serum, *Journal of Periodontology*, 61 (1990) 504-509.

[18] C. Pautke, M. Schieker, T. Tischer, A. Kolk, P. Neth, W. Mutschler, S. Milz, Characterization of Osteosarcoma Cell Lines MG-63, Saos-2 and U-2 OS in Comparison to Human Osteoblasts, *Anticancer Research*, 24 (2004) 3743-3748.

[19] A.Z. Rodrigues, P.T.d. Oliveira, A.B. Novaes Jr., L.P. Maia, S.L.S.d. Souza, D.B. Palioto, Evaluation of in vitro human gingival fibroblast seeding on acellular dermal matrix, *Brazilian Dental Journal*, 21 (2010) 179-189.

[20] P. Indovina, G. Rainaldi, M.T. Santini, Three-dimensional cell organization leads to a different type of ionizing radiation-induced cell death: MG-63 monolayer cells undergo mitotic catastrophe while spheroids die of apoptosis, *International Journal of Oncology*, 31 (2007) 1473-1483.

[21] Tulika Mishra, M. Khullar, A. Bhatia, Anticancer Potential of Aqueous Ethanol Seed Extract of *Ziziphus mauritiana* against Cancer Cell Lines and Ehrlich Ascites Carcinoma, *Evidence-Based Complementary and Alternative Medicine*, 2011 (2011) 11.

[22] M.E. Mycielska, M.B.A. Djamgoz, Citrate transport in the human prostate epithelial PNT2-C2 cell line: electrophysiological analyses, *The Journal of Physiology*, 559 (2004) 821-833.

[23] Y. Lu, J. Zhang, J. Dai, L. Dehne, A. Mizokami, Z. Yao, E. Keller, Osteoblasts induce prostate cancer proliferation and PSA expression through interleukin-6-mediated activation of the androgen receptor, *Clinical and Experimental Metastasis*, 21 (2004) 399-408.

[24] P.J. Russel, P. Jackson, E.A. Kingsley, Prostate Cancer Methods and Protocols, Methods in Molecular Medicine (2003).

[25] H.G. Rittenhouse, J.A. Finlay, S.D. Mikolajczyk, A.W. Partin, Human Kallikrein 2 (hK2) and Prostate-Specific Antigen (PSA): Two Closely Related, but Distinct, Kallikreins in the Prostate, *Critical Reviews in Clinical Laboratory Sciences*, 35 (1998) 275-368.

[26] T.K. Takayama, B.A. McMullen, P.S. Nelson, M. Matsumura, K. Fujikawa, Characterization of hK4 (Prostase), a Prostate-Specific Serine Protease: Activation of the Precursor of Prostate Specific Antigen (pro-PSA) and Single-Chain Urokinase-Type Plasminogen Activator and Degradation of Prostatic Acid Phosphatase†, *Biochemistry*, 40 (2001) 15341-15348.

[27] Y. Zick, M. Eisenstein, R. Goren, Y. Hadari, Y. Levy, D. Ronen, Role of galectin-8 as a modulator of cell adhesion and cell growth, *Glycoconjugate Journal*, 19 (2002) 517-526.

[28] N. Saeki, J. Gu, T. Yoshida, X. Wu, Prostate stem cell antigen (PSCA): a Jekyll and Hyde molecule?, *Clinical Cancer Research*, 16 (2010) 3533–3538.

[29] M. Yin, R. Dhir, A. Parwani, Diagnostic utility of p501s (prostein) in comparison to prostate specific antigen (PSA) for the detection of metastatic prostatic adenocarcinoma, *Diagnostic Pathology*, 2 (2007) 41-48.

[30] G. Davies, R.J. Ablin, M.D. Mason, W.G. Jiang, Expression of the prostate transglutaminase (TGase-4) in prostate cancer cells and its impact on the invasiveness of prostate cancer, *Journal of Experimental Therapeutics and Oncology*, 6 (2007) 257-264.

[31] R. Wang, J. Xu, O. Saramäki, T. Visakorpi, W.M. Sutherland, J. Zhou, B. Sen, S.D. Lim, N. Mabjeesh, M. Amin, J.-T. Dong, J.A. Petros, P.S. Nelson, F.F. Marshall, H.E. Zhau, L.W.K. Chung, PrLZ, a Novel Prostate-Specific and Androgen-Responsive Gene of the TPD52 Family, Amplified in Chromosome 8q21.1 and Overexpressed in Human Prostate Cancer, *Cancer Research*, 64 (2004) 1589-1594.

[32] R.E. Conway, N. Petrovic, Z. Li, W. Heston, D. Wu, L.H. Shapiro, Prostate-Specific Membrane Antigen Regulates Angiogenesis by Modulating Integrin Signal Transduction, *Molecular and Cellular Biology*, 26 (2006) 5310-5324.

[33] Y. Guo, R. Pili, A. Passaniti, Regulation of prostate-specific antigen gene expression in LNCaP human prostatic carcinoma cells by growth, dihydrotestosterone, and extracellular matrix, *Prostate*, 24 (1994) 1-10.

[34] M. Kalos, J. Askaa, B.L. Hylander, E.A. Repasky, F. Cai, T. Vedvick, S.G. Reed, G.L. Wright, G.R. Fanger, Prostein expression is highly restricted to normal and malignant prostate tissues, *The Prostate*, 60 (2004) 246-256.

[35] S.P. Balk, Y.J. Ko, G.J. Bubley, Biology of Prostate-Specific Antigen, *Journal of Clinical Oncology*, 21 (2003) 383-391.

[36] J. Kim, G.A. Coetzee, Prostate specific antigen gene regulation by androgen receptor, *Journal of Cellular Biochemistry*, 93 (2004) 233-241.

[37] Y.S. Zhu, L.Q. Cai, X. You, J.J. Cordero, Y. Huang, J. Imperato-McGinley, Androgen-Induced Prostate-Specific Antigen Gene Expression Is

Mediated via Dihydrotestosterone in LNCaP Cells, *Journal of Andrology*, 24 (2003) 681-687.

[38] Z. Rekasi, A.V. Schally, A. Plonowski, T. Czompoly, B. Csernus, J.L. Varga, Regulation of prostate-specific antigen (PSA) gene expression and release in LNCaP prostate cancer by antagonists of growth hormone-releasing hormone and vasoactive intestinal peptide, *Prostate*, 48 (2001) 188-199.

[39] Y. Fujii, S. Kawakami, Y. Okada, Y. Kageyama, K. Kihara, Regulation of prostate-specific antigen by activin A in prostate cancer LNCaP cells, *American Journal of Physiology - Endocrinology and Metabolism*, 286 (2004) 927-931.

[40] P.J. Gkonos, C.K. Kwok, N.L. Block, B.A. Roos, Identification of the human seminal TRH-like peptide pGlu-Phe-Pro-NH2 in normal human prostate, *Peptides*, 15 (1994) 1281-1283.

[41] C. Lee, D.M. Sutkowski, J.A. Sensibar, D. Zelner, I. Kim, I. Amsel, N. Shaw, G.S. Prins, J.M. Kozlowski, Regulation of proliferation and production of prostate-specific antigen in androgen-sensitive prostatic cancer cells, LNCaP, by dihydrotestosterone, *Endocrinology*, 136 (1995) 796-803.

[42] K.H. Tsui, T.-H. Feng, L.-C. Chung, C.-H. Chao, P.-L. Chang, H.-H. Juang, Prostate Specific Antigen Gene Expression in Androgen Insensitive Prostate Carcinoma Subculture Cell Line, *Anticancer Research*, 28 (2008) 1969-1976.

[43] Á. Végvári, M. Rezeli, C. Welinder, J. Malm, H. Lilja, G. Marko-Varga, T. Laurell, Identification of prostate-specific antigen (PSA) isoforms in complex biological samples utilizing complementary platforms, *Journal of Proteomics*, 73 (2010) 1137-1147.

[44] N. Heuzé, S. Olayat, N. Gutman, M.-L. Zani, Y. Courty, Molecular Cloning and Expression of an Alternative hKLK3 Transcript Coding for a Variant Protein of Prostate-specific Antigen, *Cancer Research*, 59 (1999) 2820-2824.

8

Conclusion and future work

8.1 Conclusions

This thesis enabled the development of new biosensors, based on non-invasive methods that allowed inexpensive and portable detection in point-of-care testing for PCa early detection. New synthetic receptors with high affinity for PCa biomarkers were successfully obtained. Mostly, solid-contact carbon conventional electrodes and SPEs were used, involving simple and inexpensive procedures and providing selective readings with low concentrations of analyte and low sample volumes.

Regarding the transduction, electrochemical techniques, such as potentiometry and voltammetry, were used. These techniques are easily adjusted for screening purposes, enable simple and inexpensive procedures and provide selective readings with low concentrations and low sample volumes. They may also offer portable versions to carry out tests in point-of-care.

Voltammetry has demonstrated to be a rapid and sensitive technique, in which LODs were in good agreement with other techniques reported in the literature, or better. Potentiometry was a suitable strategy, due to its low cost and portability feasibility, which was easily achieved with low cost materials. One limitation of this method is related to the composition and thickness of the PVC membrane, which is hardly controlled during its production. Overall, the potentiometric biosensor for PSA was successfully designed and results obtained

in artificial serum and different prostate cell lines were similar to those achieved by a commercial ELISA kit.

This work is also very important due to the inexistence in the literature of biosensors with the recognition element of the MIPs for the selected biomarkers. To obtain this kind of recognition element, one of the most important steps is the imprinting stage. To improve the binding affinity of the protein template to its complementary binding sites, new strategies were successfully introduced herein. Among these, the addition of charged monomers at the binding site were introduced, having the surrounding environment tailored with neutral materials. The use of CAF as monomer for molecular imprinting by electropolymerization has also been introduced herein successfully, which has never been used before for this purpose.

This work also reported the effective introduction of enzymes as recognition element for PCa biomarkers. For this purpose, the construction of SAR electrochemical biosensor was presented, based on the covalent immobilization of an enzyme on the surface of the carbon-SPE. In this work, selectivity was improved by covering the electrode surface with Nafion.

All the studied devices have introduced several technical innovations in the development of biosensors, both in terms of the assembly of the recognition element and also in system configuration for monitoring PCa biomarkers in point-of-care. Further developments may however be achieved…

8.2 Future work

The previous sensors could be favorably combined in a multi-sensorial platform for point-of-care screening, allowing the measurement of multiple analytes at once. The array of electrodes could be further turned into micro or nanosized

electrodes allowing the use of samples with small volumes (few μL), by means of screen-printed electrodes.

In addition, the application of microfluidics into the PCa biosensors would be extremely useful. This technology offers new promising avenues in point-of-care diagnostics, including high-throughput analysis, portability and disposability, low consumption of costly reagents, short reaction time, multiple sample detection in parallel, and versatility in design. It also allows the incorporation of microscale fluid regulators (e.g. valves, mixers, and pumps) on the lab-on-a-chip platform, giving an increased degree of automation.